Tracing soil particle movement. Towards a spectral approach to spatial monitoring of soil erosion

Mila Ivanova Luleva

PhD dissertation committee

Chair

Prof. Dr. A. Veldkamp	University of Twente

Promoters

Prof. Dr. Victor G. Jetten	University of Twente
Prof. Dr. Freek D. van der Meer	University of Twente

Assistant promoter

Dr. Harald M.A. van der Werff	University of Twente

Members

Prof. Dr. Wout Verhoef	University of Twente
Prof. Dr. Andrew Skidmore	University of Twente
Prof. Dr. Violette Geissen	University of Bonn
Dr. Sabine Chabrilat	Helmholtz Centre Potsdam GFZ
Dr. Eduardo Garcia-Melendez	Universidad de Leon

ITC dissertation number 228
ITC, P.O. Box 217, 7500 AE Enschede, The Netherlands

ISBN: 978-90-6164-356-2
Printed by: ITC Printing Department, Enschede, The Netherlands

UNIVERSITY OF TWENTE.

FACULTY OF GEO-INFORMATION SCIENCE AND EARTH OBSERVATION

TRACING SOIL PARTICLE MOVEMENT. TOWARDS A SPECTRAL APPROACH TO SPATIAL MONITORING OF SOIL EROSION

DISSERTATION

to obtain
the degree of doctor at the University of Twente,
on the authority of the rector magnificus,
prof. dr. H. Brinksma,
on account of the decision of the graduation committee,
to be publicly defended
on Wednesday, July 3, 2013 at 12:45

by

Mila Ivanova Luleva
born on January, 18, 1984
in Sofia, Bulgaria

This dissertation is approved by:

Prof. Dr. Victor G. Jetten (promoter)
Prof. Dr. Freek D. van der Meer (promoter)
Dr. Harald M.A. van der Werff (assistant promoter)

Contents

List of Figures

List of Tables

Introduction 1

1.1 Soil Erosion and Land Degradation

Soil is the product of complex interactions between climate, geology, vegetation, biological activity, time and land use. The proportions of its different components- sand, silt and clay particles, organic matter, water and air, as well as the way in which these components form together a stable structure, define soil's characteristics [Morgan, 2005]. Soil erosion is a naturally occurring process, which plays a major role in the process of soil formation. However, climatic conditions such as droughts, aridity, irregular and intense precipitation regimes as well as human-induced activities such as deforestation, overgrazing and soil structure deterioration, cause a shift from natural to accelerated soil erosion [Cerdan et al., 2010]. The latter is what presents a major concern and it is referred to in studies of land degradation caused by soil erosion.

Soil can be eroded under the influence of wind and water. Soil detachment is caused by raindrop impact and flow traction, while the material is transported by saltation and overland water flow. Under the influence of intense flow, a formation of small channels, also known as rills, occurs. In agricultural areas, rills are removed by ploughing, however, although the visible signs are removed, the process of erosion has still taken place. If the storms are severe, or preventive measures do not take place, soil erosion leads to forming gullies. These can be removed only by radical measures such as re-grading of entire areas. Because these methods are time and effort consuming, the gullied areas are often simply abandoned.

One of the major controlling factors that determine the rate and severity

of soil erosion is runoff. The amount of runoff is directly proportional to the difference between the amount of rainfall and infiltration of the soil. The infiltration in its turn is determined by both soil texture properties, as well as soil structure. In many areas erosion is directly associated with the loss of structure by crusting. Furthermore the degree of erosion is determined by the velocity of the runoff, which is a function of the terrain slope, surface roughness and resistance by vegetation. Although conceptually this is a well known system, the interaction of the many factors, each with its spatial variability, makes precise prediction of erosion difficult.

The impact of erosion is most commonly assessed using soil erosion models. The main limitations, however, are the variability and spatial extent of the event, which create difficulties in obtaining sufficient spatial data to calibrate erosion models and to verify the predicted results [Jetten et al., 2003]. Remote sensing can play an important role considering that it provides extensive coverage over various areas. Spatial data acquired with satellite sensors have been used as an input for estimation of erosion parameters, however the main focus is directed towards the visible and infrared parts of the spectrum [Metternicht and Zinck, 1998]. Therefore, landuse maps, vegetation cover maps and digital elevation models are the most common products of image analysis.

One of the ways to quantify erosion spatially is with chemical and radioactive tracers. Soil particle tracing using chemical tracers have been conducted over the past three decades. Several chemical soil particle tracers have been used to model spatial distribution of soil erosion [Zhang et al., 2006] and to identify suspended sediment [Onda et al., 2007]. Some of the most commonly used soil particle tracers include the Cesium 137 isotope (^{137}Cs) [Andersen et al., 2000, Chappell, 1999, Collins et al., 2001, Guimaraes et al., 2003, Porto et al., 2001, Sanchez-Cabeza et al., 2007, Timothy et al., 1997], Lead (^{210}Pb) and Beryllium (^{7}Be) [Mabit et al., 2008, Wallbrink and Murray, 1993], and Rare Earth Oxides [Polyakov and Nearing, 2004, Zhang et al., 2006]. The ^{137}Cs is considered the primary chemical tracer for detection of soil particle movement [deGraffenried Jr and Shepherd, 2009, Estrany et al., 2010, Meusburger et al., 2010, Rodway-Dyer and Walling, 2010, Xiaojun et al., 2010], however it comes with a number of limitations and assumptions. Firstly, the homogeneous distribution of

^{137}Cs fall out is limited to the Northern hemisphere, because it has been introduced to the environment after the Chernobyl incident in the late 1980s. Secondly, all particle movements are assumed to be as a result of soil erosion [Campbell et al., 1982, Chappell, 1999, Walling and Quine, 1990]. Cost of soil sampling and analysis and the limited half-life of the element are also among the main limitations preventing extrapolation of these methods to cover large areas [Boardman, 2006].

Considering that sampling large areas for determination of soil properties using spectral reflectance is relatively cheap and fast, compared to traditional field and laboratory techniques [Shepherd and Walsh, 2002], infrared spectroscopy has the potential to provide solutions to some of the problems and limitations associated with scaling of the particle tracing techniques.

Soil properties have been studied with infrared spectroscopy since the 1980's, using visible, near-infrared and shortwave infrared wavelength region (400–2500 nm). Soil spectral reflectance is determined by both physical and chemical characteristics of soils [Baumgardner et al., 1985, Ben-Dor et al., 2003, Shepherd and Walsh, 2002]. Soil spectral features result from an overtone absorption and combination of bond vibrations in molecules of three functional groups in minerals: OH, SO_4 and CO_3, [Ben-Dor and Banin, 1995, Hunt and Salisbury, 1970]. In addition, organic matter influences the spectral response because it holds most positively charged nutrient ions in soils.

To date, infrared spectra have not been put into soil erosion perspective. Low concentrations of the ^{137}Cs isotope in nature makes the identification of the element through spectral means impossible, considering the capabilities of available spectrometers.

Elements with similar chemical and biological behaviour to the isotope, such as Potassium (K), which is much more abundant in the environment but still evenly applied, are not fully explored. Potassium shares electrical, chemical and physical properties with Cs, both being members of the Group I alkali metals [Andrello and Appoloni, 2004, Relman, 1956]. Both elements have similar biological and chemical behaviour, where the difference is only in reactivity [Relman, 1956], but it has not been tested as a particle trace.

The element K is mainly present as part of preliminary soil minerals

(unavailable), in clay minerals and fine silt (slowly available), and in a water-soluble form (readily available) [Garrett, 1996, Peterburgsky and Yanishevsky, 1961, Sharpley, 1989]. Potassium occurs naturally in the environment, but it is also used on agricultural lands as a fertilizer. In general it is applied in a form of K_2O or K–P–N prior to harvesting.

1.2 Soil Erosion in Europe

Soil erosion by water is an extensive and increasing problem throughout Europe. Over the last decade, a number of reports have been produced in order to assess the affected areas and severity of degraded land. In the early 1990s, Oldeman [1991] and Van Lynden [1995] provided an overview for the Council of Europe. As stated by the European Soil Bureau [2001], with a very slow rate of soil formation, any soil loss of more than 1 t/ha/yr can be considered irreversible within a time span of 50–100 years. Losses of 20–40 t/ ha in individual storms, are measured once every two years in Europe [Morgan, 2005].

The Mediterranean region is particularly prone to erosion. According to Van Lynden [1995], areas within this region have been affected to the extent to which erosion has stopped due to lack of soil. According to the European Soil Bureau [2001], this area is characterized by long dry periods followed by heavy bursts of erosive rainfall, falling on steep slopes with fragile soils. Severe erosion is also measured in other parts of Europe mainly within Austria, Czech Republic and the loess belt of Northern France, Belgium and The Netherlands. Soil erosion can therefore be considered, with different levels of severity, an EU-wide problem.

This study is part of the DESIRE Project, funded under the EU's Sixth Framework Programme. It has an aim to develop strategies for use and protection of areas prone to soil erosion and desertification in Europe. The project is conducted by 28 research institutes, non-governmental organisations and policy makers from Europe, Australia, Africa, South and North America. In total there are eighteen study sites located across these continents, where soil is subjected to erosion due to wind or water, salinization, droughts or flash floods. More information regarding exact location and detailed description of the sites can be found in Alterra [2007].

Table 1.1: Differences and similarities between Guadalentin basin, Spain and South East Limburg, The Netherlands

	Guadalentin basin	South East Limburg
Relief	Ranging Slopes	Mainly flat
Geology	Wide range of minerals- predominantly illites, chlorites, and illite-smectites.	Predominantly limestone
Soil	Silt Loam (Calcisols)	Loess
Clay content	30–36 %	12–18 %
Precipitation	300–500 mm annual (intense rainstorm events)	820–900 mm annual (distributed throughout the year)
Erosion	Severe- due to tillage, fallow land and land	Severe- due to flooding and runoff

1.3 Study Sites

Two study sites were selected in order to conduct the present research. As part of the DESIRE Project, one of them is the Guadalentin basin, South East Spain, while the second one is located in South Limburg, The Netherlands. The two study sites differ in soil texture, relief, underlying geology and precipitation rates (see Table 1.1). Both sites, however, are affected by severe erosion.

1.3.1 Guadalentin basin

Climate, geomorphology and the impact of human activities have resulted in progressive land degradation across the Mediterranean region of Europe. In Spain, more than 22 million ha, 43.8 % of the land is affected by erosion rates higher than 12 t/ha/yr. Nearly half of this area registers soil losses higher than 50 t/ha/yr. Because of this, within the Murcia province of Spain (Figure 1.1), a number of test sites are developed especially for soil erosion and related studies.

This is an area where land degradation phenomenon can be readily

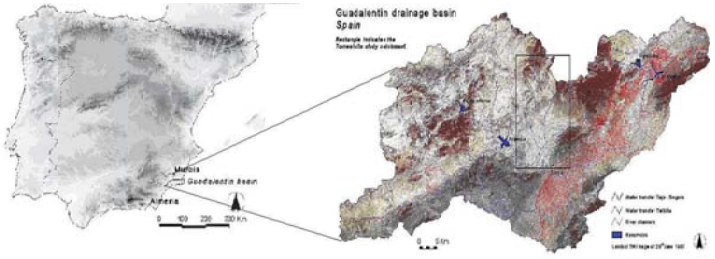

Figure 1.1: Location of the Guadalentin basin, South-East Spain [Alterra, 2007]

observed (Figure 1.2). Soil erosion by rills and gullies is common, caused by tillage, fallow land and land abandonment. Rain storms are of high intensity, while rock types are susceptible to erosion. Measures to combat these problems have been applied for over 100 years, though only in some parts they have been successful.

Guadalentin basin lies on the eastern edge of the Beltic ranges facing southwest-northeast direction and faults determine the main structure of the drainage network. The Guadalentin is an ephemeral river for the major part of its course. The upper section of the basin has a high drainage density. The middle section is characterised by an undulating landscape with long pediments and incised river terraces. The lower reach is characterised by a flat valley bottom with series of developed alluvial fans.

The basin covers an area of 3300 km^2 [Baartman et al., 2011]. The climate varies from semi-arid to sub-humid Mediterranean. Annual precipitation from 300 mm to 500 mm with average annual temperature between 12 and 18° Celcius. Summer droughts, commonly last for 4–5 months. Annual potential evapotranspiration rates of 1000–2000 mm are common [Baartman et al., 2011].

The main agricultural crops include almonds and herbaceous crops. Semi-natural ecosystems include shrublands of Stipa tenacissima, Rosmarinus officinalis and Anthyllis cytisoides. Forests are dominated by Pinus halepensis in part as a result of afforestation policies over the past 150 years [Alterra, 2007].

Soils are shallow with high Calcium Carbonate content exceeding 50 % for some areas. Texture depends mainly on the hillslope position. Stoni-

ness is high, low organic matter and moisture content. Salinity and crusting are problematic for some parts of the Guadalentin Basin, where soils are neutral to slightly alkaline. These soils are higy prone to formation of erosion features sich as rills and gullies (see Figure 1.2).

Figure 1.2: Newly formed rills and deep gully formations in the Guadalentin basin, South-East Spain. A: Rills; B: Gully system

As indicated on soil maps produced by FAO [2006], the main soil types, recognized in the region of Murcia are Calcisols, Luvisols, Regosols and Fluvisols.

Calcisols are soils with an argic horizon within 100 cm from the soil surface. The have an irregular upper boundary resulting from albeluvic tonguing into the argic horizon. Luvisols are characteristic soils for the forested regions. They are identified by the presence of eluvial (Ae) horizons and illuvial (Bt) horizons where silicate clay is accumulated. Regosols are well to imperfectly drained mineral soils which lack horizon development or have minimal A and B horizon development. Fluvisols have a salic horizon starting within 50 cm from the soil surface.

Gully erosion in the Guadalentin is estimated to produce about 37.60 t

ha^{-1} yr^{-1}, which is equivalent to 50 % of total soil loss due to rill, interrill and gully erosion [Poesen et al., 2003].

1.3.2 South East Limburg

Southeast Limburg is part of European loess belt which covers parts of England, northwest France, Belgium, The Netherlands, Germany, Poland and Russia [Kwaad et al., 2006]. They are the product of the Quaternary Glacial period and the resulting dust accumulation ranging (in Europe) from the maritime areas of NW-Europe (France, Belgium) over Central Europe to the Ukraine and the Russian plains [Haase et al., 2007]. The loess soil of Limburg is rich in lime and contains up to 70 % quartz grains in the silt fraction [Spaan et al., 2010].

The study site is located within the area of the soil erosion experimental farm at Wijnandsrade (Figure 1.3). It is characterised by a hilly relief with surface elevation up to 300 m above sea level. Typical landforms include dry valleys, incised roads and manmade cultivation terraces. The soils belong to Typic Hapludalf soil type (Soil Taxonomy) or Albic Luvisol [FAO, 2006]. The soils are developed the Holocene period and are highly susceptible to soil erosion and runoff due to their low structural stability. These processes are enhanced by continuous changes in land use and decrease of grassland in favour of arable land [Boardman et al., 1994].

Top soils have very high silt content, classified as silt or silt loam, with low organic matter content [Kwaad and Mücher, 1994]. The sub soils are very stony and dry due to underlying gravels of terraces deposited by the River Meuse. The plough layer is light in colour and has low-organic matter content, a yellowish subsurface horizon with a weak platy structure and textured subsoil with weak but coarse prismatic structure [de Bakker, 1979].

The slope varies between 2 and 12 % [de Bakker, 1979]. The annual precipitation is distributed throughout the whole year with an average of 60 mm per month with high rainfall intensities reaching 1–2 mm/min. The area is used mainly for agriculture [Winteraeken and Spaan, 2010]. The present land use in South Limburg is mainly arable crops, nearly 50 % of the area, of which is covered by sugar beets, potatoes, silage-maize and cereals [Spaan et al., 2010], while the rest is meadow, forest and residential

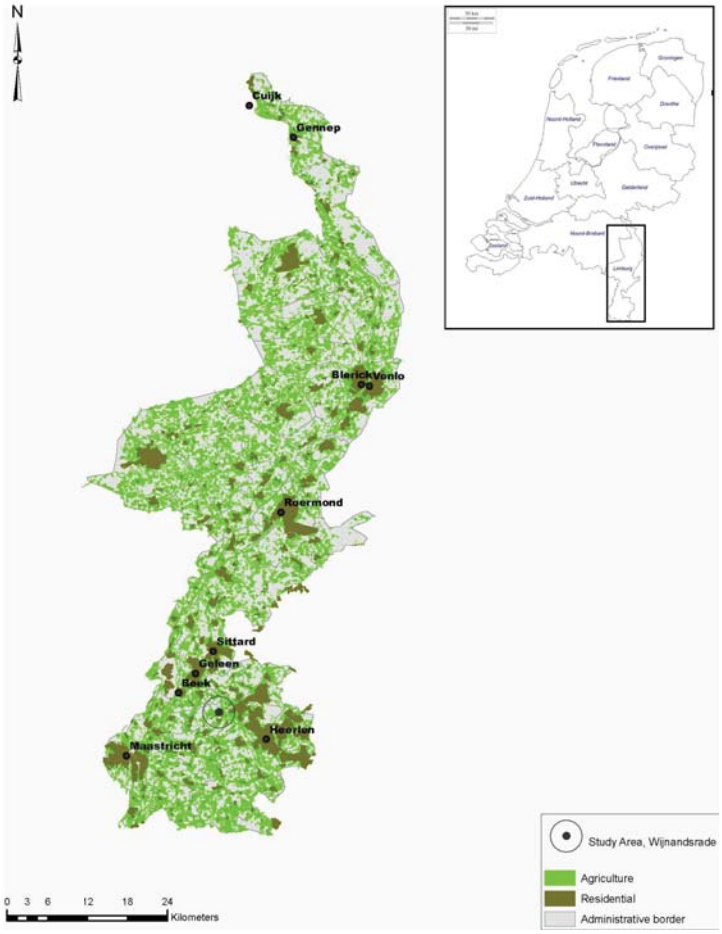

Figure 1.3: Location of soil erosion experimental farm at Wijnandsrade, South Limbourg, The Netherlands

areas.

1.4 Problem Statement

Soil erosion has been studied and modeled for decades. However, the large spatial extent of the event, as well as the insufficient data for input and validation of the soil erosion models, still create limitations. Recently, remotely sensed data have been included in various erosion studies [Vrieling, 2006]. The main use of these data is to derive spatial information from the visible and near- infrared wavelengths of the electromagnetic spectrum, for determination of parameters associated with soil erosion such as vegetation, topography and rainfall.

As part of soil erosion modeling, soil particle tracing has been explored as a technique to assess soil particle movement. The most commonly used soil particle tracer, the ^{137}Cs isotope, comes with a number of limitations and assumptions. The isotope has limited half-life, an assumed even spatial distribution and, due to the high cost of analysis, it is impractical for assessment of large areas (See also Chapter 3). Furthermore, the concentrations in which the element is found in the environment are too low to have influence on the soil spectral response of soils.

Different types of soil, water, rocks and vegetation are known to reflect, transmit or absorb electromagnetic energy coming from the Sun in a specific and characteristic manner. The spectral response of each of these targets is determined by the interaction of the incident radiation with the surface, the orientation and position of the Sun, topography and orientation of the target, the atmospheric state as well as the location of the measuring sensor. Moreover, the chemical composition and molecular structure of the object of interest, determine the wavelengths where reflection, transmission or absorption takes place within particular wavelengths of the electromagnetic spectrum. The result is a spectral response curve of for the target, also referred to as a spectral reflectance signature.

The chemical and physical properties of soil determine the amount of solar energy that is reflected back from the target. The main controlling factors that influence the shape of the soil spectrum include moisture content, organic matter, particle size distribution, soil mineralogy and soil texture. Each factor can be determined by studying the spectral curve either directly, by looking at spectral absorption features, or indirectly, through establishing statistical relationships between soil chemical composition

and soil spectral response (further described in Chapter 3 and 4).

A limited number of studies explore the use of spectral information derived from longer wavelengths. Soil chemical properties have distinct spectral signatures in the shortwave infrared spectrum (between 1100 and 2500 nm), however this information has not been implemented in soil erosion studies to date. This research focuses on, firstly, identifying potential alternative chemical soil particle tracer that has similar chemical and physical behavior as Cesium. The element has to be more abundant and less harmful to the environment, allowing practical application of the technique. Secondly, the emphasis is directed towards examining whether the shortwave infrared electromagnetic spectrum can provide sufficient information to allow identification and quantification of this element in order to establish a cost effective and rapid way for tracing of soil particle movement.

The specific aim of the study is to identify the most suitable chemical soil particle tracer, and to evaluate whether change in concentration of this element can be measured with infrared spectroscopy by establishing direct relationships between concentrations and absorption band parameters of the soil spectral signature. The scope of the research is limited by the concentrations in which the element is present. They should be high enough to have influence on the shape of the spectral curve, but low enough not to cause disturbance and contamination to the environment.

1.5 General Research Objectives

1. To identify gaps in the use of remote sensing in soil erosion studies by reviewing the latest techniques associated with modeling and assessment of the process
2. To establish direct and indirect relationships between soil chemical composition and infrared spectral response
3. To identify whether changes in Potassium concentration in soils of various textures can be observed using infrared spectral response
4. To examine whether Potassium can be used as a tracer for soil particle movement under field conditions through spectral analysis

1.6 Thesis Structure

A general introduction to the process of soil erosion, spectral characteristics of soils and problem definition is presented in Chapter 1 (this chapter). This is followed by Chapter 2, which provides an overview of the use of remote sensing in monitoring soil erosion and its contribution as an input for soil erosion modeling. By examining the different applications of these data, gaps in the current knowledge are outlined and new areas where these data can contribute are identified. Advanced stages of soil erosion have been extensively monitored using remote sensing data, however there are no methods developed for detecting early signs of erosion. This chapter identifies soil particle tracing using chemical elements as a new application of remote sensing in monitoring early stages of soil erosion.

Chapter 3 presents a method to establish direct and indirect relationships between naturally occurring soil chemical elements and infrared spectral response. Specific wavelength ranges that statistically predict and quantify soluble fractions of chemical elements, from near infrared and shortwave infrared spectroscopy are outlined.

Chapter 4 introduces the use of Potassium (K) as an alternative to Cesium 137 (^{137}Cs) as a particle tracer. The study is conducted in a laboratory on soils of various textural classes. Ranging concentrations of Potassium fertilizer are applied to the surface of the soil samples and measured for their spectral characteristics. Absorption feature parameters, including absorption band depth, center and area, are analyzed in order to determine the influence of K on the spectral absorption curve.

Chapters 5 and 6 describe the application of the technique established in field conditions. The behavior of K was tested with a flow experiment conducted in an area severely affected by soil erosion Murcia, South East Spain. Spectral field measurements are built into synthetic images to study the spatial extent and variation of the tests. The experiment resulted in identification of factors that have strong influence on the spectral response and limit the applicability of the technique. An improved experimental setup was conducted in South Limburg, The Netherlands (chapter 6), on Loess soils with limited clay content. The range of concentrations of applied fertilizer was increased, and the runoff sediment was collected. The methods of image interpretation and statistical analysis remained the

same.

Chapter 7 contains general discussion in the form of synthesis. The research objectives are answered and main conclusions are outlined based on evaluation of the findings. This section contains limitations of the current study as well as recommendations if further work is intended.

2 Gaps and opportunities in remote sensing for soil erosion assessment

Abstract

Assessing soil erosion over large areas has been a challenge for decades. The large spatial extent of the process creates difficulties in data acquisition for both measuring and validation. This chapter provides an overview of the most common applications of remotely sensed data as an input for various models and techniques in soil erosion studies. Remotely sensed data provide spatial coverage and are used to derive information for various soil erosion parameters, such as vegetation cover, topography, soil moisture, as well as to detect large erosion features. The chapter also contains a discussion on soil particle tracing using chemical elements as a method for assessment of soil erosion and deposition. By identifying the limitations associated with this technique, the gaps in the use of remote sensing for soil erosion monitoring using particle tracers are presented. Additionally, the chapter outlines a potential use of remote sensing data in order to expand the scope of already existing techniques. [1]

[1] This chapter is based on: Luleva, M.I., Van Der Werff, H., Van Der Meer, F. and Jetten, V., (2012), Gaps and opportunities in the use of remote sensing for soil erosion assessment, Chemistry, 21(5),748 - 764, Luleva et al. [2012]

2.1 Introduction

Land degradation and soil erosion have been studied since the 1940's, when the first concepts of detachment and transport of soil material were introduced [Ellison, 1944]. Various soil erosion models have been developed to predict, simulate and assess the severity of erosion. Jetten et al. [2003] mentioned that it is possible to predict quantitatively aggregated soil loss, but the exact prediction in space and time of erosion features is impossible because of the high spatial variability of all parameters involved. Remote sensing is found to provide solutions for estimating some of the related erosion parameters and for outlining already developed erosion features [Alatorre and Begueria, 2009, Jetten et al., 2003, Vrieling, 2006, Shruthi et al., 2011]. Most research, however, focused on land cover mapping, identification of bare soil regions, and mapping soil types [Alatorre and Begueria, 2009]. Shruthi et al. [2011] showed that very high resolution images are needed for erosion feature detection, while Vrieling [2006] showed that large gullies can be detected by coarser resolution images, but mainly through the presence or absence of vegetation. Various classification techniques and processing algorithms based on spectral correlation have been implemented in order to overcome some of the limitations [Shrestha et al., 2005]. Yet, the potential of using remotely sensed imagery for soil erosion studies is still not fully explored.

The aim of this chapter is to provide an overview of existing applications of remotely sensed data in soil erosion studies done in the laboratory and in the field. We provide a detailed review on the methodologies that are applied on remotely sensed imagery to estimate the main parameters used as input for soil erosion models. In addition we look into soil particle tracing techniques to identify gaps, where remotely sensed data can be integrated to widen the scope of currently existing methodologies.

2.2 Satellite remote sensing as an input for soil erosion models

The concepts and principles behind observing soil erosion over large areas are very well known and they are being continuously refined. The mecha-

nism behind the process is also clear and well defined. However, scientists are still not able to predict it very successfully mainly because of the resolution and spatial variability of erosion. In addition, the required high level of precision presents an obstacle, because erosion is an accumulative process and a small error at a particular location is accumulated into a large error on a catchment level. Therefore, the measurement technique should provide high resolution spatio-temporal data to characterize the process [Chappell et al., 2005]. Research on soil erosion is mainly focused on the use of soil erosion models in order to simulate and predict the event.

Methods and models for soil erosion assessment have been reviewed by Jetten et al. [2003] and later on Zhou et al. [2008]. The most widely applied ones include: Universal Soil Loss Equation (USLE) [Wischmeier and Smith, 1978], its revised version (RUSLE) [Renard et al., 1991, Prasannakumar et al., 2012], the Soil Erosion Model for Mediterranean regions (SEMMED) [de Jong et al., 1999], the Water Erosion Prediction Project (WEPP) [Flanagan and Laflen, 1997], Limburg Soil Erosion Model (LISEM) [Flanagan and Laflen, 1997, Jetten et al., 2003, Vrieling, 2006, Takken et al., 1999] as well as particle tracing techniques [Campbell et al., 1982, Chappell, 1999, Luleva et al., 2011, Sanchez-Cabeza et al., 2007, Syversen et al., 2001, Walling and Quine, 1990]. A main limitation of erosion models is the fact that they are applied on small scale for particular study area or catchment [Nigel and Rughooputh, 2010]. Extensive reviews of satellite-based sensors that have been used in soil studies are provided by Vrieling [2006] and later on by Mulder et al. [2011]. Another more recent review by Goldshleger et al. [2010] looks into the use of sensors with high spectral resolution for studying three specific degradation processes- soil salinity, soil crusting and post-fire mineral alterations. The authors suggest that there is potential in the use of these data for monitoring soil erosion factors.

Efforts have been put into studying land cover and land use change [Sobrino and Raissouni, 2000] focusing mainly on vegetation. When it comes to direct assessment of soil composition and degradation, however, the number of studies decreases. By using satellite imagery it is possible to observe only the surface soil characteristics and only when the signal is not masked by the vegetation cover [Vrieling, 2006]. The most commonly used remotely sensed data in soil erosion modeling come from Landsat

TM imagery. Availability and low cost of the scenes allow long term monitoring of particular areas. The main benefit of Landsat TM sensor is the multi-temporal aspect [de Jong et al., 1999], although the low spatial and spectral resolution of the scenes present a limitation. Parameters associated with soil erosion, estimated from imagery, include assessments of vegetation cover, calculation of vegetation indices, changes in topography, and outlining of bare ground Alatorre and Begueria [2009]. However, often bare ground is interpreted as degraded areas which is not necessarily the case. In addition, ground survey should always be done when interpreting vegetation cover.

It is important to note that the information provided by remote sensing is limited to the surface characteristics, although some statistical relationships are established between the surface and depth properties [Vrieling, 2006]. Monitoring visible signs of degradation such as sheet, rills or gullys as well as physical deteriorations such as crusting, hard setting and compaction, total erosion can be estimated over time [Boardman, 2006, Omuto and Shrestha, 2007].

Table 2.1 gives an overview of the various studies that used remote sensing data to estimate erosion related parameters or erosion itself.

Identification and mapping erosion features is performed by automated or supervised extraction of digital information based on spectral and/or structural pattern recognition [Alatorre and Begueria, 2009]. Classifiers based on statistical probability functions are commonly used to allocate ground pixels to a given surface type. Based on the composition of vegetation abundance and the identification of soil degradation features, linear mixture modeling has shown useful to map land degradation [Metternicht and Fermont, 1998].

Models and techniques, used to study soil related processes, provide spatial coverage but they do not show reality, only a simulation. The measurements are point-based, apart from a few examples of erosion feature mapping [Takken et al., 1999] and therefore there is a clear need for developing new methods that integrate the spatial extent of the event, the development of the process over time, and the factors affecting soil behavior.

2.3 Soil erosion parameters

2.3.1 Vegetation related erosion parameters

Vegetation cover has been widely studied with remote sensing [Shoshany, 2000], due to its distinct signature in the visible and near-infrared part of the electromagnetic spectrum. The most commonly used imagery is provided by Landsat TM and SPOT HRV, although limited number of studies attempted to implement airborne hyperspectral remote sensing from HyMap [Asner and Heidebrecht, 2003, Shrestha et al., 2005, de Jong and Jetten, 2007]. Vrieling [2006] provides an extensive review on the different satellite sensors used for detection of vegetation in soil erosion.

The bulk of research has focused on estimating Normalized Difference Vegetation Index (NDVI), Leaf Area Index (LAI) and Land Surface Temperature (LST) from satellite imagery. These are used as indicators for spatial and temporal changes in soil fertility [Julien and Sobrino, 2009, Nicholson and Farrar, 1994, Park et al., 2004]. In their study, Troufleau and Sogaard [1998] used LST and NDVI to derive soil surface moisture status while Unganai and Kogan [1998] used standardized difference of NDVI and LST to estimate drought-prone areas in Southern Africa. In addition, Park et al. [2004] used vegetation indices to estimate the impacts of hydrologic properties. They showed that values for NDVI and LST are related to soil runoff potential. Considering that soil is classified in hydrologic soil groups, based on runoff potential and soil physical conditions, it is suggested that physical degradation can influence LST and NDVI [Omuto and Shrestha, 2007, Park et al., 2004].

2.3.2 Topography

Slope is an important controlling factor for development and formation of soil erosion. Some of the best transport equations are based on stream power, which is the product of slope and discharge [Hessel and Jetten, 2007]. Since discharge itself is also determined by slope, the relation between erosion and slope is a power function and therefore it is very sensitive. In addition, the accuracy of a DEM is very important. Since courser DEMS often generate lower slopes than high resolution DEMS this will influence greatly the soil loss estimation.

As stated by Smith and Clark [2005], remote sensing provides the most effective way of developing Digital Elevation and Terrain models (DEM, DTM). The main sources of such data have been reported to be ASTER and Landsat TM [Thurmond et al., 2006].

The resolution of the produced DEMs plays a crucial role. LiDAR cloud point data provide means for more accurate building of DEMs, however this usually requires great amount of time, effort and resources [Liu, 2008], limiting their use.

2.3.3 Soil Moisture

Soil moisture content influences soil infiltration, which determines soil runoff. Hence, it is also considered as an indirect indicator of erosion. Methods applied for determining soil moisture content cannot often be extrapolated spatially due to variation over time. On the soil surface, moisture content influences the process of exchange of heat between land surface and atmosphere [Owe et al., 2001], as part of the environmental water cycle. Research focuses on potential use of infrared spectra for estimating surface soil moisture. It is known to affect spectrum shape in the visible, near infrared (VNIR) and shortwave infrared (SWIR) spectral range (350 nm and 2500 nm) [Doerr et al., 2000, Haubrock et al., 2008], where increasing moisture content leads to decreasing reflectance [Baumgardner et al., 1985, Lobell and Asner, 2002, Weidong et al., 2002]. Estimations from optical measurements in the VNIR and SWIR are considered increasingly important, not only for improving existing hydrological models at different scales [Doerr et al., 2000]but also for estimation of ground cover properties.

The overtone and combination absorption bands of molecular water around 900 nm, 1400 nm and 1900 nm are indicative regions for soil moisture variability [Haubrock et al., 2008, Weidong et al., 2002]. Soil moisture influences background reflectance and therefore affects quantification of soil parameters [Haubrock et al., 2008]. For instance, Iron oxides, soil organic matter and Phosphorus prediction from VNIR and SWIR have been tested by Bogrekci and Lee [2006] and Galvao and Vitorello [1998], who developed calibration models for estimation of these parameters using specific bands as a function of moisture.

Problems related to estimation of surface soil moisture from spectra, are mainly related to validation of the results. A number of moisture indices have been developed, including Modified Temperature- Vegetation Dryness Index (MTVDI) [Kimura, 2007], Normalized Difference Water Index (NDWI) [Dasgupta et al., 2007], Normalized Soil Moisture Index (NSMI) [Haubrock et al., 2008]. The correlation coefficients between the certain bands and the actual moisture content, however, have not been shown to be higher than 0.71 [Haubrock et al., 2008].

MTVDI [Kimura, 2007], for instance, can be calculated from satellite-derived surface temperature, and aerodynamic minimum and maximum surface temperatures estimated from meteorological data. The main purpose of this index was to help identifying wet-edge index, by combining the MTDVI with the commonly used NDVI. The authors, however, reported lack of sufficient data for drawing strong conclusions. NDWI takes into account the bands at 860 nm and 1240 nm [Dasgupta et al., 2007], however the study acknowledged uncertainties up to 66% associated with the index. The most recent one reported in the literature was introduced by Haubrock et al. [2008] (NSMI). From a systematic study over the whole spectral range from 350–2500 nm, the NSMI based on the reflectance at 1800 nm and 2119 nm has been determined to be suitable quantifier of water content for the surface. The authors claim that NSMI can be seen as a generally applicable parameter, which can be used without any a priori knowledge about the target. The index should be tested for its applicability from remote sensing data, where resolution and atmospheric effect complicate spectral measurements.

In arid regions, surface soil moisture is a dynamic variable at a relatively low level, making optical remote sensing useful for assessment of degradation. In such regions, moisture indices have great potential for rapid and efficient surface soil moisture estimations [Famiglietti et al., 1999, Khawlie et al., 2002, Zribi et al., 2005, 2003].

Table 2.1: Key soil parameters studied with remote sensing

Parameters	Sensors/Platforms	Cited Literature
Vegetation related parameters:	Landsat TM, NOAA AVHRR, Spot HRV, ERS SAR, RADARSAT	Reviewed in Shoshany [2000], Mulder et al. [2011]
-NDVI and LST		[Nicholson and Farrar, 1994, de Jong et al., 1999, Khawlie et al., 2002, Asner and Heidebrecht, 2003, Park et al., 2004, Shrestha et al., 2005, 2004, Sharma, 2010]
-Active Fires	Landsat TM, HyMap* Radarsat SAR	
-Land Cover and Ecology	AVIRIS*, Landsat TM, Spot HRV, Hyperion*	[de Jong et al., 1999, Khawlie et al., 2002, Asner and Heidebrecht, 2003]
Hydrological Variables -Surface Soil Moisture -Rainfall and cloud cover	SPOT, Landsat TM, ASTER, Ikonos, Quickbird Laboratory spectra acquired with ASD spectrometers, NOAA AVHRR- thermal bands, MODIS, SAR	Reviewed in King et al. [2005] [Famiglietti et al., 1999, Zribi et al., 2005, 2003, Dasgupta et al., 2007, Kimura, 2007, Haubrock et al., 2008]
Topography: Slope and Morphology	ASTER, Landsat TM, LiDAR	[Betts and DeRose, 1999, de Jong et al., 1999, Evans, 2002, Hessel and Jetten, 2007]
Soil Chemical and Physical Properties -Chemical Composition and Crusting -Roughness, Texture	Laboratory spectra acquired with ASD spectrometers Laboratory spectra acquired with ASD spectrometers SAR, Laboratory spectra acquired with ASD spectrometers. Suggestions* for using CHRIS, MISR, Proba	[Baumgardner et al., 1985] [Ben-Dor, 2002, Ben-Dor et al., 2003, Shepherd and Walsh, 2002, Udelhoven et al., 2003, Goldshleger et al., 2012, Casa et al., 2013] [Anderson and Kuhn, 2008, Croft et al., 2009, Moran et al., 2002]
Particle tracers	ASD Spectrometer	[Luleva et al., 2011, Schmid et al., 2012]

2.4 Integration of high spectral resolution remote sensing data in studies on soils

In Section 2.3, it was shown which satellite remote sensing data can be used as an input for soil erosion modeling. The spatial extent of these data has been explored to some degree, however the spectral properties of these images have been somewhat neglected. Most soil erosion studies have used only the information in the visible and near-infrared wavelengths of the electromagnetic spectrum, although research have already established methods that can aid the determination of soil erosion parameters. This section will look into established methods for high resolution image analysis that can potentially be integrated in soil erosion research.

Literature covers the use of spectral data in identifying organic matter, moisture content, soil chemistry and roughness either directly [Baumgardner et al., 1985, Ben-Dor et al., 2003, Shepherd and Walsh, 2006], or indirectly through analyzing and relating factors [King et al., 2005]. The aim of most laboratory based studies is to establish methodologies that can be applied on remotely sensed imagery to extrapolate results in the spatial dimension. The focus is on detecting changes in soil structure, which determine the impact of degradation and regenerative processes of soil, indicating soil erosion [Chappell et al., 2005]. Research efforts have been put into successfully linking soil erosion to particular soil types, where studies from the 1960's were first used [Holden, 1968]. Laboratory analysis of soil spectra have also been conducted, to estimate chemical constituents and predicting crust formation [Ben-Dor et al., 2003, Udelhoven et al., 2003]. Not much has been done in terms of scaling these to image data.

Silt and silt loam soils have a low to medium clay content (10-20 %), hence they are weak because the structure easily brakes down,making them highly susceptible to erosion and soil crusting [Le Bissonnais et al., 2005]. Soil crust decreases infiltration and causes runoff, which in turn washes off nutrients and important chemical components of the soil at the surface [Eghbal et al., 1996].

The challenge is to determine a method that predicts soil surface chemical properties using remote sensing techniques and to investigate ways

of deriving sub-surface soil spectral information. An attempt was recently made by Ben-Dor et al. [2008], introducing an extension to an ASD spectrometer, specifically designed for sub-surface spectral measurements. The authors demonstrated the application of the technique on four different soil profiles. Although the method was not tested on independent locations, it provides the bases for future robust soil mapping. Others refer to more conventional methods of implementing geophysical measurements using gamma-ray spectrometers [Tyler, 2008].

In order to implement the use of remotely sensed data for quantifying soil chemical properties, a method to separate noise caused by different atmospheric and environmental factors from actual signal, should be established. However, the transition from laboratory scale analysis through filed measurements to satellite imagery presents a challenge. As it has been pointed out by Vrieling [2006] "due to the complexity of erosion processes, regional differences, and scale dependency, it cannot be expected that a standardized operational erosion assessment system using satellite data will develop in the near future".

2.4.1 Chemical Properties of Soils

It has been established that soil physical degradation is a relatively slow process [Morgan, 2005]. It begins with structural deterioration culminating into soil loss through erosion after many years [Jones et al., 2003]. Visible signs in the field such as rills, gullies or sediment deposits are manifestations of advanced stage of degradation. To detect early warning signs, it is important to study soil properties sensitive to the degradation.

Spectral reflectance is a property of soil that integrates many functional processes influencing physical conditions [Ben-Dor et al., 2003, Shepherd and Walsh, 2006]. It is sensitive to soil constituents such as Iron Oxide, Carbon content and Calcium Carbonate that influence aggregation [Baumgardner et al., 1985, West et al., 2004] and soil crust formation. Furthermore, large-area sampling for spectral reflectance is more effective compared to conventional sampling methods for laboratory analysis [Janik et al., 1998, Shepherd and Walsh, 2006].

Some efforts have been put into studying soil properties from spectra. As stated by Udelhoven et al. [2003], soil parameters are neither static nor

homogeneous in space and time. Costs of analytical procedures are often a limiting factor when spatial soil variability in large-scale is addressed. Reflectance spectra have been used extensively to determine variation in the Earth's surface composition [van der Meer, 2004].

Soil properties derived from spectra have been studied long before the 1980's. Soil research has focused on VNIR and SWIR regions of the spectrum [Baumgardner et al., 1985] and the trend has been followed to date, with some relationships established from data in the thermal and microwave regions [Barnes et al., 2003, Yitagesu et al., 2011]. The basic physical and chemical soil properties show high correlation with derivative reflectance values within the visible and short-wave infrared wavelengths [Shepherd and Walsh, 2006].

Subtle differences in the spectral shape can serve as a valuable base for identifying soil properties mainly due to the fact that the soil spectra forms as a result of the overlap between absorption features of many organic and inorganic compounds [Shepherd and Walsh, 2006]. According to Ben-Dor et al. [2003], changes in spectral response occur due to changes in soil albedo and soil mineralogy, where the former is strictly related to the physical soil properties, while the latter is strictly related to the chemical. Soil albedo is strongly influenced by soil color, organic matter, moisture content and iron content [Post et al., 2000].

Literature covers extensively in-situ laboratory procedures for estimating and predicting soil properties. These procedures, however, are rarely applicable to satellite imagery. As identified by Ben-Dor [2002], the main limitations are that only the top few centimeters can be studied and vegetation masks the response from the soil surface.

Recent efforts include aerial photographs and satellite images of bare soil and related soil erosion parameters [Schmid et al., 2012]. Others estimate Organic Matter and Phosphorus levels, however, as pointed out by Lopez-Granados et al. [2005], these approaches were limited to linear regression with brightness values from the blue, green and near infrared bands. Chabrillat et al. [2002], suggests an improvement to these methods by stating that unlike multispectral imagery, hyperspectral remote sensing with its continuous spectrum for each pixel, enables the spectral identification of minerals, rocks, or soils at image level [Ben-Dor, 2002, Chabrillat et al., 2002].

2.4.2 Chemical Soil Particle Tracing

As it was discussed in the previous section, data acquired with field and laboratory spectrometers have been widely applied in studies on soils in order to examine the soil chemical properties. These data and the corresponding analytical techniques, however, have not been yet integrated in studies of soil erosion, most likely because of the limited reference to soil chemical composition. One of the few lines of research that can potentially benefit from these data is the concept of chemical soil particle tracing for monitoring soil movement due to erosion.

The Cesium-137 isotope (^{137}Cs) is the most widely used chemical soil particle tracer. Soil particles move according to their size, under the influence of wind, water or gravity [Morgan, 2005]. Using tracers for soil erosion originated in China, shortly after the Chernobyl incident in the late 1980s. The use of ^{137}Cs in soil erosion modeling has been identified as a very effective technique in assessing both spatial patterns and rates of soil redistribution in the landscape [Li et al., 2000].

Distribution of ^{137}Cs in soil profiles at undisturbed sites shows an exponential decrease with depth while ploughed soils show uniform mixing of ^{137}Cs in the ploughed layer [Belivermis, 2012]. Although biological and chemical processes can move some amount of ^{137}Cs , the dominant factors affecting its movement within landscapes, are the same physical processes that affect the movement of soil particles to which it is attached [Warren et al., 2005]. As suggested by Chappell [1999], ^{137}Cs offers the greatest potential for measuring net soil flux in semi-arid environments where soil flux monitoring is limited due to considerable spatial and temporal variability of the controlling factors.

There is a number of assumptions behind the models that use ^{137}Cs distribution. Chappell [1999] explains in more detail the problems related to them. First, it is assumed that there is a spatially uniform distribution of ^{137}Cs within a climatologically uniform area. Secondly, the fixation of ^{137}Cs to the clay size fraction of different minerals is considered immediate and permanent, and the redistribution of soil corresponds to the movement of ^{137}Cs . The reasoning behind this is that Cs is rapidly adsorbed by clay particles in the surface soil and it is essentially none-exchangeable once adsorbed to the clay surfaces. The extent of adsorption and fixation of

^{137}Cs to clay particles depends largely on the clay type. Generally, ^{137}Cs is adsorbed irreversibly by micas and hydrobiotite, while montmorillonite, kaolinite and vermiculite hold ^{137}Cs much less strongly

Models developed for calculation of redistribution rates of soil have been derived from ^{137}Cs measurements and summarized by Li et al. [2000]. Although ^{137}Cs isotope has been extensively used to model soil redistribution, little has been reported on the integration of spectral data. Limited number of studies have attempted the use of remote sensing to map ^{137}Cs net soil flux with SPOT imagery, but the results were poor [Chappell, 1998].

The limited use of spectral data in monitoring ^{137}Cs distribution is mainly related to the small chemical difference between the isotopes of Cs, which is associated with reaction kinetics. Therefore, all isotopes behave in the exact same way and it is very difficult to determine each of them with any techniques different from laboratory based mass spectrometry. Moreover, the relatively low concentrations of the chemical prevent the formation of a distinct absorption. Anything below 3300 Bq of activity (or 1 nano gram per gram of soil) is already under the detection limit of the main analytical instruments.

Considering that Cs is an alkaline metal, its physical and chemical behavior is similar to those of Potassium (K) and Sodium (Na), extensively studied by spectral analyses. Luleva et al. [2011] suggest that K can be used as a potential alternative tracer that could be observed using soil spectral response, allowing rapid spatial mapping. Table 2.2 outlines the differences and similarities between the two elements, as well as the advantages and limitations of each one in their use as particle tracer. Introducing K is a soil particle tracer can introduce a number of advantages to erosion studies. The element has potential to be measured using spectral measurements which can increase the spatial representation. It has been shown that K concentrations can be quantified measured using spectral means [Luleva et al., 2011], however there is a need to test whether tracing patterns can be established spatially using spectral data.

2.5 Conclusions

Over the recent years, the problem of soil erosion has received much broader acknowledgment in literature. Time and effort associated with

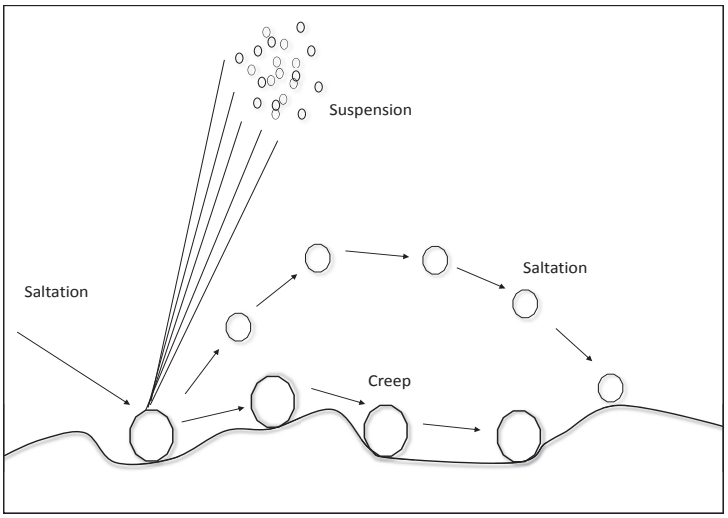

Figure 2.1: Simplified diagram of soil particle transport under the influence of wind by creep, saltation and suspension. Based on Lyles [1988]

field sampling and analytical techniques due to the large scale of the event, however, still present a major limiting factor. Remote sensing provides some solutions to spatial data acquisition; however the potential of these data is not yet fully explored. General conclusion is that change detection of vegetation cover alongside with change in land use are soil erosion parameters most widely studied with remote sensing.

Landsat TM, ASTER and SPOT HRV are most frequently used, however it can be argued that the availability and price of the science determine their use, rather than sensor capabilities. There is a clear gap in the use of remotely sensed data with high spectral resolution. Chemical soil particle tracing of soil movement due to erosion is a line of research that can benefit from the development of a methodology that combines the spatial and the high spectral properties of remotely sensed data. The two upcoming international missions —Enmap, scheduled to launch in year 2013 and HyspIRI, expected to launch between year 2013 and 2016— promise to provide satellite hyperspectral data that would allow detailed and repetitive analysis of surface parameters.

Table 2.2: Differences and similarities between ^{137}Cs isotope and K, for soil particle tracing

	^{137}Cs	K
Introduction to the environment	Introduced in the environment due to the Chernobyl incident in the late 1980s	Naturally occurring, but also introduced to the environment as an agricultural fertilizer.
Distribution	The even distribution of Cs is always assumed and therefore it has been a cause of debate, although some studies have provided supporting arguments based on climatological factors and study area locations [Chappell, 1999]	Although K fertilizer should be applied evenly to all agricultural fields in order to maintain optimal crop production [Jalali, 2007], the distribution of the element should be measured in order to account for natural variation.
Displacement	Radioactive Cs is assumed to move only due to erosion as it binds strongly to the soil particles.	K can be moved due to uptake by plants or by leaching.
Cost of analytical measurement	High	Low
Previously used as a tracer	Yes	No*
Detection using spectral response	No	Yes

Spectrally active chemical elements as potential soil particle tracers

3

Abstract

In chapter 2, various applications of remotely sensed data in soil erosion studies were reviewed. The use of the information derived from the shortwave infrared wavelengths of the electromagnetic spectrum was identified as a major gap in current research [Luleva et al., 2012]. A way to integrate these data in studies of soil erosion is to detect chemical composition of the soil and apply the method for chemical soil particle tracing. To identify a potential soil particle tracer that has similar physical and chemical properties as the commonly used radioactive isotope Ceasium-137 (^{137}Cs), and at the same time has a spectral signature, a number of abundant in the environment chemical elements were tested. In this chapter, wavelength ranges that statistically predict and quantify soluble fractions of chemical elements, from near infrared and shortwave infrared spectroscopy are identified. Partial least squares regression (PLSR) was used to develop prediction models for naturally occurring Calcium (Ca), Magnesium (Mg), Potassium (K), Sodium (Na), Iron (Fe), and acidity (pH) in silt loam soil samples. Significant wavelength ranges were determined by establishing direct and indirect relationships between soil spectra and soluble fractions of these elements. [1]

[1]This chapter is based on: Luleva, M, van der Werff, H, van der Meer, F., Jetten, V. , Predicting Water Soluble Fractions of Chemical Elements in Silt Loam Soils Using ASD-derived Reflectance Spectroscopy, Pedosphere (submitted)

3.1 Introduction

The chemical composition of soils determines nutrient availability, plant growth and soil dynamics. Estimating the concentration of chemical elements in soils requires extensive sampling and laboratory testing, which is time consuming and expensive. In this chapter, infrared spectral data were used to develop statistical models that predict and quantify amounts of soluble fractions of soil chemical composition by identifying spectral subsets of spectral wavelength regions.

Reflectance spectra have been used for the last four decades to describe the Earth's surface composition [van der Meer, 2006]. Studies mostly looked at the visible, near-infrared (VNIR), and shortwave-infrared (SWIR) regions of the electro-magnetic spectrum. In the early 1980s, it was reported that soil moisture content, organic matter, soil texture and iron content influence the spectral response in VNIR and SWIR [Baumgardner et al., 1985]. A decade later, multivariate statistics were introduced to studies on chemical elements in soils [Palacios-Orueta and Ustin, 1998]. As stated by Stenberg et al. [2010], the influence of chemical bonds on reflectance is explained by broad molecular overtone and combination bands in the VNIR spectral region of three functional groups in minerals: SO^3 , CO^4 , and OH. The abundance of compounds is mainly determined by soil type and parent material. The effect of major soil constituents and chemical bonds in minerals on infrared spectra has been extensively reported in literature [Ben-Dor et al., 2003, Viscarra Rossel et al., 2006]. The resulting complex spectra have been found to present a challenge when assigning specific absorption features to individual chemical elements [Ali et al., 2010]. Soluble fractions of these elements determine chemical processes and concentrations available to plants. To gain insight, influence of inorganic chemicals on specific parts of the spectral response, attention has been paid on multivariate statistics [Ben-Dor and Banin, 1995, Shepherd and Walsh, 2002, Udelhoven et al., 2003].

Some efforts to relate soil spectra to chemical constituents have been directed towards spectral math using reference [Ben-Dor and Banin, 1995, Ben-Dor et al., 2003, Farifteh et al., 2007, Stenberg et al., 2010, Viscarra Rossel et al., 2006]. For example, multiple linear regression analysis was applied for identifying the presence of Nitrogen [Dalal and Henry, 1986],

Carbonates and organic matter [Ben-Dor and Banin, 1995, Gomez et al., 2008]. Multivariate adaptive regression splines were used for identification of Calcium, Magnesium and Organic Carbon [Shepherd and Walsh, 2002]. Unlike principal component analysis or multi linear regression, Partial Least Squares Regression (PLSR) handles correlated, many and noisy data. PLSR has been used to prevent correlation from being explained as meaningful information [Wold et al., 2001]. Specific to soil constituents, PLSR has been applied to Infrared spectra in the 400 to 2500 nm wavelength range for Nitrogen [Reeves III et al., 1999], Magnesium and Manganese [Janik et al., 1998] as well as inorganic Carbon and total Carbon [McCarty et al., 2002, Reeves III et al., 1999]. PLSR was also applied in several other studies [Lee and Ramsey, 2001, Udelhoven et al., 2003, Viscarra Rossel et al., 2006], showing its use for determination of soil nutrient status, soil development and soil degradation. Moreover, wavelength regions, that result from molecular overtones, have been defined for identifying and quantifying chemical elements in soil [Farifteh et al., 2007, Gomez et al., 2008, Lee and Ramsey, 2001, Udelhoven et al., 2003, Viscarra Rossel et al., 2010, Yitagesu et al., 2009]. The applied methods were based on direct and indirect relationships between compounds and soluble fractions.

However, there are two gaps in the studies listed in literature. Firstly, there is no conclusion on whether specific absorption features can be associated with soluble fractions of chemical elements in soils, either directly or indirectly. Secondly, a specific wavelength range associated with each element, covering a 50–70 nm range in VNIR or SWIR, has not been reported to date. Such a narrow range of wavelengths would be important for separating and defining regions associated with respective soluble fractions of elements in silt loam soils. Currently, overlap between constituents makes diffuse reflectance spectroscopy in VNIR and SWIR to be considered non-specific [Stenberg et al., 2010]. Direct or indirect relationships between soluble fractions of elements and infrared spectra aid differentiating. Identification of relevant spectral features in a PLSR calibration is important for several reasons. Firstly, it serves as a stepping stone to understanding physical basis, and secondly, the selection of only important features can decrease the risk of over-fitting, allowing the obtainment of more robust models with fewer parameters.

The aim of this chapter is to identify specific wavelength ranges that

statistically predict and quantify, Calcium (Ca), Magnesium (Mg), Potassium (K), Sodium (Na), Iron (Fe) and acidity (pH) in silt loam soils by applying PLSR techniques on spectral features within the VNIR and SWIR wavelength regions. The current study focuses on silt loam soils in Southeast Spain, outlining relationships of the elements with spectra acquired for this soil textural type.

3.2 Methodology

3.2.1 Sampling and laboratory data collection

The study area is located within the Guadalentin Basin of Murcia Province, Spain. This area was selected as part of the European Union DESIRE Project, on desertification and soil erosion [Alterra, 2007]. The area is part of an alluvial plain formed by the Guadalentin River. The soil material consists of sediments and salt-rich transported material from nearby slopes [Hernandez Bastida et al., 2004]. A total of 60 surface soil samples were collected using a sampling spade, following a random sampling strategy. The common attribute of the soils is a silt loam texture with 20–25 % clay and more than 50% silt. Although similar in texture, the samples belong to three different soil types as defined by the FAO [2006]. Different soil types were sampled to ensure variation in soil chemical composition. The sampled soils include Calcisols, soils with substantial accumulation of lime (A and D); Regosols, well drained mineral soils which lack of horizon development or exhibit minimal A and B horizon development (B); and Fluvisols with distinct topsoil horizon (C) [FAO, 1998].

Each soil sample was air-dried for 48 hours at room temperature. The soil material was sieved through a 2 mm sieve. To determine chemical concentrations, we followed procedures for water extractable soils [Van Reeuwijk, 2002] in 1:20 dilutions with demineralized water. Inductively Coupled Plasma-Optical Emission Spectroscopy (ICP-OES) was used with a detection limit of 0.01 ppm to estimate the chemical concentrations of soluble Ca, Mg, K, Na, and Fe. Acidity (pH) was determined using a standard hand held Horiba pH Probe with a glass electrode, in a pH range of 0–14 following Van Reeuwijk [2002]. Spectra were acquired using an Analytical Spectral Devise (ASD) Fieldspec Pro Spectrometer with a 450–

2500 nm wavelength range at 3–10 nm resolution and a contact probe as fore-optic. Averages of 25 spectral measurements per sample, collected by moving the probe, were used in the modeling. The internal average of the instrument was kept as default at 10 iterations.

3.2.2 Partial Least Squares Regression Models

PLSR models were built using Unscrambler X software version 10.0.1 [CAMO Software AS, 2010]. The produced prediction model is a set of equations (or PLSR factors) computed as linear combinations of spectral amplitudes, by using a regression coefficient (known as b-coefficient) for each wavelength position [Yitagesu et al., 2009]. The larger the values of these coefficients, the more important the wavelength is for the model [Gomez et al., 2008]. Considering the nature of the prediction models, possible autocorrelation between sampling points is neglected since it is handled by the software. This is automatically done by transforming the original variables into a set of orthogonal latent variables, which also results in noise reduction [Seiden et al., 1996].

Spectra were normalized by dividing the reflectance values for each sample by the maximum spectral value. This is to ensure a normal distribution of the data needed to avoid uncontrolled scale variation [Lai et al., 2007, Yitagesu et al., 2009]. The spectra were smoothed with a Savitzky Golay filter [Savitzky and Golay, 1964] in Unscrambler software. The filter was characterized by a second order polynomial fit and 7 smoothing data points, to remove spectral noise spikes while preserving chemical information, as suggested by Savitzky and Golay [1964] and Bogaert and D'Or [2002]. All samples were included in the prediction model development. The chemical elements Ca, Mg, K, Na, and Fe, as well as acidity, were used as input prediction variables. For each input variable, a set of latent variables (principal components) were selected, based on cross-validation, explained variance and correlation between attributes (loadings). The sum of the selected components explained a minimum of 85 % of the residual variance (first local maximum), to avoid over-fitting. High number of latent variables is known to lower the prediction error, however it introduces bias to the interpretations [Stevens et al., 2010]. The explained variance and loadings are used to assess the relevance of an individual component

to the overall model [Westad et al., 2003]. Loadings explain the importance of the variables, where the number of variables included in the models and their standard deviations influence the actual correlation structure [Westad et al., 2003]. PLSR regression coefficients (raw b-coefficients) were used for selecting specific wavelength ranges associated with each variable [Haaland and Thomas, 1988]. These were computed by Unscrabler software and their accuracy was assessed for 95 % confidence interval based on computation of t-values from Student t-distribution. The significance level was estimated and represented by comparison of t-values and their theoretical distribution resulting in computation of p-values. P-values lower than 0.05 (95 % confidence) were associated with significant wavelengths for prediction of the elements. T-values were calculated as a ratio between deviation from the mean and the standard error of the mean.

To assess each prediction model, a full cross validation, applying leave-one-out method, was performed. This validation method was preferred taking into account the limited number of samples [Stenberg et al., 2010, Viscarra Rossel et al., 2006, Yitagesu et al., 2009]. Root mean-square error (RMSE) of cross validation were used together with the loadings and b-coefficients [Gomez et al., 2008, Stenberg et al., 2010, Viscarra Rossel, 2008, Westad et al., 2003]. These were automatically calculated by the Unscrambler software in units same as the input data. The coefficients of determination for the identified wavelengths were compared to literature [Udelhoven et al., 2003, Viscarra Rossel et al., 2006], in terms of establishing whether the identified absorption features corresponded to already reported soil constituents or molecular overtones.

3.3 Results and Discussion

3.3.1 Sampling and laboratory data collection

The results obtained through laboratory analysis are summarized in Table 3.1 and 3.2, for all samples. All data are skewed, indicating the need for normalization prior to modelling. Table 3.1 contains description and expected concentrations per soil type to emphasize variation between and within samples (Table 3.1), based on FAO [2006]. It can be noted that the soils are characterized with high Ca levels, while Na is present in low quantities. The

Table 3.1: Soil characteristics [FAO, 2006] and mean concentrations per soil type. Each soil type contents 15 sampling units

Soil Type	Soil Texture	Parent Material	Processes and Characteristics	Mean measured concentrations at depth of 0–20cm (ppm)				
				Ca	Mg	Fe	K	Na
Calcisols	Sandy Loam	Alluvial, colluvial and aeolian deposits of weathering material	Water erosion	680.4	13.9	2.9	16.7	3.1
Regosols	Silt Loam	Unconsolidated, finely grained material	Water erosion; Deposition	623.1	10.8	2.5	15.2	2.4
Fluvisols	Sandy Loam	Alluvial and marine deposits	Water Erosion; Deposition	225.4	5.3	2.6	12.7	2.0

texture of all samples comprises of more than 50 % silt. Hence, variation in chemical composition is mainly determined by the difference in soil type. High Ca concentrations were found in soil samples that belong to Calcisols, as expected. The smallest variation in elements concentration is noted for Fluvisols (see Table 3.1), which is associated with formation of a salt crust at the surface (Table 3.1).

3.3.2 Partial Least Squares Regression

The results from each prediction model are summarized in Table 3.3. Root mean square error (RMSE) values indicate the quality of performance of the model. The wavelength ranges associated with the each property are

Table 3.2: Mean, minimum, maximum and standard deviation of soil property concentrations for the total of 60 samples, determined following a reference method for ICP-OES

Soil property	Mean	Min	Max	Std Dev.
pH	6.70	5.85	7.43	0.43
Ca(ppm)	580.68	21.58	2144.84	525.10
Mg(ppm)	11.60	2.07	43.85	9.33
K(ppm)	15.59	6.61	35.32	6.54
Na(ppm)	2.68	0.77	8.17	1.24
Fe(ppm)	2.79	1.52	5.73	0.94

listed with corresponding R^2 (Table 3.3). The highest correlation is noted for K and Ca. The values for significance (p values) of b-coefficients per element were used for selection of specific wavelength ranges and are shown in Table 3.3. RMSE values range between 0.80 ppm for Na to 3.73 ppm for K. Full record of all statistical parameters estimated during the cross validation per soil property is included in Figures 3.1- 3.6.

PLSR uses correlated variables and relates them to a set of output variables by projecting the data into a low dimensional space, defined by orthogonal latent vectors [Dayal and MacGregor, 1997]. The presence of exchangeable ions in soils that are high in clay content can influence the prediction of soluble fractions of elements [Gomez et al., 2008]. Moreover, as stated in Stevens et al. [2010], the use of spectral data derived from heterogeneous areas in terms of soil type, has been reported to diminish the predictive ability of VNIR-SWIR spectroscopy. Hence, the results of this study should not be extrapolated to not sampled soil types. To establish relationships between absorption and chemical elements for clay-rich soils, representative samples would need to be included in the PLSR analysis.

The specific wavelength ranges predicted for soluble fraction of Ca coincide with reports in literature on Calcium Carbonate overtone vibrations at 2333 nm [Baumgardner et al., 1985, Gomez et al., 2008, Shepherd and Walsh, 2006, Udelhoven et al., 2003]. This is expected since the concentrations of Ca in these soils are determined by the presence of lime. Figure 3.1 shows PLSR model performance for Ca. Three distinct clusters can be identified associated to the differences in concentration between soil types.

Table 3.3: Results of PLSR models: coefficients of determination, Root Mean Square Error (RMSE) of Cross Validation (leave-one-out) and wavelengths associated with individual chemical elements found in soils.

Soil property	RMSE of CV	Significant wavelength range	R-Square per band	Mean P values for B-coefficient per band range
Ca	3.270	2310–2379	0.904	0.007
Mg	3.570	1693–1722; 2350–2410	0.754; 0.829	0.030; 0.028
K	3.730	1628–1699; 2440–2480	0.883; 0.913	0.021; 0.01
Na	0.808	2025–2103	0.774	0.033
Fe	0.909	2225–2261	0.738	0.023
pH	2.360	1001–1096; 2334–2379	0.731; 0.885	0.021; 0.019

The b-coefficients, combined with coefficients of determination for Fe, indicate a specific wavelength range between 2225–2261 nm (Table 3.3). This wavelength range is associated with the presence of clay particles in soils, and the high coefficient values are likely caused by Fe-OH bonds [Herrmann et al., 2001]. The expected absorption feature near 1000 nm for Fe was not selected, which could be caused by low abundance of this element in the top soil at all sampling locations (Table 3.1 and 3.2). This is also the reason for the lowest R^2 values derived from the PLS model (R^2 =0.73). As shown on Figure 3.3, prediction values are underestimated by the model for soluble K, the model outlined absorption bands centred near 2470 nm with a R^2 of 0.91 and RMSE of cross validation of 3.73 (Table 3.3). Figure 3.3 shows the model performance, indicating the fit between regression lines for predicted and measured values. Literature does not report on influence of molecular overtones or certain chemical bonds in this region. However, investigation with different concentrations

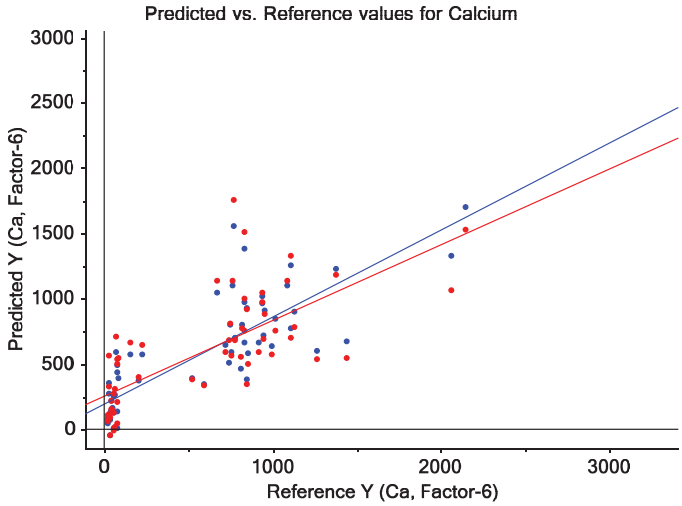

Figure 3.1: Cross validation for Calcium in all 60 samples, predicted versus reference values for soluble fractions of chemical elements against the full spectrum. Blue line: calibration line. Red line: validation line.

of these soluble fractions established the direct influence of the element on absorption [Luleva et al., 2011]. The wavelength range identified for Mg between 2350–2400 nm (Table 3.3) can be explained by the Mg–OH feature reported in literature [Clark et al., 1990, Herrmann et al., 2001]. The model performance, shown on Figure 3.4, indicates the suitability of the technique for the prediction of this element with R^2 values of 0.83 and RMSE of 3.57. PLSR models for Na, as seen in Table 3.3, produce R^2 of 0.77 for the significant wavelength range between 2025–2103 nm. The difference between regression lines that correspond to predicted and measured values (Figure 3.5) can be explained by the difference in soil salinity between the soil types. Wavelength regions associated with soil pH have been found to overlap with those corresponding to Ca, showing a R^2 of 0.89 for the wavelength range between 2334–2379 nm (Table 3.3). This can be explained by soil pH that is directly influenced by calcium carbonate contents, higher concentrations leading to a higher pH. This is also shown on Figure 3.1 and Figure 3.6, where the similar performance of

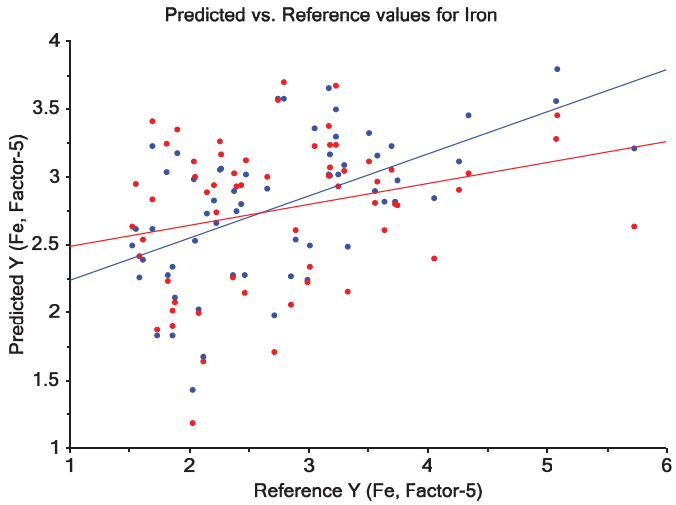

Figure 3.2: Cross validation for Iron in all 60 samples, predicted versus reference values for soluble fractions of chemical elements against the full spectrum. Blue line: calibration line. Red line: validation line.

the models indicated by the regression lines, can be seen.

Full cross validation following leave-one-out approach was found to be the most effective technique for model assessment based on the number of samples available for this study Viscarra Rossel et al. [2006], Viscarra Rossel [2008]. The cross validation results shown in Table 3.3 indicate that PLSR models can be used in prediction and quantification of soluble fractions of individual elements. Figure 3.1 shows that the models overestimate fractions of elements present in low concentrations (Na and Fe), while the predicted values for the remaining elements of interest (Ca, Mg, K) are lower than the measured. Based on the calculated b-coefficients, RSME and R^2 values, it can be stated that the identified spectral wavelength ranges are associated with the respective property of interest. Wavelengths are associated with certain properties, which cannot be observed from visual inspection of the spectra alone. This is especially the case of elements present in low quantities, such as Na and Fe.

PLSR uses correlated variables and relates them to a set of output

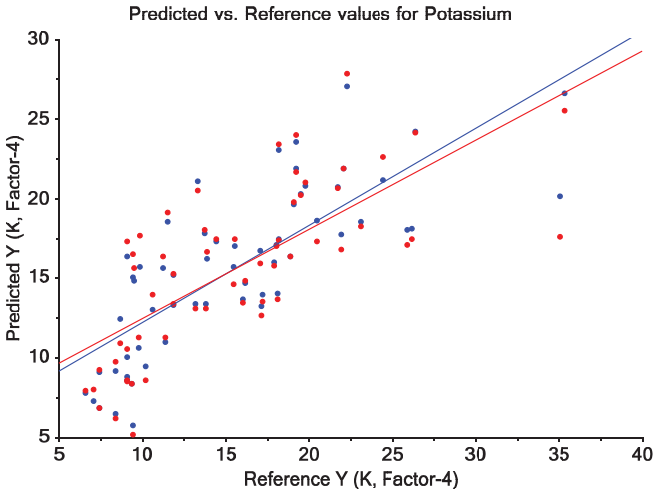

Figure 3.3: Cross validation for Potassium in all 60 samples, predicted versus reference values for soluble fractions of chemical elements against the full spectrum.Blue line: calibration line. Red line: validation line.

variables by projecting the data into a low dimensional space, defined by orthogonal latent vectors [Dayal and MacGregor, 1997]. The presence of exchangeable ions in soils that are high in clay content can influence the prediction of soluble fractions of elements [Gomez et al., 2008]. Moreover, as stated in Stevens et al. [2010], the use of spectral data derived from heterogeneous areas in terms of soil type, has been reported to diminish the predictive ability of VNIR-SWIR spectroscopy. Hence, the results of this study should not be extrapolated to not sampled soil types. To establish relationships between absorption and chemical elements for clay-rich soils, representative samples would need to be included in the PLSR analysis.

These results show the feasibility of the proposed methodology for identifying soluble fractions of soil chemical elements in silt loam soils using infrared spectroscopy. The influence of each element on specific wavelength ranges can be explained by the molecular overtones of the compounds present in the soil samples. The prediction models associated with soluble fractions of various concentrations (Ca, Mg and K) gave overall

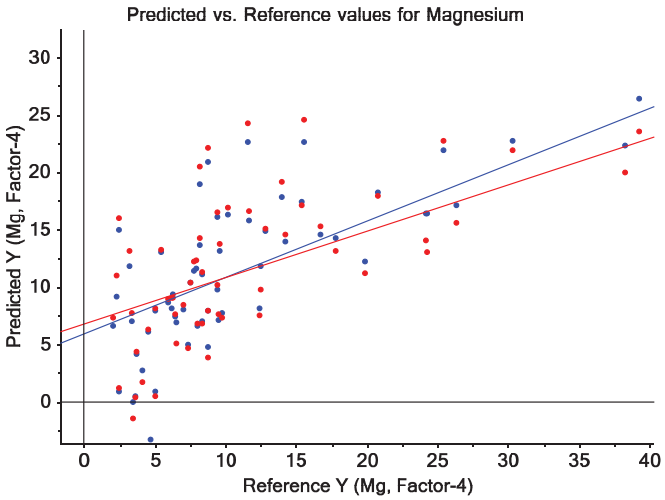

Figure 3.4: Cross validation for Magnesium in all 60 samples, predicted versus reference values for soluble fractions of chemical elements against the full spectrum.Blue line: calibration line. Red line: validation line.

higher R^2 and lower RMSE values. This suggests that the methodology can potentially be applied to other soil types in order to develop a more generalized soil model for prediction of soluble fractions of individual chemical elements.

3.4 Conclusions

This chapter reports on an approach for identification of soluble fractions of Calcium, Magnesium, Potassium, Sodium, and Iron as well as acidity (pH) through laboratory spectral response. The highest coefficients of determination were reported for Calcium, Magnesium and Potassium. Elements such as iron and sodium were strongly correlated only to specific wavelength ranges with limited influence over the full wavelength range. The chapter presents an attempt to identify the influence of individual soluble fractions of chemical elements in silt loam soils on infrared spectra.

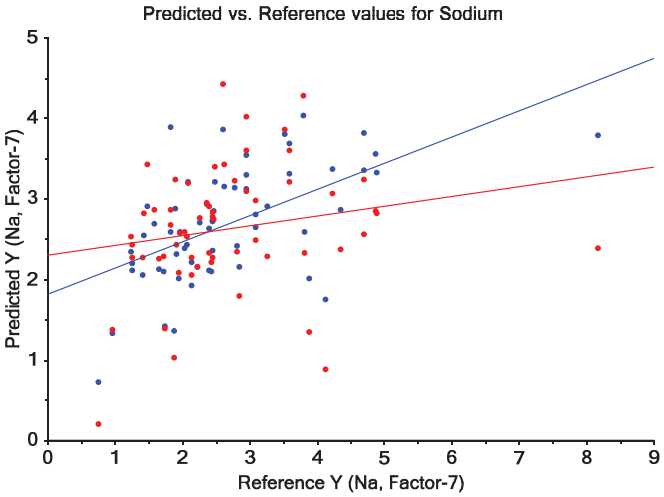

Figure 3.5: Cross validation for Sodium in all 60 samples, predicted versus reference values for soluble fractions of chemical elements against the full spectrum.Blue line: calibration line. Red line: validation line.

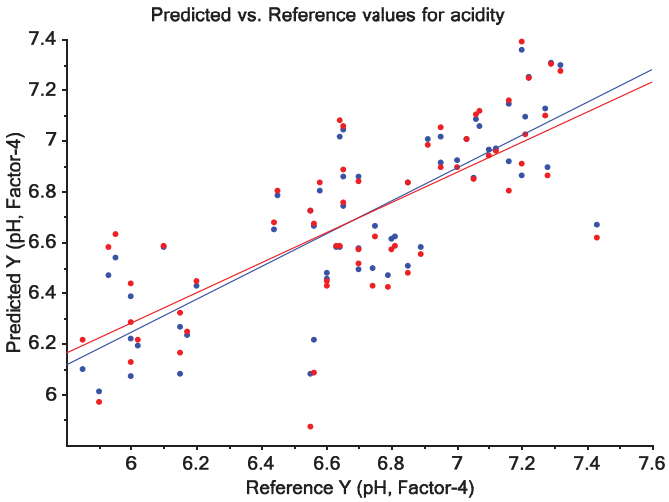

Figure 3.6: Cross validation for pH in all 60 samples, predicted versus reference values for soluble fractions of chemical elements against the full spectrum.Blue line: calibration line. Red line: validation line.

4 Spectral sensitivity of Potassium as a proxy for soil particle movement

Abstract

In Chapter 3, the feasibility of using Partial Least Squares Regression for identifying soluble fractions of soil chemical elements in silt loam soils using infrared spectroscopy was tested. By outlining wavelength ranges where the change in reflectance is associated with change in the concentration of the element, Potassium was identified as having the closest to ^{137}Cs properties that can be predicted from infrared spectra.

This chapter presents a laboratory based study on the use of Potassium (K) as a potential replacement of Cesium (Cs) in soil particle tracing. The element has similar electrical, chemical and physical properties. In order to test this, heavy clay, clay loam, loam, silty loam and sandy loam and fine sand soils were sampled for the study. Sensitivity analyses were performed on soil chemical properties and spectra to identify the wavelength range related to K concentration. Different concentrations of K fertilizer were added to soils with varying texture in order to establish spectral characteristics of the absorption feature associated with K. [1]

[1]This chapter is based on: Luleva, M.I., van der Werff, H., Jetten, V., van der Meer, F., (2011). Can Infrared Spectroscopy Be Used to Measure Change in Potassium Nitrate Concentration as a Proxy for Soil Particle Movement?, Sensors (11), 4188–4206.

4.1 Introduction

Land degradation is a relatively slow process [Omuto and Shrestha, 2007]. Physical and chemical degradation, under the influence of wind and water, leads to loss of nutrients, soil instability, subsoil exposure and desertification. Well-known erosion features such as rills and gullies are manifestations of an already advanced degradation [Boardman et al., 2009, Boardman and Evans, 2006]. To detect early warning signs, however, it is important to monitor soil properties sensitive to degradation, such as chemical composition, runoff and sediment yield. Natural variation in soil chemical composition is associated with bedrock geology and soil type, although agricultural practices and overgrazing also influence surface soil chemistry and quality [Lemenih et al., 2005, Nael et al., 2004, Zhang et al., 2006]. Hence, studies on soil erosion have focused on using soil chemical composition mainly for particle tracing.

Various chemical soil particle tracers have been used to obtain spatially distributed data for soil erosion [Zhang et al., 2006] and used to identify suspended sediment [Onda et al., 2007]. Commonly used soil particle tracers are the Cesium 137 isotope (^{137}Cs) [Andersen et al., 2000, Chappell, 1999, Collins et al., 2001, Guimaraes et al., 2003, Porto et al., 2001, Sanchez-Cabeza et al., 2007, Timothy et al., 1997], Lead (^{210}Pb) and Beryllium (^{7}Be) [Mabit et al., 2008, Wallbrink and Murray, 1993], and Rare Earth Oxides [Polyakov and Nearing, 2004, Zhang et al., 2006]. Although ^{137}Cs is considered the primary chemical tracer for detection of soil particle movement [deGraffenried Jr and Shepherd, 2009, Estrany et al., 2010, Meusburger et al., 2010, Rodway-Dyer and Walling, 2010, Xiaojun et al., 2010], one has to assume a homogeneous distribution of ^{137}Cs fall out limited to the Northern hemisphere, and that all particle movements are a result of soil erosion [Campbell et al., 1982, Chappell, 1999, Walling and Quine, 1990]. Cost of soil sampling and analysis and the limited half-life of the element are the main limitations to extrapolate these methods to cover large areas [Boardman, 2006].

Soil properties have been studied with infrared spectroscopy since the 1980's, using visible, near-infrared and shortwave infrared wavelength region (400–2500 nm). Spectral reflectance is determined by both physical and chemical characteristics of soils [Baumgardner et al., 1985, Ben-Dor

et al., 2003, Shepherd and Walsh, 2002]. Soil spectral features are mainly a result of overtone absorption and combination of bond vibrations in molecules of three functional groups in minerals: OH, SO_4 and CO_3, [Ben-Dor and Banin, 1995, Hunt and Salisbury, 1970]. Organic matter is also found to have influence on spectral response since it holds most positively charged nutrients in soils. However, due to the relatively weak attraction between K and this soil constituent, K absorption is not found to be affected [Schulte and Kelling, 1998]. Results obtained using regression models for detection of soluble fractions of Potassium, only have moderate accuracy and vary according to study sites [Stenberg et al., 2010]. Sampling large areas for determination of soil properties using spectral reflectance is relatively cheap and fast, compared to traditional field and laboratory techniques [Shepherd and Walsh, 2002]. To date, infrared spectra have not been put in use when studying soil erosion with ^{137}Cs . Low concentrations of the isotope in nature makes the identification of the element through spectral means impossible, considering the capabilities of available spectrometers [Stevens et al., 2010].

The element Potassium (K) shares electrical, chemical and physical properties with Cs, both being members of the Group I alkali metals [Andrello and Appoloni, 2004, Relman, 1956]. Both elements have similar biological and chemical behaviour, where the difference is only in reactivity [Relman, 1956], but it has not been tested as a particle tracer. Potassium occurs naturally in the environment, but it is also used on agricultural lands as a fertilizer. The amount of K fertilizer (in a form of K_2O or K–P–N) typically applied by farmers, according to EU Directives: Nitrates Directive (91/676/EC) and Water Framework Directive (2000/60/EC), as well as EU commission recommendations, is 183 kg of solid fertilizer per hectare or in dissolved solution 1.83 g of solid fertilizer per 10 ml of water for sandy silt soils, although there is no specific policy adopted for the EU region. In practice, the range of totals of applied amount may reach 5–8 g/10ml according to soil type and water conditions. In soils, K is mainly present as part of preliminary soil minerals (unavailable), in clay minerals and fine silt (slowly available), and in a water-soluble form (readily available) [Garrett, 1996, Peterburgsky and Yanishevsky, 1961, Sharpley, 1989]. When K fertilizers are applied, they dissolve and K becomes part of the soil-water solution [Garrett, 1996]. Fertilizers are applied prior to

harvesting. To maintain optimal crop production, uniform application of the fertilizer is the most desired practice [Jalali, 2007]. Potassium remains immobile as long as soils are not chopped or plowed. The mobility and distribution of this element has also been discussed by Askegaard and Eriksen [2000], Jalali and Rowell [2009, 2003]. These authors explain the behaviour of the element determined by soil physical properties such as texture, porosity, organic matter and water holding capacity. They also state that due to low cation exchange capacity and organic matter content, sandy soils are more likely to experience K leaching than clays. Furthermore, soil texture combined with chemical composition (presence of Calcium, Sodium or Gypsum, of both soil and water used for irrigation) determine the rates of leaching of K [Jalali and Rowell, 2003, Kolahchi and Jalali, 2007]. Establishing the behaviour of K in soils can prevent under or overestimating of predicted sediment deposits in studies where the element is used as a tracer.

The aim of this chapter is to determine spectral characteristics of K in soils and its capability to replace ^{137}Cs in large scale soil erosion monitoring. This is examined by measuring infrared spectral response of soils of different texture. The laboratory analysis comprises of two experimental stages, with varying concentrations of added K fertilizer. Fertilizer concentrations, in range of three times higher than typically applied by farmers, are used to quantify K through spectral analysis and establish wavelength ranges sensitive to change in concentration of the element. The findings are subsequently compared to literature based on Partial Least Squares Regression modelling and derivative manipulations. The second stage of the experiment includes application of typically used in agricultural field concentrations, to determine the lowest detectable concentrations.

4.2 Methods

4.2.1 Laboratory Experiment

Eight locations in central, east and southeast Netherlands were chosen for soil sample collection, according to soil type and soil texture. The collected material varied from heavy clay (Fluvisol- Eutric), clay loam (Fluvaquent-

Typic), loam (Fluvisol- Calcaric), silty loam (Luvisol- Orthic) and sandy loam (coarse sand) (Podzol- Humic), to fine sand (Arenosols- Albic). Description of each soil type can be found in Table 4.1.

At each location, 1–2 kg of material was collected using a clean spade to form a composite sample of the surface soil (0–5 cm). Each composite sample comprised of ten combined discrete samples collected around a single location, in order to represent all components of the sampled body material. Duplicates were acquired for silty and sandy loam soils. The samples were air dried for two days and subsequently sieved to remove particles larger than 5 mm. First, each sample was divided and placed in four identical metal dishes (30 g of soil each). The soil material in three of the dishes was fertilized with respectively 8, 16 and 32 g/10ml solution of Potassium Nitrate Fertilizer (46 % K_2O 13 % N, Organic matter). The use of fertilizer in the experiment allowed strict control over the added concentrations. To the fourth, demineralised water was added for use as a reference. Prior to acquiring spectra, samples were dried overnight at 30 degrees Celsius, to remove the effect of moisture on the spectral reflectance. The percentage Sand-Silt-Clay content was determined through bulk density and soil texture analysis, following standard laboratory procedures [Van Reeuwijk, 2002]. An Analytical Spectral Devices (ASD) Fieldspec Pro Spectrometer with a 450–2500 nm wavelength range coverage at 3–10 nm spectral resolution was used to acquire reflectance spectra. A high-intensity contact probe with internal light source was used as fore-optic with a spot size of 10mm. An average spectrum was created per soil textural type and amount of K, based on 10 measurements repeated for 20 iterations.

In the second stage of the experiment, three soil textural types (heavy clay, fine sand and silt loam) were selected, as these clearly show the effect of each textural component (sand, silt, clay) on spectra. The same procedure as above was followed, but now nine dilutions of fertilizer in the range of 1.13 g/10ml to 1.93 g/10ml were applied to each soil class, and one set was used as a reference. Spectra were collected in the same setup as described above.

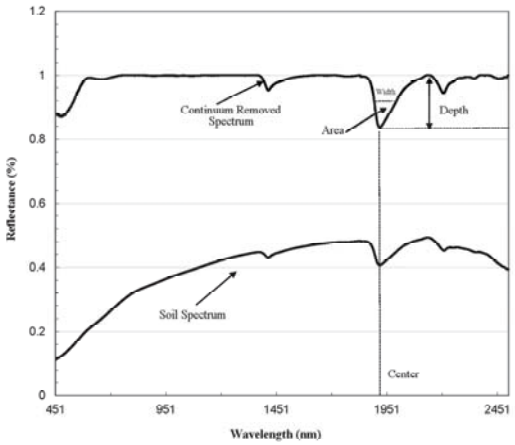

Figure 4.1: Absorption feature parameters: absorption band depth, absorption band width, absorption band center., after van der Meer [2004]

4.2.2 Absorption Feature Parameters

To determine the wavelength range influenced by change in K concentrations, and to compare the parameters from a common base line, an absorption feature analysis using continuum removal was performed following Richter et al. [2009]. This method is found to enhance differences in shape between individual features [Noomen et al., 2006]. Mathematically, it is calculated by dividing each individual spectrum by the corresponding continuum line [Kokaly and Clark, 1999]. Absorption features were associated with K through sensitivity analysis to assess the impact of added fertilizer on specific absorption features. After identifying the wavelength range related to K, absorption feature characteristics including absorption depth, absorption center, absorption area and absorption width of the individual feature were calculated using IDL-ENVI software [ITT Visual Information Solutions, 2009]. Figure 4.1 is an example to illustrate each absorption feature parameter. Equations implemented in IDL scripts are reported in van der Meer [2004].

Table 4.1: Soil types [FAO, 2006, de Bakker, 1979] and typical texture characteristics per soil type. Each soil type contents 15 sampling units

Map Unit	Soil Type	Description and Properties [FAO, 2006]	Texture
Rn95C	Fluvaquent-Typic	Originate from Clayey marine and fluvial sediments. Typically sandy loam or fine sand texture.	Clay loam
Rd10A	Fluvisol-Calcaric	Originate from predominantly recent fluvial and marine deposits. Calcaric material between 20 and 50 cm from the surface	Loam
Rn44C	Fluvisol-Eutric	Originate from predominantly recent fluvial and marine deposits. Having a base saturation of 50 % or more in the major pat between 20 and 100cm from the soil surface.	Heavy Clay
Zd21	Arenosols-Albic	Originate from unconsolidated, finely grained material. Relatively young, sandy soils with no profile development	Fine Sand
Hd30	Podzol-Humic	Originate from weathering materials of siliceous rock. Spodic illuviation horizon under a subsurface horizon that has the appearance of ash and is covered by an organic layer	Coarse Sand
Bld6	Luvisol-Orthic	Originate from unconsolidated material. Pedogenetic clay differentiation between topsoil and subsoil. Prone to erosion due to high silt content.	Silty Loam

4.3 Results

4.3.1 Laboratory Testing of Potassium Influence on Spectra

Based on results from continuum removal and sensitivity analyses, the wavelength range that relates to Potassium concentration was found to be 2450–2470 nm. For this wavelength range, coefficients of determination values vary between 0.918 for clay loam samples to 0.984 for silty loam samples. Figure 4.2 shows changes in absorption at 2450–2470 nm caused by changes in K concentration, based on the first stage of laboratory experiments. The deepest point of absorption was observed between 2450 nm and 2470 nm. With addition of fertilizer, the depth of absorption increases accordingly. This is also observed when small quantities of fertilizer were applied (Figure 4.3). This figure shows changes in absorption after application of fertilizer in quantities between 1.13 g/10ml and 1.93 g/10ml, for the heavy clays, fine sand and silt loam soil samples. Changes are noted for fine sand and silt loam samples, the absorption in the heavy clay soil samples is not clear.

4.3.2 Absorption Feature Analysis

Figure 4.4 shows variation per soil textural type in absorption depth, width and center of absorption in the 2450–2470 nm wavelength range. Figure 4.5 shows changes in absorption feature characteristics due to increase in K concentrations. Both figures show that the spectral response of soils with higher clay content is characterised by noisier spectrum. A shift of 5–10 nm in center of absorption is most profound in the clay samples, although all samples show a shift to lower wavelengths with increase of K concentration. An increase in band depth is noted for soil samples that belong to the silty loam textural class. This cannot be observed for the heavy clay and fine sand samples.

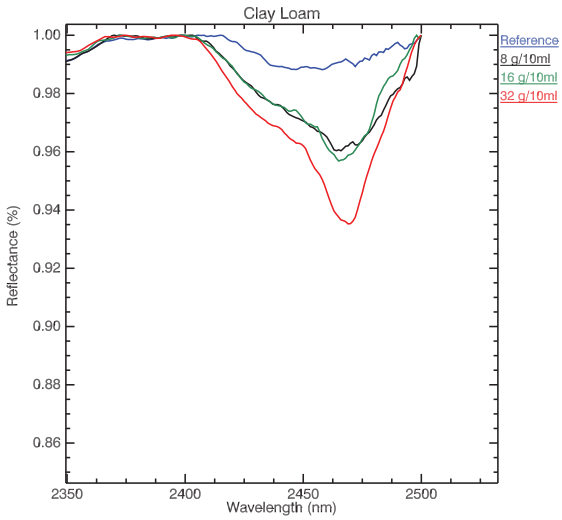

[a]

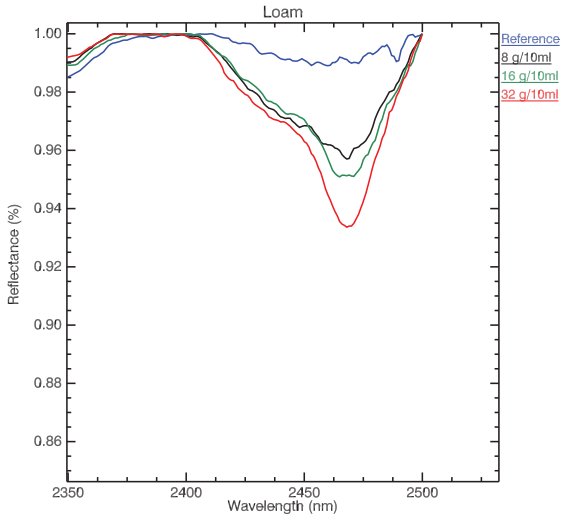

[b]

Figure 4.2: Change in absorption at 2450–2470 nm with change in K concentration. Each spectrum is shown in continuum removed reflectance and it is an average of 10 measurements. The blue lines belong to soils with no added fertilizer and used as a reference. The deeper absorption features belong to samples with addition of K fertilizer in concentrations 8, 16 and 32 g/10ml, indicated with black, green and red line respectively. The sub-figures show (a) Clay Loam, and (b) Loam.

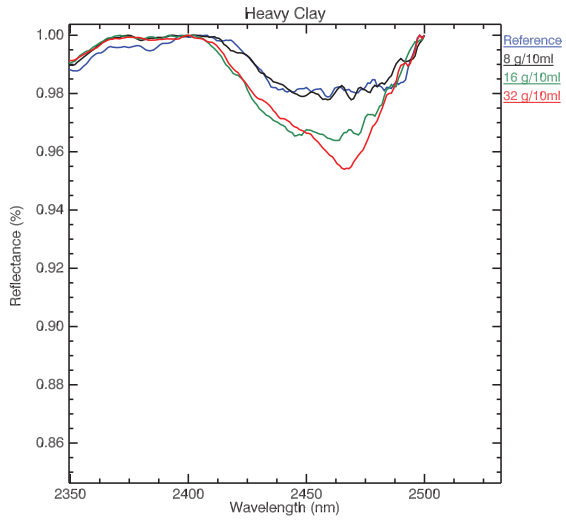

[a]

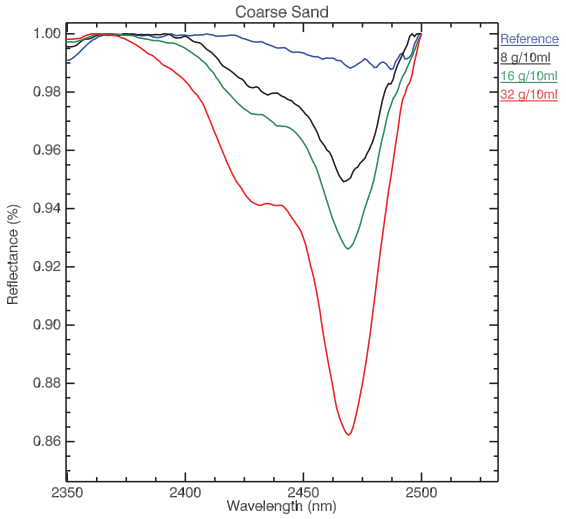

[b]

Figure 4.3: Change in absorption at 2450–2470 nm with change in K concentration. Each spectrum is shown in continuum removed reflectance and it is an average of 10 measurements. The blue lines belong to soils with no added fertilizer and used as a reference. The deeper absorption features belong to samples with addition of K fertilizer in concentrations 8, 16 and 32 g/10ml, indicated with black, green and red line respectively. The sub-figures show (a) Heavy clay, and (b) Coarse Sand.

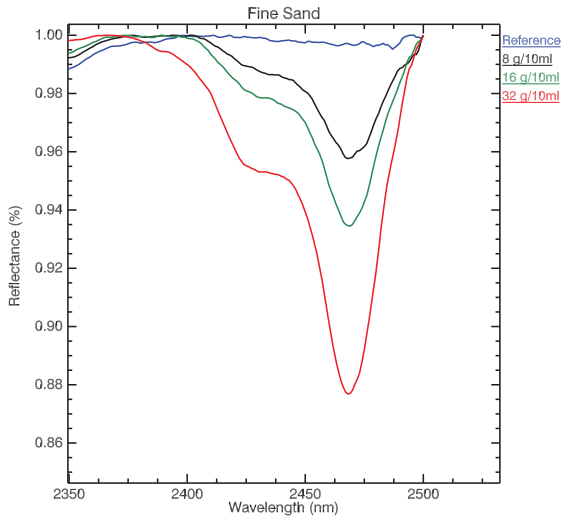

[a]

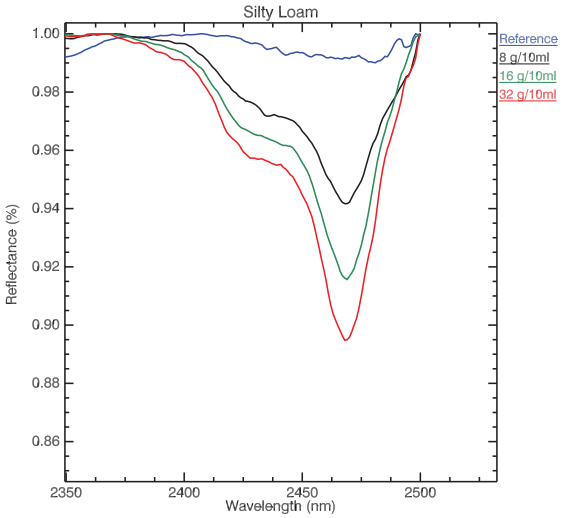

[b]

Figure 4.4: Change in absorption at 2450–2470 nm with change in K concentration. Each spectrum is shown in continuum removed reflectance and it is an average of 10 measurements. The blue lines belong to soils with no added fertilizer and used as a reference. The deeper absorption features belong to samples with addition of K fertilizer in concentrations 8, 16 and 32 g/10ml, indicated with black, green and red line respectively. The sub-figures show (a) Fine Sand, and (b) Silt loam.

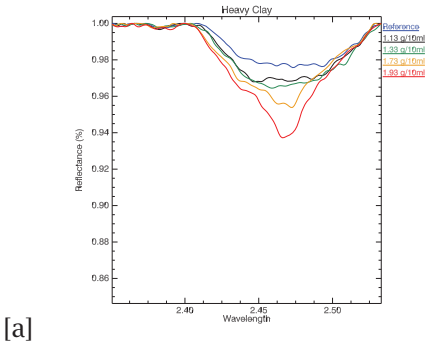

[a]

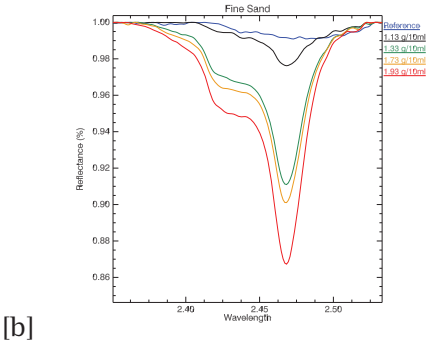

[b]

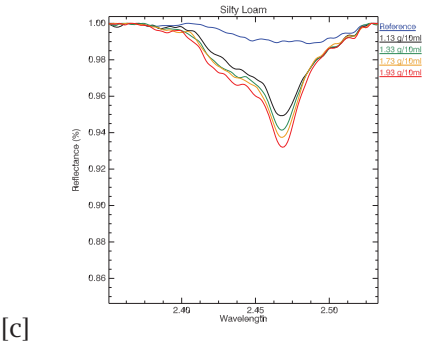

[c]

Figure 4.5: Change in absorption at 2450–2470 nm with change in K concentration. Each spectrum is an average of 10 measurements. The blue lines belong to soils with no added fertilizer and used as a reference. The deeper absorption features belong to samples with addition of K fertilizer in concentrations 1.13 g/10ml (black), 1.33 g/10ml (green), 1.73 g/10ml (orange) and 1.93 g/10ml (red); (a) Heavy clay, (b) Fine Sand, (c) Silt Loam.

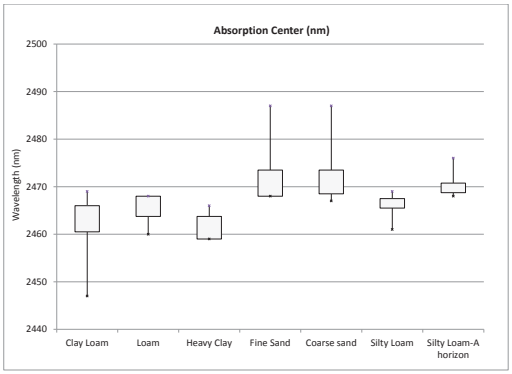

[a]

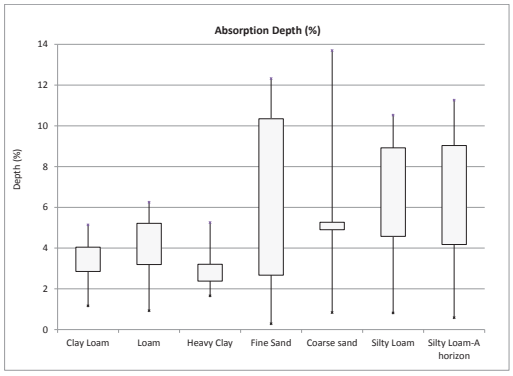

[b]

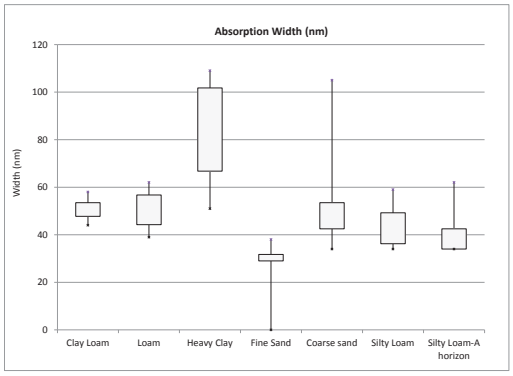

[c]

Figure 4.6: Variation in absorption feature parameters per soil textural type. (a) Absorption center, (b) Absorption depth, (c) Absorption width.

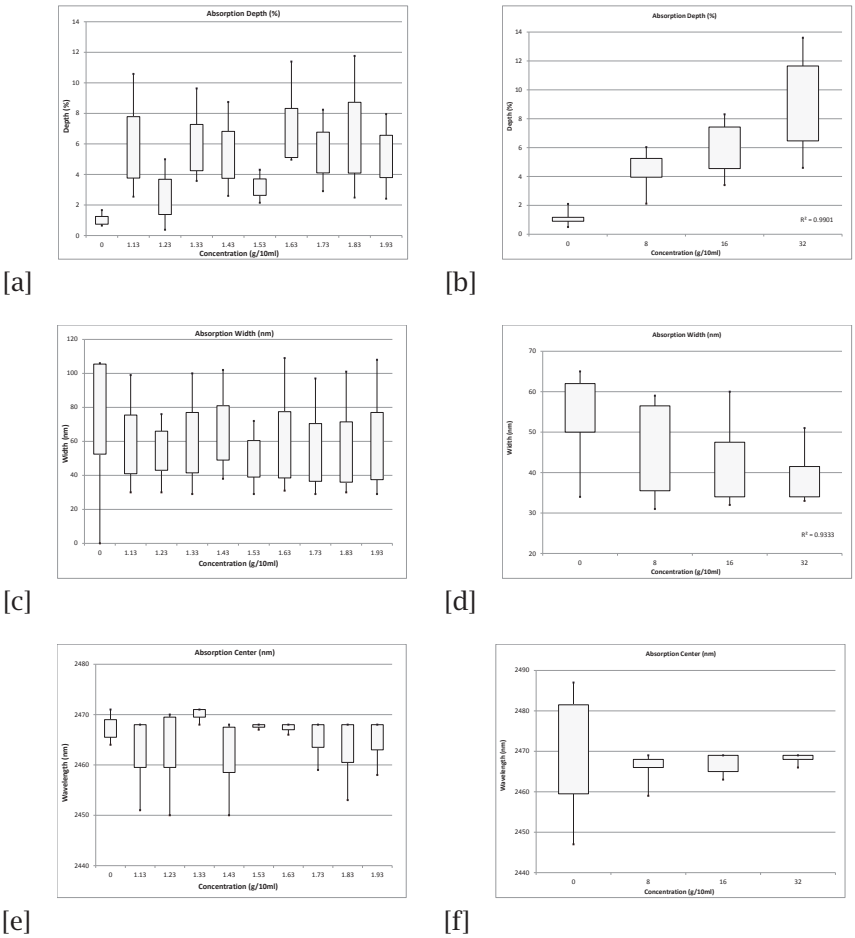

Figure 4.7: Change in absorption feature parameters- depth of the absorption, width and center, classes based on varying concentrations of added K fertilizer 0 to 32 g/10ml for all samples and soil textural types: (a) Absorption band depth for 0 to 1.93 g/10ml, (b) Absorption band depth for 0 to 32 g/10ml, (c) Absorption width for 0 to 1.93 g/10ml, (d) Absorption width for 0 to 32 g/10ml, (e) Absorption center for 0 to 1.93 g/10ml, (f) Absorption center for 0 to 32 g/10ml.

4.4 Discussion

4.4.1 Potassium Influence on Spectra

From continuum removal and sensitivity analysis performed on laboratory derived spectra, the wavelength range where the center of K absorption can be found is 2450 to 2470 nm. This falls within the range reported in literature using second derivative calculations [Ben-Dor and Banin, 1995] and Partial Least Squares Regression models [Udelhoven et al., 2003]. These studies reported optimal calibration equations for K that produce R^2 of 0.89 for wavelengths between 2396 and 2462 nm. The characteristic feature can be accounted to possible absorptions of combination modes between the free K ions and OH functional group.

Minor change in depth of absorption with addition of K fertilizer, is observed in samples with high clay content, that belong to soil textural classes clay loam and heavy clay (Figures 4.2 and 4.3). This is explained by the fact that clay content in samples prevents significant spectral changes caused by non-clay minerals [Ben-Dor et al., 2003]. Potassium is held at the edges of the clay particles, causing easy replacement by other positive ions [Johnston, 2010]. The soil textural types that show consistency between change in K concentration and depth of absorption are also the ones most prone to soil erosion: silty loam and fine sand (Figures 4.3(a), 4.3(b) & 4.4(a)), and Figures 4.5(b) & 4.5(c)).

4.4.2 Absorption Feature Analysis

The center wavelength and depth of the K absorption feature becomes better defined with an increase in concentration of added fertilizer. This is observed in the findings that emerge from both stages of laboratory analysis for all soil textural types (Figure 4.2 and 4.5). Changes in absorption feature parameters appear when 8, 16 and 32 g/10ml of fertilizer are applied. Figure 4.4(a) shows that soil texture defines the position of K absorption center. High clay content in soils causes greater fluctuations in absorption center values. The increase in concentration, as seen in Figure 4.7(e) and 4.7(f)), has strong influence on the peak position only above 8 g/10ml of fertilizer. The effect K concentration has on spectra is

highlighted in the case of absorption band depth for concentrations higher than 8 g/10ml (Figure 4.7(b).

Samples with high clay content experience smaller changes in absorption compared to those belonging to highly erosive soil textural types - sand and silt loam. This is explained by the abundance of free K ions in clays and the formation of illite-like [Barre et al., 2008] groups, where K replaces water and fills the interlayer clay sites. The presence of clay particles in soils causes shifts in clay absorption from 2200nm towards longer wavelengths, and therefore influencing the features at 2400–2500 nm [Hasegawa, 1963]. On the other hand, as stated in Kolahchi and Jalali [2007], when K fertilizer is applied to soils with low clay content, K ions do not interact strongly with the soil matrix. As a result, a localized increase in K concentration in the soil solution can be observed. The influence of texture on spectral absorption of K can be seen in Figure 4.6(a–c). Values for absorption feature parameters: center of absorption, depth and width, are dependent on soil textural type. The figure shows how higher percentage of each textural component- clay (Clay loam, Loam, Heavy clay), sand (Fine sand, Coarse sand) or silt (Silty loam), influences the results. Therefore, the influence of soil texture prevents the computation of a universal statistical model for all textural classes.

Reflecting back on erosion, it is the silty soils that are most prone to erosion. Heavy Clays are rarely found in landscape positions prone to erosion since they are associated with floodplain soils. All the other texture types can occur on hill slopes, but of those, the higher the sand content, the higher the infiltration rate, meaning less runoff. This leaves the silty soils and loamy sands to be the most interesting in this context.

Both experiments indicate that quantification of K depends on the amount of fertilizer added to the soil samples, as well as the soil sand-silt-clay content. In order to serve as particle tracer, the initial amount of K present in the soil should be established by collection of spectra prior to fertilizer application. This serves as a baseline and it should be accounted for when change in concentration occurs due to removal of fertilizer by erosion agents. Furthermore, particle tracing using K fertilizer is limited by K uptake by plants, and therefore cannot be performed after vegetation cover has emerged. Nevertheless, K can be quantified, through spectral response when more than 1.73 g/10ml of K fertilizer is present in the soil.

As shown in Figures 4.6(a–c) and 4.7, the degree of change above this value becomes more constant for all textural types, while the fluctuation in parameter values for lower concentrations can be explained by noise in the spectra. In relation to common agricultural practices, this amount is the minimum quantity of needed fertilizer recommended for crop production. Higher amounts of available K in soils have not been found to cause contamination or have a negative effect on agricultural practices. This laboratory experiment to detect and quantify K concentration in soils using spectral response, suggests that the technique can be applied in field and possibly on airborne hyperspectral imagery in order to achieve rapid and extensive spatial coverage over large areas affected by soil erosion.

4.5 Conclusions

This chapter presents a new approach to soil particle tracing using infrared spectroscopy, allowing a rapid monitoring of soil particle movement, towards monitoring soil erosion. The aim was to find a chemical element that can replace radioactive ^{137}Cs , while allowing fast and relatively inexpensive way of obtaining spatial data. Potassium is known to have the same physical and chemical behaviour in soils differing only in reactivity. Similarly to studies on ^{137}Cs , near-even distribution of the element can be assumed based on the annual application of fertilizer over soil erosion affected fields. Limitations in K quantification are an unknown initial concentration of available and unavailable K, as well as the effect of uptake by plants. If fertilizer is present in concentrations higher than 1.73 g/10ml, our technique can be applied. Best results are achieved when the method is used on soils high in sand and silt content.

The defined absorption feature with a peak center positioned between 2450 and 2470 nm, in the infrared spectrum associated with Potassium, makes it possible to detect and quantify using spectroscopy. Spectra should be acquired before and after the application of the fertilizer, to establish reference concentration.

Tracing Potassium in a silty loam soil with field spectroscopy

5

Abstract

In Chapter 4, tracing soil particles using K fertilizer and infrared spectral response was identified as suitable technique for quantification of K in soils with sandy and sandy silt texture. It was suggested as a new approach that can potentially grow to a technique for rapid monitoring of soil particle movement.

The aim of this chapter is to identify soil particle movement using Potassium fertilizer and infrared spectral response. Flow experiment was conducted in the area of the Guadalentin basin in Murcia, South East Spain. The severe soil erosion that takes place in the region, as well as the silty loam texture of the soil, determined the selection of the field area. The study was used as a pilot experiment to identify possible limitations of an experiment of this type.

5.1 Introduction

Soil properties sensitive to soil erosion, such as chemical composition, moisture content, runoff and sediment yield, can serve as an indicator for monitoring and detecting early signs of degradation. Agricultural practices and changes in landuse influence the quality and chemical composition of the surface soil material, although natural variation associated with bedrock geology determines the soil type and composition [Lemenih et al., 2005, Nael et al., 2004, Zhang et al., 2006].

As already discussed previously in Chapter 2, an approach to predict soil erosion is to use chemical tracers [Onda et al., 2007] as a proxy for tracking of soil particles movement [Zhang et al., 2006]. Soil particle tracing is an approach to detect early signs of hazard in arid and semi-arid environments [Chappell, 1996]. The Cesium 137 isotope (^{137}Cs) is considered to be the primary chemical tracer for detection of soil particle movement and has been used in soil erosion studies for over 40 years. The ^{137}Cs was introduced to the environment between the 1950s and 1970s through nuclear fallout of atomic bomb tests, and in 1986 through the Chernobyl power plant accident (see Chapter 3). The applicability of the technique is limited by the half-life of the isotope and the cost of soil chemical analysis, preventing its use over large areas [Boardman, 2006].

Remote sensing allows the acquisition of continuous spatial information over larger areas [Alatorre and Begueria, 2009, Jetten et al., 2003, Vrieling, 2006], which, combined with the information about soil chemical composition, provided by the shortwave infrared wavelengths in the electromagnetic spectrum, could allow extensive soil particle tracing. As presented in Chapter 3, the spectrally active element Potassium (K) can be used as a proxy to ^{137}Cs in soil particle tracing [Luleva et al., 2011]. A spectral absorption feature near 2465 nm is indicative for the abundance of K in soils, and absorption band depth is linearly related to concentration [Luleva et al., 2011]. Potassium (K) can be introduced as a fertilizer in the form of Potassium Oxide (K_2O) and Potassium-Phosphorus-Nitrogen (KPN). The recommended amount of fertilizer for EU countries is 0.6–2 mg/g of soil, although quantities may be higher. When applied as a fertilizer, the majority of available K ions adsorb onto the surface of soil particles in the first 30 seconds to 2 minutes after application When soils are not plowed,

1.003 mg of K per gram of soil is adsorbed, while if disturbed, this amount reduces depending on quantity of removed organic matter in soil [Wang and Huang, 2001]. The mobility of K is determined by various factors, the most important of which include physical and chemical properties such as soil texture [Luleva et al., 2011], organic matter [Askegaard and Eriksen, 2000], cation exchange capacity and presence of Calcium, Sodium and Gypsum [Jalali, 2007, Jalali and Rowell, 2009].

The aim of this chapter is to examine the possibility to use Potassium (K), in the form of an agricultural fertilizer, as a soil particle tracer in field conditions. Moreover, the chapter aims to outline key limitations and provide suggestions for improving the used methodology.

5.2 Methodology

5.2.1 Study site

The study site is located in the Guadalentin basin, within the province of Murcia, Southeast Spain. This is an area severely affected by soil erosion (Figure 5.1). Rills and gullies are the most common soil erosion feature, caused by tillage, fallow land and land abandonment. Rain storms are of high intensity, while rock types are susceptible to erosion.

Guadalentin basin lies on the eastern edge of the Betic ranges facing southwest-northeast direction and faults determine the main structure of the drainage network. The basin covers an area of 3300 km^2. Soils are shallow with high Calcium Carbonate content exceeding 50 % for some areas. Texture depends mainly on the hillslope position. Stoniness is high, low organic matter and moisture content. Salinity and crusting are problematic for some parts of the Guadalentin Basin, where soils are neutral to slightly alkaline. According to FAO [2006] the main soil types, recognized in the region of Murcia are Calcisols, Luvisols, Regosols and Fluvisols. The area has a typical semi-arid climate Mediterranean. Annual precipitation ranges from 300 mm to 500 mm with average annual temperature between 12 and 18° C [Alterra, 2007].

Figure 5.1: Advanced soil erosion in the Region of Murcia, South East Spain

5.2.2 Experimental setup and data collection

In this chapter, the field-based experiment was based on two experimental plots placed in bare agricultural field with silty loam Calcisols with ranging clay content between 30 and 36%. One of the plots (Plot A) was sprayed with K–P–N fertilizer (24%, 12%, 16%), diluted with 20% water by volume (1:1.5 ratio) recommended by the manufacturer to avoid crystalization, while the second plot (Plot B) was used as a reference with no added fertilizer.

The plots were 2.5 m in length and 0.6 m in width, following the set up in Morgan (2005).

Each plot was evened out and cleared from larger soil aggregates or loose vegetation residuals to achieve optimal flow conditions. The degree of slope of the plots was 12 %. Controlled water flow was generated to trigger particle movement. A water tank with volume of 10 l with dispenser was used to generate water flow for a total of 15 min per plot.

Infrared spectral measurements were acquired with an Analytical Spectral Devices (ASD) Fieldspec Pro instrument with a 450–2500 nm wave-

length range coverage at a 3–10 nm spectral resolution, following a grid sampling strategy. The fore-optic was a high-intensity contact probe with internal light source and a spot size of 10 mm in diameter. The measurements were collected in three stages: prior to application of fertilizer to determine background values of K, after application of fertilizer to establish the distribution of fertilizer, and after water flow to observe particle displacement. Data were obtained in a grid with 10 measurements across flow direction and 11 measurements along flow direction, to a total of 110 measurements per plot per stage. The same locations were measured at each stage of the experiment.

A spectral library was built from spectra collected during the experiment. These were mosaicked to produce artificial images, each representative for a plot in one of the three stages of the experiment. Each pixel within an image contains the spectral information collected from the corresponding sampling point in a plot. A spectral subset of bands was created for the 1800–2500 nm wavelength range to include the water absorption band around 1900 nm, the clay feature near 2200 nm and the K absorption feature near 2465 nm [Luleva et al., 2011]. A continuum removal conversion was applied to all spectra to eliminate brightness differences and thus enhance colour difference while standardizing the shape of absorption features [Noomen et al., 2006]. The absorption feature parameters- depth, position and area were computed for each pixel in IDL ENVI software, following van der Meer [2004].

The images were spatially interpolated using ordinary kriging with a spherical semivariogram model in ArcGIS 10 software. Validation of the spectrally obtained images was done by comparison with laboratory determined K concentrations in the collected soil samples, as well as digitized images of the flow patterns.

5.2.3 Sensitivity analysis on spectral data

The collected ASD infrared spectra were built into artificial images that represent each of the three stages of the experiment. A pixel within an image contains the spectral information collected from the corresponding sampling point in a plot. A spectral subset of bands was created for the 2000–2500 nm wavelength range to include the clay feature near 2200 nm

and the K absorption feature near 2465 nm [Luleva et al., 2011]. A continuum removal conversion was applied to all spectra to eliminate brightness differences and thus enhance colour difference while standardizing the shape of absorption features [Noomen et al., 2006]. The absorption feature parameters- depth, position and area (described in Chapter 4) were computed for each pixel in IDL-ENVI software, following van der Meer [2004]. Each image pixel was then assigned the corresponding absorption parameter values for clay and K absorption feature. The images were spatially interpolated using ordinary kriging with a spherical semivariogram model in ArcGIS 10 software. The absorption depths for clay (near 2200 nm) and K (near 2465 nm) absorption bands were plotted to determine the relation and coefficient of determination between clay content and K content. The procedure was applied for both plots on values derived after each stage of the experiment.

5.3 Results and Discussion

5.3.1 Potassium Fertilizer Mobility

Although the plots were not fully covered by the flow, the sampling points were deliberately kept the same, in order to examine the whether change is caused by the flow. This was mainly due to the fact that the soil was fully dried and large lumps were formed. This allowed the water to accumulate near the water tank, before it could trigger a flow. It is possible, that this has caused leaching down the soil profile, or further dilution of the applied fertilizer. Therefore, it can only be assumed that fertilizer is removed with the particles under the influence of the water flow. The runoff water was not collected, and therefore this could not be tested with the available dataset.

Figures 5.2 and 5.3 show the change in absorption band depth for clay absorption feature near 2200 nm and K absorption feature near 2460 nm. The pixels shown in white colour are these with deepest absorption, while the green indicate the shallowest.

Figure 5.4 shows scatter plots and coefficients of determination calculated based on absorption band depth values for clay and K absorption features.

The plot received no fertilizer, however difference is still noted. The flow in the top 1/3 has decreased the K absorption, while the flow line to the right coincides with an increase in K. This might indicates that the higher concentration of K has deposited.

Higher values of absorption depth represent higher concentrations. The representation of the plots before addition of fertilizer or water flow, indicated on Figures 5.2 and 5.3, show that the K pattern follows clay content as expected. The application of K solution results in a heterogeneous image, where the center has much higher K values, while the upper right where water pooled, due to difference in surface roughness caused by the flow.

The results clearly show that there is change after each stage of the experiment, however the concentrations of applied fertilizer might be too low to indicate whether particles have moved.

The images after water flow resemble the original situation, except for the accumulation of water at the top right. There is little evidence of flow. The fact that in the areas of the image where no flow has taken place the values are back to near original, suggests that leaching of K away from the surface has occurred.

Study site with soils with lower clay content than the one at the present location should be selected in order to minimize the influence of clay absorption on K feature. Furthermore, in order to attempt quantification of fertilizer using infrared spectra, ranging concentration of fertilizer should be applied and threshold values and statistical relationships should be established.

Delineation of the plots is recommended, so that the flow can remain within the area of interest. In case the soil is dry and prone to formation of lumps, the flow should have higher intensity and longer duration.

To estimate the deposition, all runoff water should be collected, and the collected sediment should be analysed for its K content. Soil samples should also be collected from the plots after each stage of the experiment in order to validate the produced images.

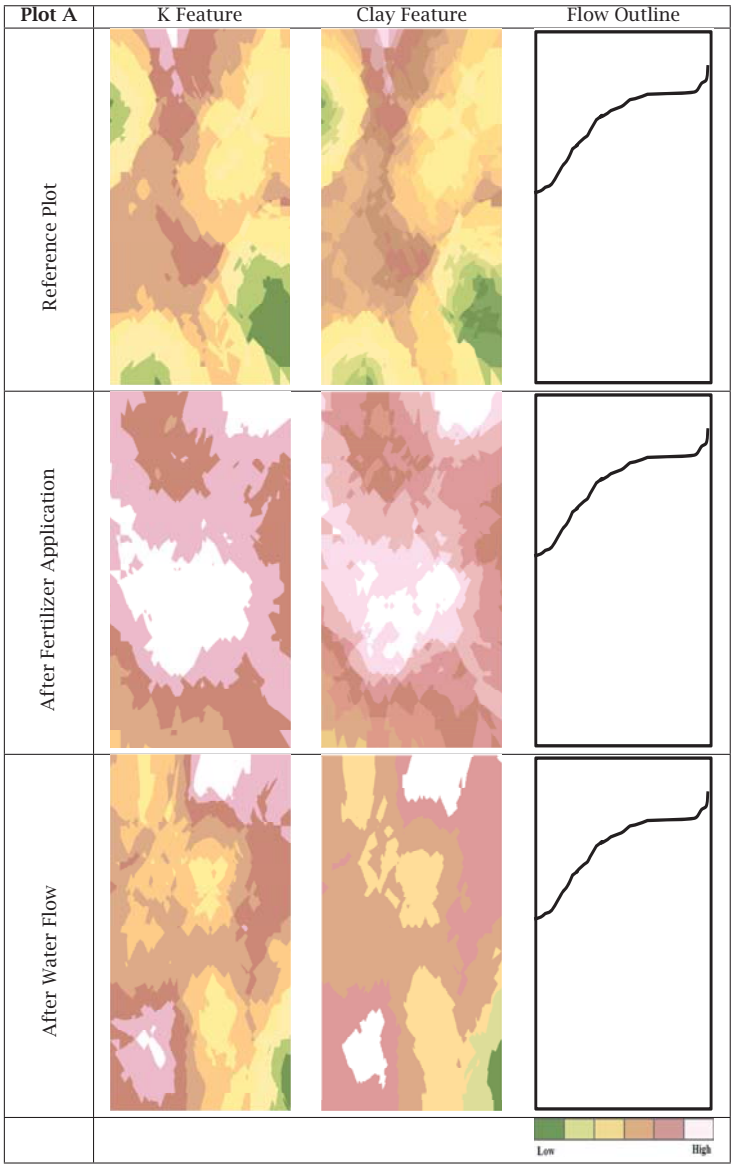

Figure 5.2: Spatial representation of K absorption feature depth near 2465 nm and clay absorption feature depth near 2200 nm for plot A. This plot was treated with 2.4 mg/g of added fertilizer. Each image comprises 110 sampling points collected after each stage of the field experiment (before treatment, after addition of fertilizer, and after water flow)

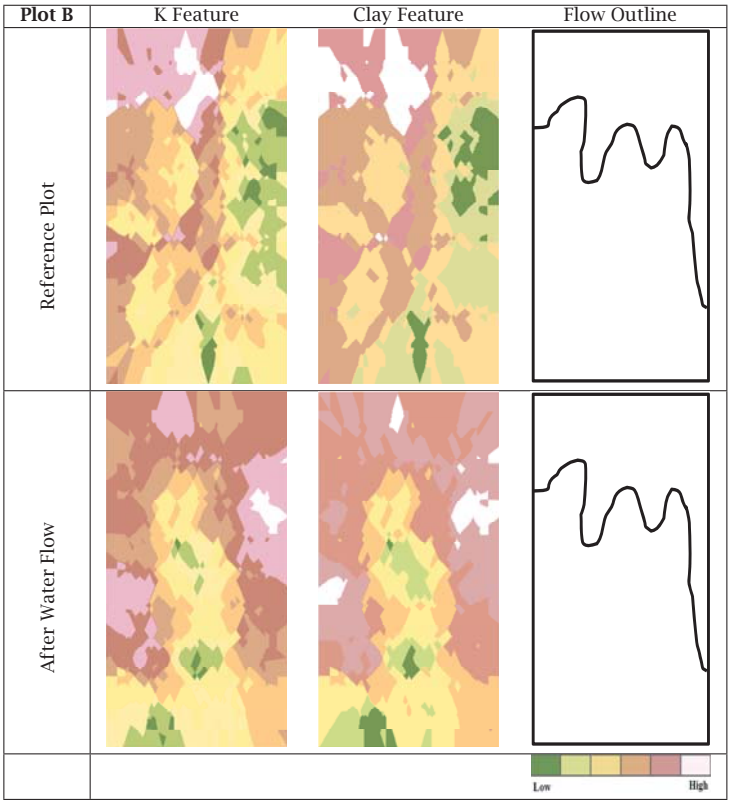

Figure 5.3: Spatial representation of K absorption feature depth near 2465 nm and clay absorption feature depth near 2200 nm for plot B. This plot was not treated with fertilizer. Each image comprises 110 sampling points collected after each stage of the field experiment (before treatment, after addition of fertilizer, and after water flow)

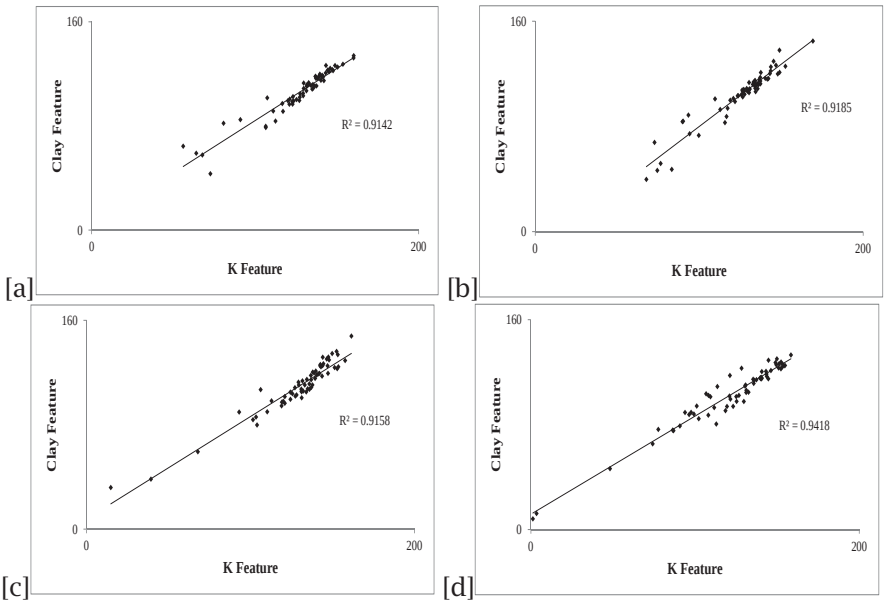

Figure 5.4: Relationships between band depth near 2465 nm (K feature) and band depth near 2200 nm (Clay feature) expressed using coefficient of determination (R^2) for experimental plot A [a,b] and plot B [c,d] for each stage of the experiment.

5.3.2 Change in absorption feature depth in relation to K concentrations

Using contact probe mode of the ASD field spectrometer has limited the influence of external factors. This allowed the estimation of absorption feature parameters at wavelength near 2460 nm. As previously discussed in Chapter 4, clay absorption near 2200 nm strongly influences the identified K absorption feature near 2460 nm. Therefore, both features had to be examined and compared statistically in order to establish if the amount of clay present in the soil is sufficient to affect the depth of absorption of the K feature.

On Figure 5.4 shows the relationship between depth of absorption near 2200nm and 2460nm. The values for coefficient of determination that were calculated for all plots indicate R^2 of 0.9 and above between the two

variables. This can also be observed from the images shown on Figures 5.2 and 5.3, where the change in absorption band depth are illustrated.

5.4 Conclusions

The research hypothesis states that flowing water moves surface soil particles with adsorbed K and can be traced by observing the change in absorption feature characteristics. The experiment was conducted on two plots- one was fertilized with a commercial Potassium fertilizer, by applying recommended by the manufacturer concentrations. The second plot was used as a reference in order to determine any natural change in surface composition under the influence of water flow. Soil spectral measurements were collected using ASD Fieldspec Pro Spectrometer, in a contact probe mode, prior application of fertilizer, after application of fertilizer and after water flow.

Change in depth of absorption near 2460nm was observed. However, from the experiment, it is not clear whether the movement of K is due to runoff or infiltration. More detailed analysis of clay movement and moisture patterns could aid the interpretation of the sampling plots.

Tracing Potassium in a Loess soil with field spectroscopy

6

Abstract

In Chapter 5, a number of limitations of the field based experiment for tracing soil particle movement using Potassium fertilizer and infrared spectral measurements were outlined. The most important of these were the presence of high clay content, the insufficient runoff data, as well as the low variation in applied fertilizer concentrations. These prevented the drawing of optimal conclusions, however it resulted outlining of key recommendations for improvement of the experiment. A field-based water flow experiment, conducted on 6 plots on silt loam Loess soils in the Netherlands, is presented in this chapter. The field area was selected due to the fact that the soils are developed on Loess, and are characterized with limited clay content. The plots were treated with various concentrations of K_2O and one plot was used as reference. Infrared reflectance spectra were collected to observe spatial variation in available K, before and after application of fertilizer, and after runoff simulation by water flow. The runoff sediment was also collected in order to establish potential removal of fertilizer under the influence of the water flow. [1]

[1] This chapter is based on: Luleva, M, van der Werff, H, van der Meer, F., Jetten, V. (2013), Observing change in potassium abundance in a soil erosion experiment with field infrared spectroscopy, Chemistry, 22, pp 91–109, Luleva et al. [2013]

6.1 Introduction

Soil erosion and sedimentation have been studied extensively in the last decades [Boardman, 2006]. An approach to predict soil erosion is to use chemical tracers [Onda et al., 2007] as a proxy for tracking of eroding soil particles [Zhang et al., 2006]. Soil particles are moved by wind, water or gravity [Moran et al., 2002]. Soil particle tracing is an approach to measure net soil flux in arid and semi-arid environments and to detect early signs of hazard [Chappell, 1999]. The Cesium 137 isotope (^{137}Cs) is considered to be the primary chemical tracer for detection of soil particle movement. This element has been used in a number of soil erosion studies for over 40 years. Most recent publications cover the use of ^{137}Cs either for comparison between various methods [Sac et al., 2008, Xiaojun et al., 2010], or as a validation technique of historical records [deGraffenried Jr and Shepherd, 2009, Estrany et al., 2010, Meusburger et al., 2010, Rodway-Dyer and Walling, 2010]. Cesium- 137 was introduced to the environment between the 1950s and 1970s through nuclear fallout of atomic bomb tests, and in 1986 through the Chernobyl power plant accident. Once fallen onto the Earth surface, ^{137}Cs attaches to soil particles. Its redistribution is mainly controlled by erosion, transport and deposition of sediments [Porto et al., 2001]. The use of ^{137}Cs for soil particle tracking has some assumptions [Parsons and Foster, 2011]: The distribution of ^{137}Cs fall out is homogeneous (while being limited to the Northern hemisphere), and particles would only move by the influence of soil erosion [Campbell et al., 1982, Chappell, 1999, Walling and Quine, 1990]. Furthermore, the use is limited by the half-life of the isotope and the cost of soil chemical analysis, preventing its use over large areas [Boardman, 2006]. There is hence a demand for a substitute of ^{137}Cs by a chemical element that has similar physical and chemical behaviour, can be distributed evenly in the environment and can be measured with already established analytical techniques.

Remote sensing allows the acquisition of continuous spatial information over larger areas [Alatorre and Begueria, 2009, Jetten et al., 2003, Vrieling, 2006]. Recently, we suggested in Luleva et al. [2011] that the spectrally active element Potassium (K) can be used as a proxy to ^{137}Cs in soil particle tracing. Potassium has similar electrical, chemical and physical properties

to Cs [Andrello and Appoloni, 2004, Relman, 1956], and both elements show similar chemical behaviour in the environment [Relman, 1956]. A spectral absorption feature near 2465 nm is indicative for the abundance of K in soils, and absorption band depth is linearly related to concentration [Luleva et al., 2011].

Potassium (K) is found in soils in three forms: readily available to plants in a water soluble form, slowly available when released from clay minerals, and unavailable as part of the crystalline structure of soil minerals. Potassium (K) can be introduced as a fertilizer in the form of Potassium Oxide (K_2O). The recommended amount of fertilizer for EU countries is 0.6–2.0 mg/g of soil, although quantities may be higher. When applied as a fertilizer, the majority of available K ions adsorb onto the surface of soil particles in the first 30 seconds to 2 minutes after application When soils are not plowed, 1.003 mg of K per gram of soil is adsorbed, while if disturbed, this amount reduces depending on quantity of removed organic matter in soil [Wang and Huang, 2001]. The mobility of K is determined by various factors, the most important of which include physical and chemical properties such as soil texture [Luleva et al., 2011], organic matter [Askegaard and Eriksen, 2000], cation exchange capacity and presence of Calcium, Sodium and Gypsum [Jalali, 2007, Jalali and Rowell, 2009].

The aim of the study presented in this chapter is to determine whether change in K concentration, when applied in the form of commercially available K fertilizer in concentrations commonly applied in agriculture, can be observed using field infrared spectroscopy on Loess soils with limited clay content.

We will examine this by answering three questions:

- Can a relative change in abundance of K in the field be observed with spectroscopy using the absorption feature near 2465 nm?
- Does a change in absorption depth of the 2465nm absorption feature correspond with the controlled addition and removal of K?
- Does the amount of K removed by water flow correspond to the concentration of K found in runoff water?

6.2 Methodology

6.2.1 Site Description

The experiment was done in an agricultural field in South Limburg region, The Netherlands. This region is part of the European Loess belt which covers parts of England, Northwest France, Belgium, The Netherlands, Germany, Poland and Russia [Kwaad et al., 2006]. Typical landforms include dry valleys, incised roads and manmade cultivation terraces. The soils belong to Typic Hapludalf soil type (Soil Taxonomy) or Albic Luvisol [FAO, 2006] and were developed on the Loess during the Holocene period. These soils are highly vulnerable to soil erosion and runoff due to their low structural stability. Top soils contain up to 60 % silt, while sub soils are stony and dry due to underlying gravel of palaeo river terraces deposited by the river Meuse. The slope varies from 2 to 12 % [de Bakker, 1979]. The annual precipitation is distributed throughout the whole year with high-intensity rainfall restricted between April and October. The average rainfall is 60mm per month, with maximum reaching 1–2 mm/min [Kwaad et al., 2006]. Erosion is enhanced by a continuous change in land cover and decrease of grassland in favour of arable land [Boardman et al., 1994]. The area is mainly used for crop production, therefore the soil is bare for the period outside the growing season [Winteraeken and Spaan, 2010].

6.2.2 Field Experiment Design

A standard practice in soil erosion studies is the use of experimental plots [Morgan, 2005]. In this chapter, the field-based experiment was based on six experimental plots. Each plot was sprayed with a different concentration of K fertilizer. Controlled water flow was generated to trigger soil erosion and runoff. The six plots were 2.5 m in length and 0.6m in width, following Morgan [2005]. Each plot was evened out and cleared from larger soil aggregates or loose vegetation residuals to achieve optimal flow conditions. Plot edges were raised 5–10 cm above the soil surface to contain the runoff. The degree of slope naturally varied from 9.0 % to 9.6 %. 30 l water tanks with dispenser were used to generate water flow and doormats to distribute the flow evenly. Galvanized steel sheets placed

[a]  [b] 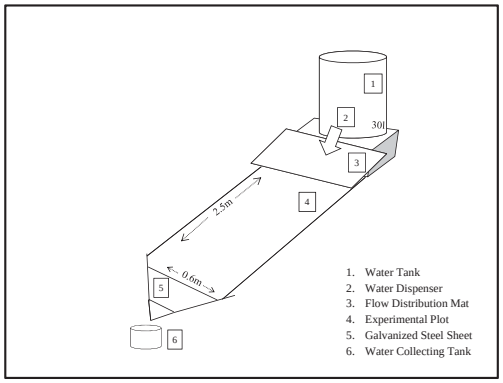

Figure 6.1: Experimental plot set up and components. a) photo of the setup in the field, b) a schematic diagram of the setup.

at the bottom of each plot (20 cm below the surface) were used to collect runoff into collector tanks (Figure 6.1).

400 ml of commercially available K fertilizer (K_2O) solution was sprayed onto each plot (except the reference plot C) with a plant sprayer, applying a fixed volume as evenly on the plot as possible. The concentrations of applied fertilizer were 0.6 mg/g (plot A and plot F), 2.48 mg/g concentration (plot B), one with 1.18 mg/g (Plot D) and 1.76 mg/g (Plot E). Plot C was used as a reference to observe the behaviour of naturally occurring K under the influence of flowing water. The duration of the flow was 14–20 min., depending on the path of the flow. 10 l of runoff water and eroded soil were collected at the bottom of the plot during the flow simulation, which corresponds with a rainfall event of 90 mm per hour.

6.2.3 Field Data Collection

Before and after the flow experiment, Loess soil samples for validation were collected from the surface (0–2 cm) and at 15 cm depth of each plot, following a grid-point sampling strategy [Hengl et al., 2003]. Initial moisture content was measured in the field using an IRROMETER Watermark soil moisture meter. Water samples were collected per litre of runoff water, up to a maximum of 10 samples or until runoff had stopped. Mixed water

samples were collected from the runoff tank, taken from the surface, 10 cm and 20 cm depth.

Infrared spectral measurements were acquired with an Analytical Spectral Devices (ASD) Fieldspec Pro instrument with a 450–2500 nm wavelength range coverage at a 3–10 nm spectral resolution. The fore-optic was a high-intensity contact probe with internal light source and a spot size of 10 mm in diameter. The measurements were collected in three stages: prior to application of fertilizer to determine background values of K, after application of fertilizer to establish the distribution of fertilizer, and after water flow to observe particle displacement. Data were obtained in a grid with 6 measurements across flow direction and 18 measurements along flow direction, up to a total of 108 measurements per plot per stage. The same locations were measured at each stage of the experiment.

6.2.4 Geochemical analysis

The soil samples were dried overnight at 30° Celsius and sieved through a 2 mm sieve to remove large particles. Water samples were filtered using laboratory membrane filters and the residual sediments were air dried overnight. All samples were analysed for total K content following standard laboratory procedures [Van Reeuwijk, 2002] with Inductively Coupled Plasma-Optical Emission Spectroscopy (ICP-OES) with a detection limit of 0.01 mg/ml. Texture and bulk density analyses were performed to determine the sand-silt-clay fractions.

The relationship between water contents and spectral absorption of K was analysed in a laboratory. A soil sample was passed through a 2 mm sieve and evenly distributed in three sample dishes, each dish containing approximately 50 grams of dry material. Three different concentrations of K fertilizer were added. The first set as a reference with addition of 10 ml of demineralized water and 0 mg/g of K, the remaining two with addition of 1.20 mg K/ g of soil and 2.48 mg K/g of soil in 10 ml solution respectively.

Spectral absorption was measured under laboratory conditions using the same instrument specifications and settings as during the field experiment (section 6.2.2).

Collection of spectra was done for 6 contiguous hours over 2 days,

adding up to a total of 117 measurements. Each sample was weighed before spectra were collected in order to measure the amount of moisture that had evaporated. The experiment was terminated when the initial moisture content of the samples was reached.

6.2.5 Spectral analysis

All ASD infrared spectra were mosaicked to produce artificial images, each representative for a plot in one of the three stages of the experiment. Each pixel within an image contains the spectral information collected from the corresponding sampling point in a plot. A spectral subset of bands was created for the 1800–2500 nm wavelength range to include the water absorption band around 1900 nm, the clay feature near 2200 nm and the K absorption feature near 2465 nm [Luleva et al., 2011]. A continuum removal conversion was applied to all spectra to eliminate brightness differences and thus enhance colour difference while standardizing the shape of absorption features [Noomen et al., 2006]. The absorption feature parameters- depth, position and area were computed for each pixel in IDL ENVI software, following van der Meer [2004].

The values of absorption band depth were mosaicked into artificial images, following the sampling pattern in IDL ENVI software. Each image pixel was then assigned the corresponding absorption parameter values for the water, clay and K absorption feature. The images were spatially interpolated using ordinary kriging with a spherical semivariogram model in ArcGIS 10 software. Validation of the spectrally obtained images was done by comparison with laboratory determined K concentrations in the collected water and soil samples, as well as digitized images of the flow patterns.

A spectral library was built from spectra collected during the controlled moisture experiment. Absorption band depth was calculated in IDL ENVI software [ITT Visual Information Solutions, 2009] following van der Meer [2004]. The absorption depths of the water (near 1900 nm), clay (near 2200 nm) and K (near 2465 nm) absorption bands were plotted to determine the relation and coefficient of determination between moisture content, clay content and K content. The Normalized Soil Moisture Index (NSMI) was calculated in order to minimize the influence of varying soil

texture and albedo [Haubrock et al., 2008]. The index was chosen because it has linear correlation with soil moisture but is not influenced by surface crusting or substrate heterogeneity. It is calculated by combining reflectance values at 1800 and 2119 nm [Haubrock et al., 2008]. The resulting values are in spectral reflectance units. The same procedure was applied to the images corresponding to each experimental field plot.

6.3 Results

K adsorbs onto the surface of soil particles at the latest 10 minutes after application of fertilizer [Wang and Huang, 2001]. Once attached, K remains immobile [Garrett, 1996] unless displaced by water or taken up by plants [Jalali and Rowell, 2009]. Soil particles are considered displaced if measured K concentrations are lower than what has been applied in the form of a fertilizer, or are similar to the concentration prior to application of fertilizer.

Moisture influences the results, so it is hard to distinguish the effect of K alone because of moisture changes during and after application. In addition, K is absorbed by the clay particles,which could influence the results, together with the exchange between absorbed K and K in solution.

In the context of soil erosion, clay particles move and create a movement of free K, absorbed K and clay. Furthermore the top few centimeters of the soil dry out and reach an equilibrium value, such as field capacity, which depends partly on the amount of clay and partly on the soil structure. The drying out affects the depth of absorption features and the rate with which clay and K can be detected.

These processes are illustrated on figures 6.5 and 6.6. Figures 6.7– 6.12 show whether K movement can be isolated and distinguished.

6.3.1 Laboratory analysis

Table 6.1 shows the characteristics of the soil found in each plot. These consist of the amount of fertilizer applied, initial soil moisture temperature values, water fraction per volume (WFV), total salt content, texture characteristics and bulk density per plot. The table shows that, in all plots, the K concentration at 15 cm depth is lower than at the surface. Bulk

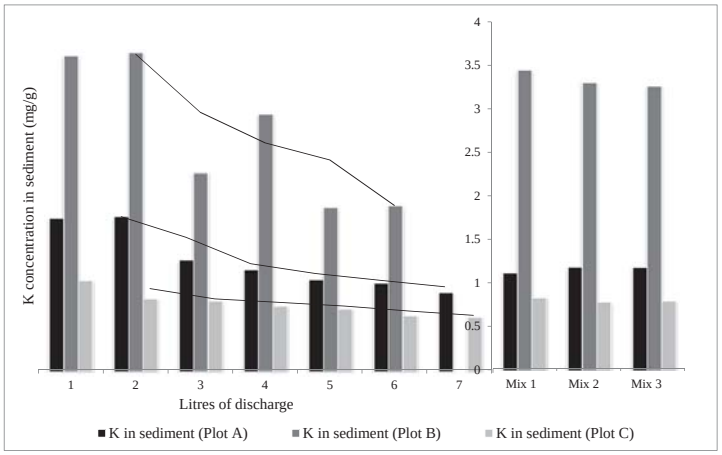

Figure 6.2: Bar chart showing a decrease in K concentration measured in sediment per litre of discharge (1 to 7) for plots A, B and C. The values under Mix 1, 2 and 3 are derived from analysis of water samples at three depths from the total collected runoff.

density varies with 0.03 g/cm3 between the plots. Texture characteristics indicate that these soils have typical characteristics of silt loam derived from Loess with silt content 53–58 % and maximum clay content of 18% (see table 6.1).

Figure 6.2 shows the change in K concentration per litre of discharge during the flow experiment. The concentration of K in the collected sediment collected decreases indicating removal of fertilizer.

Figure 6.3 shows the area of each plot covered by water flow after the experiment was completed. It can be noted that parts of plots A, B and E were not affected by runoff water.

6.3.2 Spectral analysis

Figure 6.4 shows the change in K absorption feature depth (near 2465 nm) for each plot at each stage of the experiment. It can be observed that for most pixels, depth of absorption features increases with addition of fertilizer. After water flow, K absorption continues to increase for all plots.

Table 6.1: Field conditions in the experimental plots, obtained by geochemical analysis of soil samples from each plot.

Plot	Reference K, depth cm		Added K_2O	Moisture Characteristics			Texture %			Bulk Density
	0-2cm (mg/g)	5-20cm (mg/g)	0-2cm (mg/g)	Temp. (C)	WFV	Total Salt (s/m)	Sand	Silt	Clay	g/cm3
A	2.61	0.72	0.6	14.9	0.34	0.29	31	56	13	1.32
B	2.93	0.87	2.48	15.1	0.34	0.35	30	58	12	1.29
C	2.60	0.57	0	15.7	0.34	0.28	29	53	18	1.32
D	4.23	0.72	1.18	17.4	0.35	0.29	32	53	18	1.35
E	3.21	0.67	1.76	17.6	0.32	0.27	30	52	18	1.36
F	2.74	0.63	0.6	17.5	0.34	0.28	29	53	18	1.32

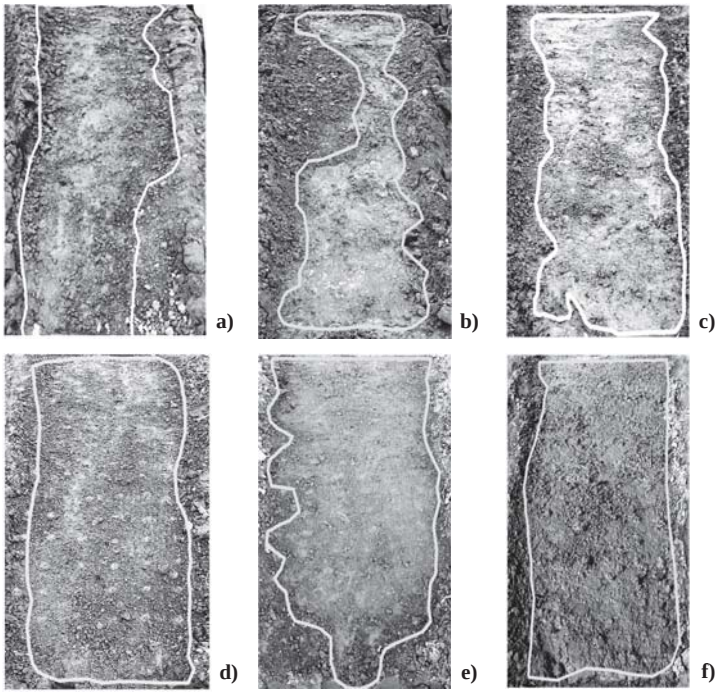

Figure 6.3: Schematic outline of each plot with the area inside the white polygon that was covered by flowing water. The area outside the polygon remained dry.

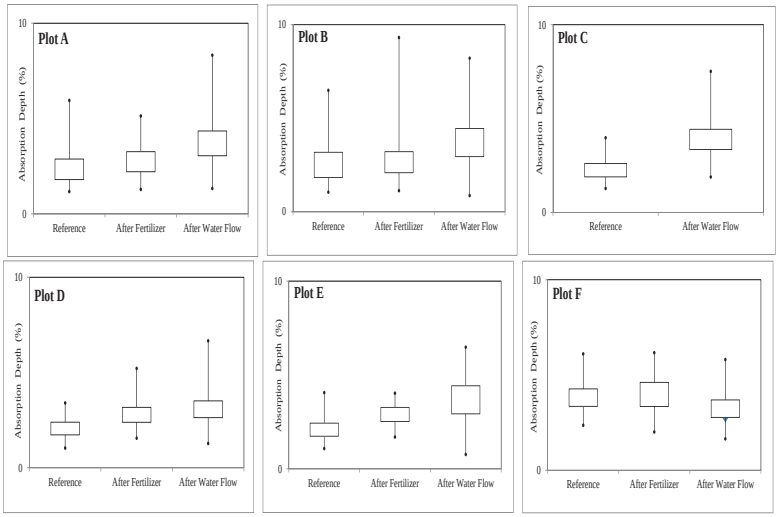

Figure 6.4: Change in K absorption feature depth, for each plot for each stage of the experiment.

Figure 6.5 and figure 6.6 show relationships between the NSMI index (soil moisture), clay absorption bands at 2200 nm and K absorption bands at 2465 nm. For all plots, after application of fertilizer, the values for R^2 indicate that the influence of moisture on K absorption is higher than it is of clay. After water flow, however, R^2 values between clay and moisture, as well as clay and K feature increase.

Figures 6.7– 6.12 show the results of absorption feature analysis. The natural variation in K can be observed from Figures 6.7– 6.12(top rows) for each plot. The range of K absorption band depth is 1.3–8.3 % for plot A, 1.3–8.5 % for plot B, and 3.2–4.5 % for plot C. In all images, NSMI is highest after water flow. The images showing clay absorption band depth show a decreased absorption after water flow (figures 6.7– 6.12, right column).

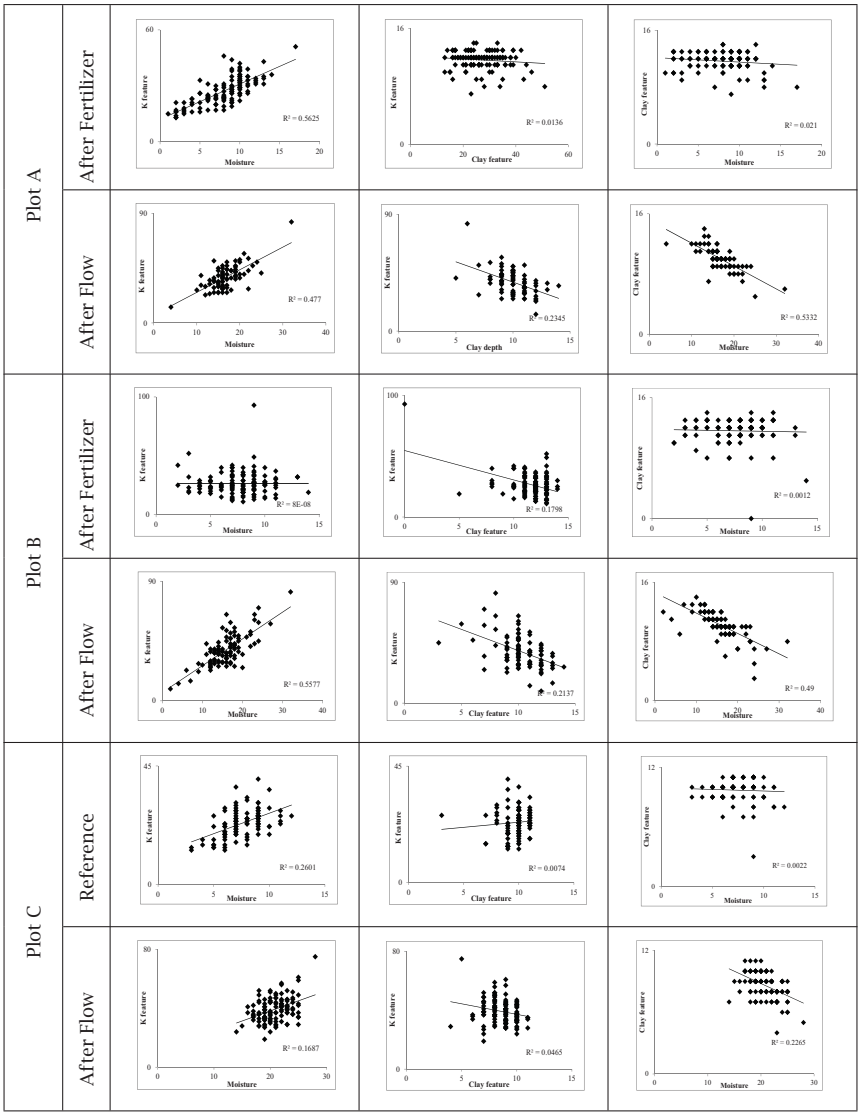

Figure 6.5: Relationships between band depth near 2465 nm (K feature), band depth near 2200nm (Clay feature) and NSMI values (Soil moisture) expressed using coefficient of determination (R^2) for experimental plots A, B and C.

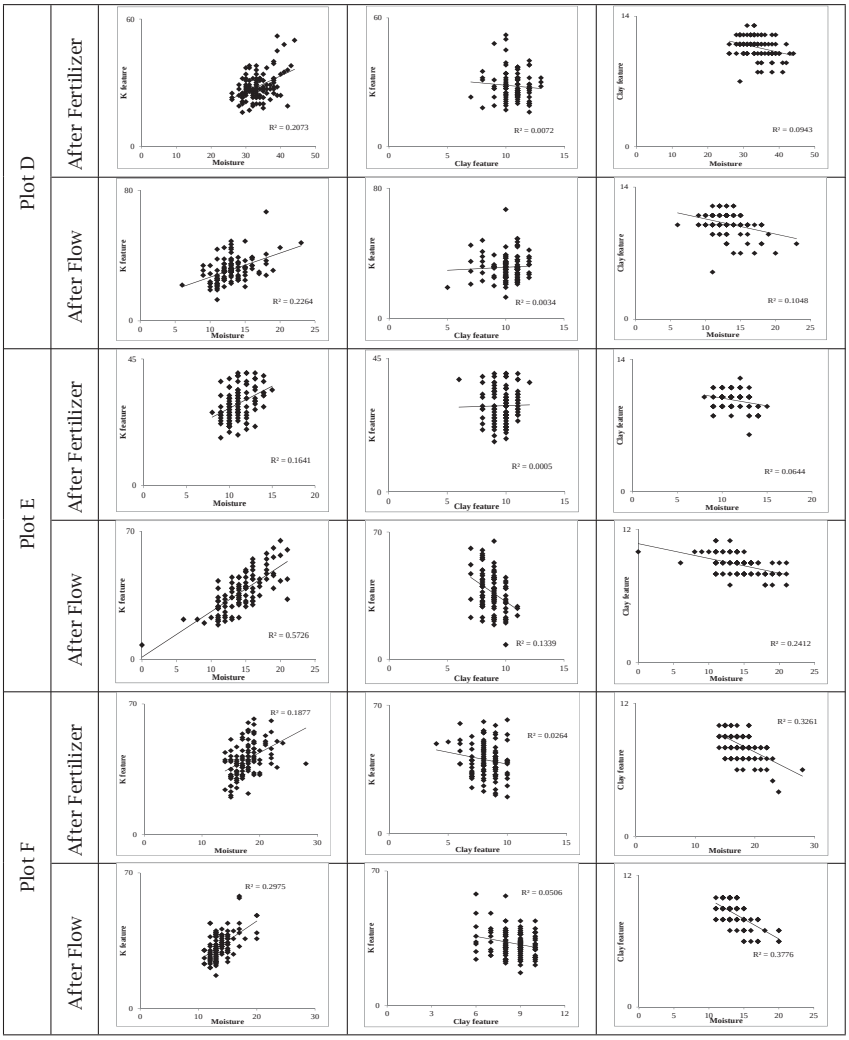

Figure 6.6: Relationships between band depth near 2465 nm (K feature), band depth near 2200 nm (Clay feature) and NSMI values (Soil moisture) expressed using coefficient of determination (R^2) for experimental plots D, E and F.

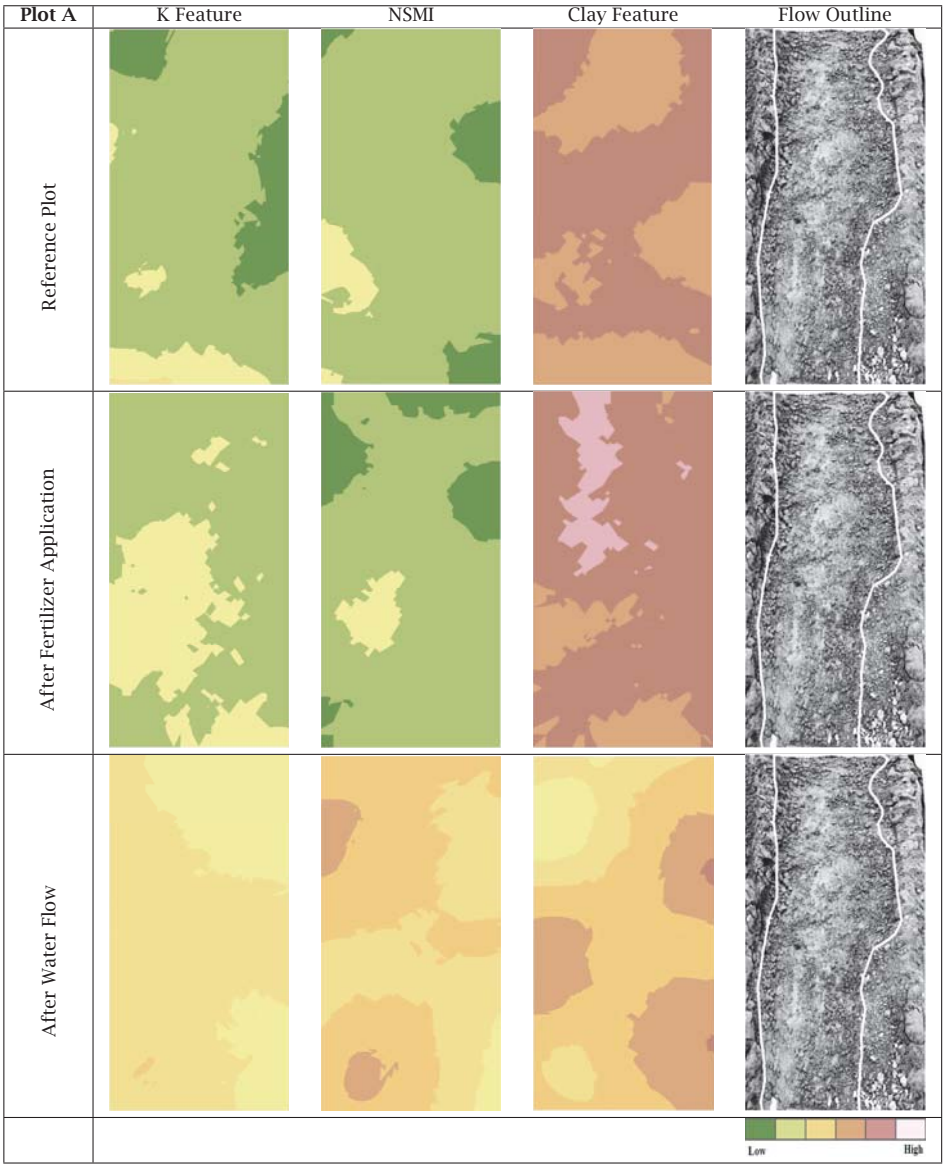

Figure 6.7: Spatial representation of K absorption feature depth near 2465 nm, Normalised Soil Moisture Index (NSMI) and clay absorption feature depth near 2200 nm for plot A. This plot was treated with 0.6 mg/g of fertilizer. Each image comprises 108 sampling points collected after each stage of the field experiment (before treatment, after addition of fertilizer, and after water flow).

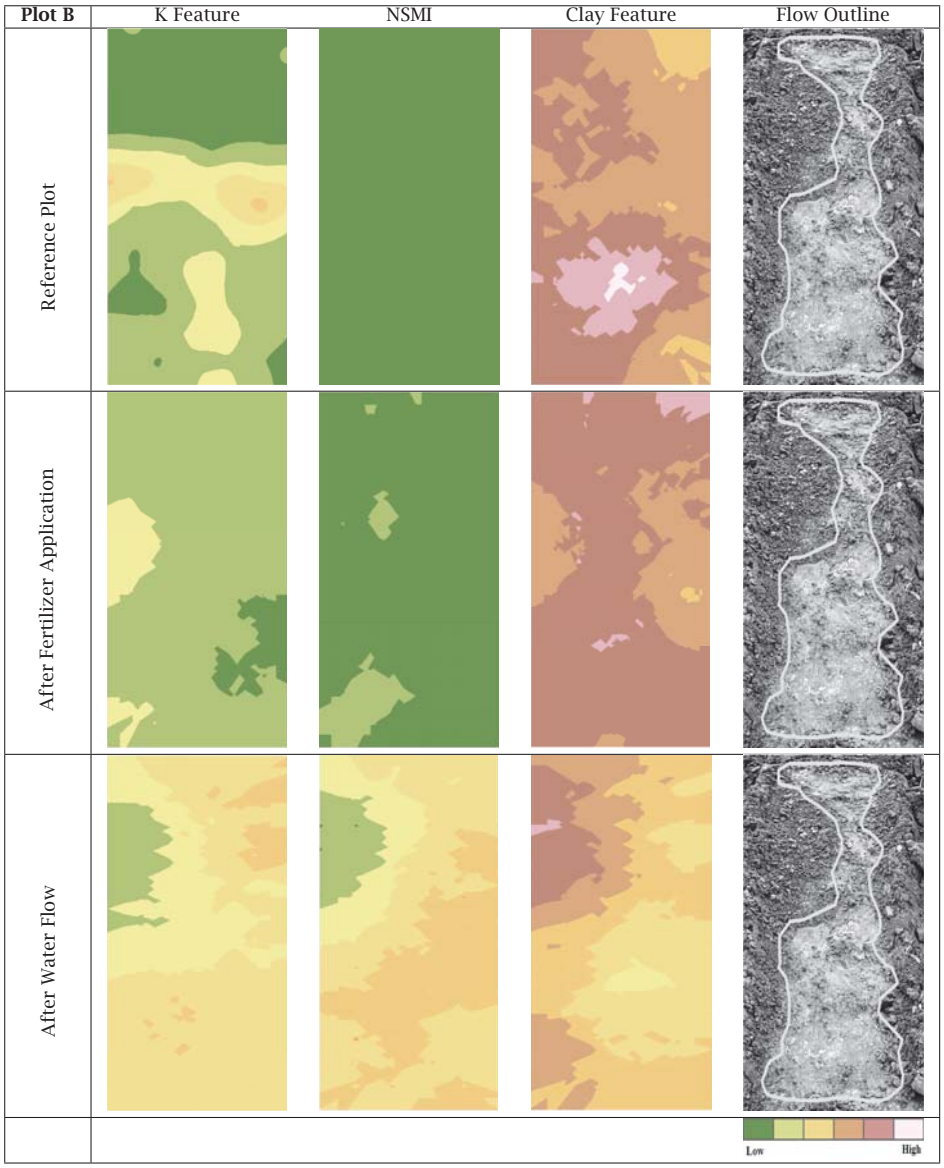

Figure 6.8: Spatial representation of K absorption feature depth near 2465 nm, Normalised Soil Moisture Index (NSMI) and clay absorption feature depth near 2200 nm for plot B. This plot was treated with 2.4 mg/g of added fertilizer. Each image comprises 108 sampling points collected after each stage of the field experiment (before treatment, after addition of fertilizer, and after water flow)

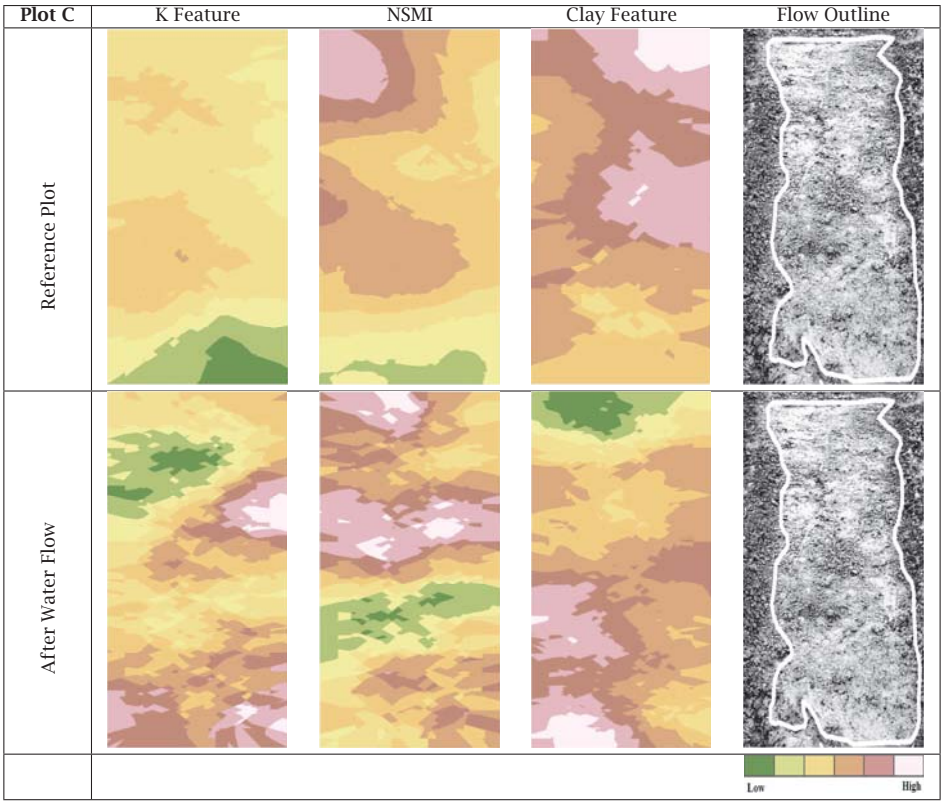

Figure 6.9: Spatial representation of K absorption feature depth near 2465 nm, Normalised Soil Moisture Index (NSMI) and clay absorption feature depth near 2200 nm for plot C. This plot had no added fertilizer. Each image comprises 108 sampling points collected from the untreated plot and after water flow.

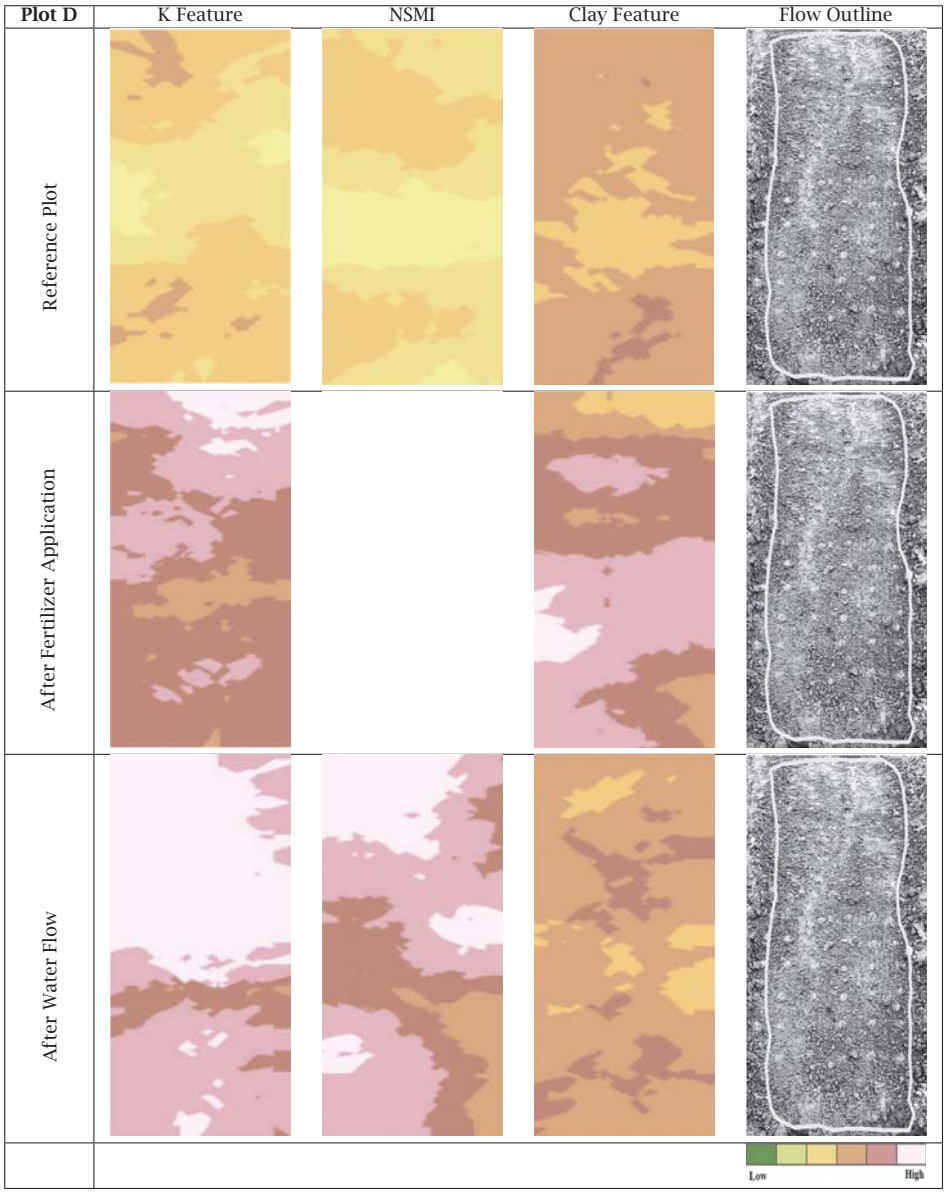

Figure 6.10: Spatial representation of K absorption feature depth near 2465 nm, Normalised Soil Moisture Index (NSMI) and clay absorption feature depth near 2200 nm for plot D. This plot was treated with 1.18 mg/g of added fertilizer. Each image comprises 108 sampling points collected after each stage of the field experiment (before treatment, after addition of fertilizer, and after water flow)

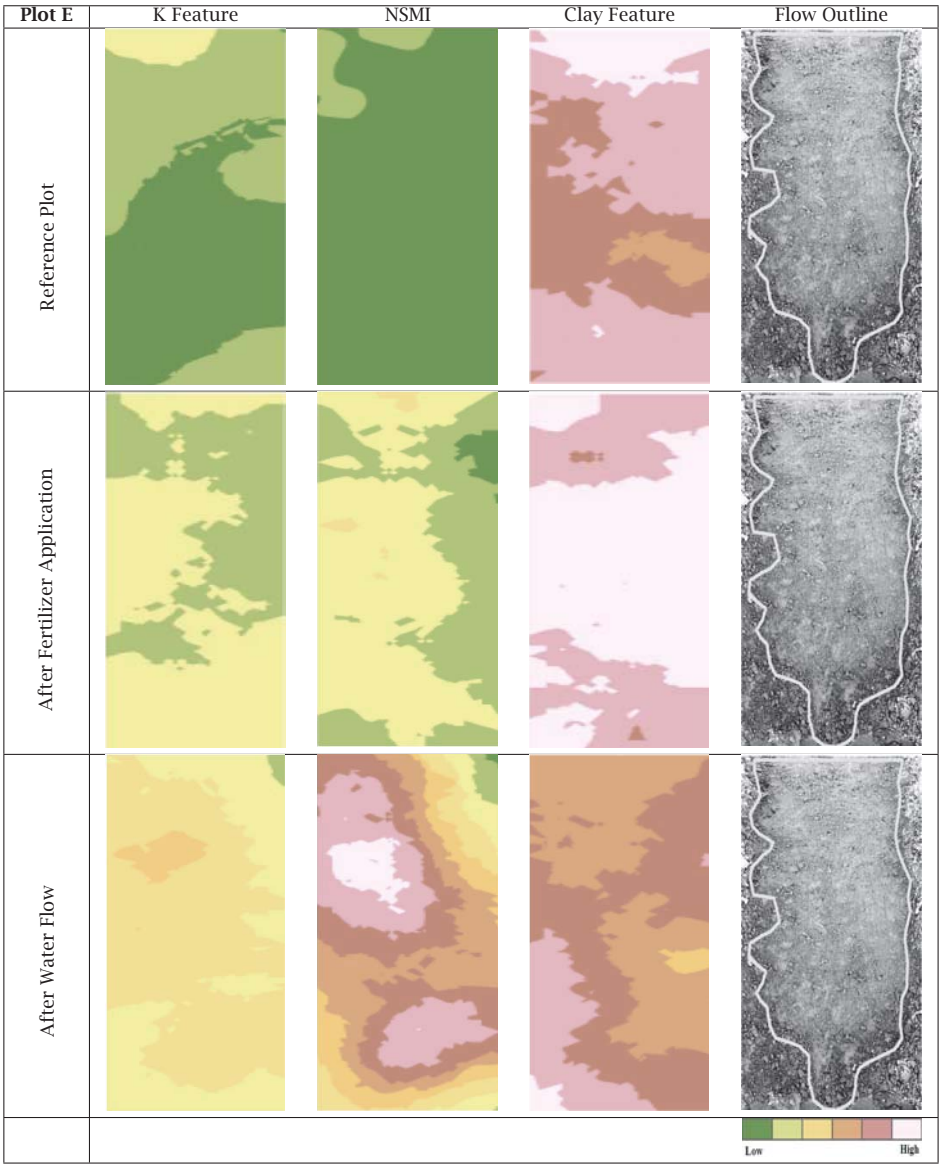

Figure 6.11: Spatial representation of K absorption feature depth near 2465 nm, Normalised Soil Moisture Index (NSMI) and clay absorption feature depth near 2200 nm for plot E. This plot was treated with 1.76 mg/g of added fertilizer. Each image comprises 108 sampling points collected after each stage of the field experiment (before treatment, after addition of fertilizer, and after water flow)

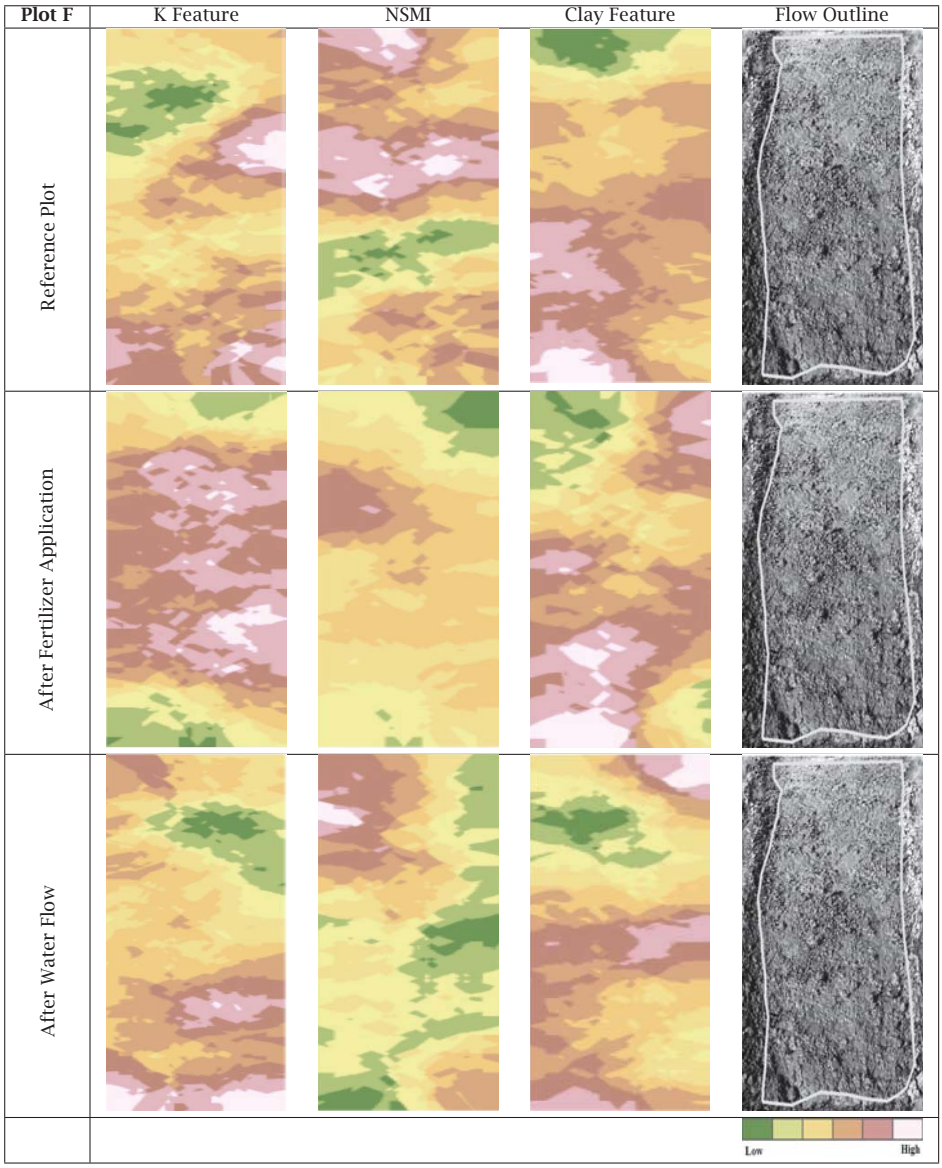

Figure 6.12: Spatial representation of K absorption feature depth near 2465 nm, Normalised Soil Moisture Index (NSMI) and clay absorption feature depth near 2200 nm for plot F. This plot was treated with 0.6 mg/g of added fertilizer. Each image comprises 108 sampling points collected after each stage of the field experiment (before treatment, after addition of fertilizer, and after water flow)

6.4 Discussion

6.4.1 Potassium Fertilizer Mobility

The K concentration in the mixed runoff sediment samples was 1.2 mg/g, which is 0.6 mg/g higher than the amount of K that was added with the fertilizer (0.6 and 2.4 mg/g for plot A and plot B respectively). This might be due to the release of slowly available K under the influence of water flow. Alternatively, it may so result from K fertilizer that had been applied by farmers before the experiment, as the experiment took place in an agricultural field. Unknown concentrations of K in the water that was used for the experiment could also add to these amounts. Soil texture is not considered to have an influence, since the texture analysis of the soil material indicates a comparable sand-silt-clay content of all plots (table 6.1).

6.4.2 Change in absorption feature depth in relation to K concentrations

For all plots, figures 6.5 and 6.6 show that after applying fertilizer, the increase in K is associated with increase in moisture, indicating that more K was added. In addition, there is no relation between K and clay, which is expected due to the fact that K was added to the plots and the concentrations became higher than the natural K that is already attached to the clay. The lack of relationship between moisture and clay can be explained by the soil saturation, which is irrespective of clay content.

After the flow, the relation between K and moisture is generally decreasing. K and clay relation increases, because clay starts absorbing K, so more clay means less free K. The moisture is removed from the top soil so the clay content causes the moisture to be retained and shows a high relation again.

Figures 6.7–6.12 show the change in surface soil moisture, K absorption band depth and clay absorption band depth for all plots and all stages of the experiment. With the addition of K, a change in depth of the feature near 2465 nm is observed. Although the fertilizer was applied as evenly as possible to the surface of all plots, a uniform distribution cannot be observed. This is likely to be a result of natural variation in the initial K

concentration, application of fertilizer by farmers prior to the experiment, or due to the difference in surface roughness.

On Figure 6.7 the reference images clearly indicate that K in concentrations of 0.6 mg/g cannot be used to explain soil erosion. K has low values, absorption feature depth increases as fertilizer solution is added and stays higher as additional water is added with the flow. The high moisture values indicate that the plot has not dried out completely. A general decrease in clay can be due to erosion and movement of particles. However since the central plot shows a higher content of clay, there is interference from moisture and K.

Figure 6.8 shows the images from the plot with 2.4 mg/g of added fertilizer. Although the added concentrations are much higher, the results do not indicate runoff. The wetter plots after the experiment show that the plots have not dried out completely. The decrease in clay could again be associated with movement of particles due to erosion.

Figure 6.9 shows the results from the reference plot with no added fertilizer. All measurements were collected from points on the plot covered by the flow. The variability suggests movement of K downslope after the flow experiment. Clay content shows a similar pattern to K, and therefore there is an indication that clay has moved downslope. This suggests that K movement is caused by the movement of clay particles with the flow.

Figure 6.10 illustrates the plot with added 1.18 mg/g of fertilizer. The image in the middle shows that moisture was evenly distributed after applying the fertilizer solution. The added K has moved down and spread over showing a clear movement of K. Moisture has influenced clay absorption, and therefore movement cannot be established.

Figure 6.11 shows the results from the plot with added 1.76 mg/g of K fertilizer. After the flow, loss of K can be observed in some parts of the image. The moisture values indicate that the plot has not dried out completely. The clay images show small movement of clay away form the plot at the lower and upper middle portions.

Figure 6.12 illustrates the results from the experiment with 0.6 g/mg of added fertilizer. The low K concentrations show a little bit of movement from the applied K in the center to the bottom of the plot. Moisture image suggests moisture is relatively homogeneous and so not of great influence. Clay does not seem to show changes.

In general, after water flow, the K absorption feature appears deeper. From Figure 6.3 that shows flow coverage, and Figures 6.7–6.12 showing change in absorption depth, it can be observed that the patches that were not covered by the water flow have the shallowest spectral absorption features. Variations within the plots can also be due to larger particles that travel shorter distances and might be deposited early [Morgan, 2005], before reaching the end of the plot.

The spatial representation of soil moisture and clay content, as presented by NSMI and clay absorption band depth, show their influence on spectroscopic detection of K in soils.

In all images, NSMI increased after each stage of the experiment (Figures 6.7–6.12). The depth of clay absorption feature decreased after water flow, which can be explained by the removal of fine clay particles by flowing water.

Based on the work of Luleva et al. [2011] and Yitagesu et al. [2009], it was expected that clay content would influence the depth of absorption near 2465 nm. The experimental field was hence selected in the Loess derived soils, which only have a maximum of 18 % clay [Jacobs and Mason, 2007]. However, as stated by Jacobs and Mason [2007], clay content in Loess soils can be higher if post sedimentation has taken place. The concentration of K applied to the plots was insufficient to show a spectral signature given the high amounts of water and clay are present. Additional tests are required in order to establish whether decrease in clay absorption can be used to indicate removal of particles due to erosion.

A direct relationship between the K absorption band depth near 2465 nm and its distribution in the field could not be established. This would probably be possible if higher amounts of fertilizer would have been added (as done in Luleva et al. [2011]). These amounts however exceed what is recommended for agricultural practices. Exploring absorption features associated with K in the thermal (mid) infrared could minimize the influence of moisture and clay. Imaging spectrometers that acquire spatial data simultaneously could limit the noise that was now introduced while measuring individual points.

6.4.3 Potential use of Potassium as a tracer for soil erosion

In all soil erosion studies using chemical particle tracers, the even distribution of the chemical has been assumed [Chappell, 1999]. The natural variation of the element due to parent material or crop residue, as well as previously applied fertilizer, presents a limitation. This could however be overcome by collecting and analysing soil spectra prior to fertilization.

Knowing the concentration of K prior to fertilizer application is crucial for using the element as a tracer. Compared to ^{137}Cs , however, Potassium (K) is spectrally active, and the absorption feature near 2465 nm allows rapid detection of its abundance in the environment prior to additional application of the element. Furthermore, this provides an opportunity to collect measurements before each stage of the field experiment. This helps determining the natural distribution of the element or previously applied quantities of fertilizer, as well as testing the method and distribution of added K before the flow experiment.

A factor that should be considered when using K as a tracer is its behaviour when introduced to the environment. While radioactive elements are considered to move only due to erosion, when attached to soil particles, K can be moved due to uptake by plants or by leaching into the subsurface. To prevent vegetation uptake and to allow collection of soil spectra using hyperspectral imagers, measurements are limited to the time between fertilizer application and crop growth. In addition, clay and moisture content restrict the applicability of the method at concentrations of applied fertilizer lower than 2.48 mg/g soil, as presented in this study.

6.5 Conclusions

In this chapter, we discussed the use of infrared spectroscopy for detecting changes in K concentrations in soils. Potassium (K) fertilizer for commercial use was applied in various concentrations to six experimental plots on silt loam soils. A flow experiment was conducted, and spectral measurements were collected to determine change in K before application of fertilizer, after application of fertilizer and after water flow. Laboratory and spectral analyses were performed to determine the change in absorption characteristics associated with K.

The study aimed to provide answers to three main questions.

- Can a relative change in abundance of K in the field be observed with spectroscopy using the absorption feature near 2465 nm? A relative change in abundance of K could be observed in the field using the spectral absorption feature near 2465 nm.
- Does the amount of K removed by water flow correspond to the concentration of K found in runoff water? The amount of K removed with water flow corresponds to concentrations of K found in the sediment of the runoff water, although background concentrations from either naturally occurring K or previously applied fertilizer had increased the amount of K.
- Does a change in depth of the 2465 nm absorption feature correspond with the controlled addition and removal of K? Change in the 2465 nm absorption feature depth does not seem to correspond to the controlled addition and removal of K. This is likely to be a result of external influences such as moisture and clay content.

Although previous studies indicate the suitability of the method at laboratory level [Luleva et al., 2011], in the field, the absorption feature near 2465 nm, associated with K, is highly influenced by moisture and clay content, at concentrations of K typically applied to agricultural fields.

If further work is intended, the method can only be applied successfully using quantities of fertilizer higher than 2.48 mg/g, or on soils with lower than 18 % clay content. Establishing K as a particle tracer can provide an opportunity for increase in size of study area and density of sampling points. This however could be possible only give that the limitations, identified in the current study, can be overcome at field level.

7 General Discussion and Conclusions

The aim of this research was to identify the most suitable chemical soil particle tracer, and to evaluate whether change in concentration of this element can be detected with infrared spectroscopy by establishing direct relationships between concentrations and absorption band parameters of the soil spectral signature. The scope of the research is limited by the concentrations, in which the element is present. They should be high enough to have influence on the shape of the spectral curve, but low enough not to cause disturbance and contamination to the environment.

In Chapter 2, the use of remote sensing techniques in land degradation and soil erosion studies was evaluated. It was established that the majority of studies used data derived only from the visible and near infrared part of the spectrum. There are a number of reasons behind this, most probable of which are the low cost and availability of the imagery, as well as the relatively easy to apply analytical techniques. Shortwave infrared spectrum, covered by many of the available sensors, however, contains information about soil chemical composition that has not been fully explored in studies of soil erosion. Soil particle tracing technique was outlined, where shortwave infrared data could be used to improve the findings. To date, the most commonly used soil particle tracer is the isotope Cesium 137 (^{137}Cs). There are a number of limitations associated with the use of this isotope, including its limited half-life, assumed even spatial distribution as well as high cost of measuring techniques. Hence in this chapter it is suggested that there is a clear gap and need in finding an alternative soil particle tracer that can be measured using remote sensing techniques.

Following in Chapter 3, a method to establish direct and indirect relationships between soil chemical composition and infrared spectral response is presented. The aim of the chapter was to evaluate common elements abundant in prone to erosion soils that have the potential to be used as an alternative particle tracer. Specific wavelength ranges that statistically predict and quantify soluble fractions of chemical elements, from near infrared and shortwave infrared spectroscopy were outlined. Partial least squares regression (PLSR) was used to develop prediction models for Calcium (Ca), Magnesium (Mg), Potassium (K), Sodium (Na), Iron (Fe), and acidity (pH) in silt loam soil samples. The element that showed highest coefficients of determination with spectra and had the closest physical and chemical properties as ^{137}Cs was Potassium.

The study was then focused more closely on testing whether Potassium can serve as a potential soil particle tracers as an alternative to Cesium 137 (^{137}Cs). When large areas are considered, the expensive soil sampling and analysis present an obstacle for determining concentrations of this isotope. Infrared spectral measurements provide a solution, however the small concentrations of the isotope do not influence the spectral signal sufficiently. Therefore, based on the fact that Potassium (K) has similar electrical, chemical and physical properties it was initially hypothesised that it can be used as possible replacement in soil particle tracing. The study was conducted under laboratory conditions on soils of six different texture types. The results were promising, identifying wavelengths between 2450 and 2470 nm to be affected directly by the amount of applied K. Absorption feature parameters (absorption band depth, width and area) were also found to change with K concentration with coefficient of determination between 0.85 and 0.99. In order for this methodology to work, however, there were two main aspects that had to be considered. First, the presence of high clay content in the soil sample, showed to have influence on the depth of absorption near 2460 nm. Second, at low concentrations, change in absorption of Potassium was observed with addition of fertilizer, however statistical relationships between absorption band parameters and added concentrations were not established, and therefore quantification could not be performed.

Based on these findings, the study was taken to the field, where the behaviour of K was tested by applying typically used concentrations of K

fertilizer. Chapter 5 and 6 describe the flow experiment that was conducted on silt loam Calcisols and Loess soils. Spectral measurements were built into synthetic images to represent the spatial extent and variation of the tests. In Chapter 5, the study was conducted in highly susceptible to erosion area in Murcia, Spain. Clay content of Calcisols, however, showed to be sufficiently high, while the concentration of fertilizer applied to the experimental plot was too low. Moreover, the runoff sediment were not collected, and therefore it could not be shown if the fertilizer was removed by the water flow with the soil particles, or it has been diluted or has leached down the soil profile. However, the methodology of spectral data collection and analysis proved effective in terms of minimizing the amount of noise caused by external factors in the far end of the shortwave electromagnetic spectrum, and at the same time allowed spatial representation of absorption caused by K presence.

Taking these limitations into account, a second field experiment took place, described in Chapter 6. The study area in Southeast Limburg, The Netherlands, was selected due to the fact that the soil is Loess, characterized by minimal clay content. The setup was improved by including more plots and adding various concentrations of fertilizer. The runoff sediment was collected together with soil samples for validation. The presence of moisture and clay in the soils, however, still proved to mask the influence of K on the spectral signal.

The advantage of using K as a particle tracer and measuring it with infrared spectroscopy is that the initial distribution of the element can be determined prior and after additional application. By doing so, the distribution of the element can be established and assumptions do not need to be made. In comparison, the even distribution of ^{137}Cs is always assumed and therefore it has been a cause of debate, although some studies have provided supporting arguments based on climatological factors and study area locations [Chappell, 1999].

Knowing the concentrations of K prior to fertilizer application is crucial for using the element as a tracer. The natural variation of K due to the nature of the parent material or crop residue, as well as previously applied fertilizer should be established or measured. One way is to analyse reference soil samples prior to annual fertilizer application, as shown in the current study, or consult reference soil maps and farmers.

A factor that should be considered when using K as a tracer is its behaviour when introduced to the environment. While radioactive elements are considered to move only due to erosion, as attached to soil particles, K can be moved due to uptake by plants or by leaching. To prevent the vegetation uptake, a soil erosion study using K should take place between the time of fertilizer application and crop growth. The study should also be performed on silt loam soils, characteristic for soil erosion, and at the same time limiting K leaching by having higher organic matter contents [Askegaard and Eriksen, 2000].

Exploring K as a soil particle tracer introduces a number of advantages to current erosion studies. It is applied annually as a fertilizer and therefore does not have a half-life as radioactive elements do. The scope of the study, however, was limited to K concentrations that are not harmful to the environment, and are regularly applied during agricultural practices. Thus, a methodology would be suitable for effective monitoring of early signs of soil erosion. Although high concentrations of Potassium in the laboratory showed promising results, high amounts of fertilizer were not used in the field experiments. The focus of this study was put on the removal of K under the influence of water flow. Therefore, in order to establish whether sedimentation and deposition can be measured, additional tests should be conducted at the locations where the flow stops. Additionally, it is recommended that further tests on K leaching are performed, despite that, as described in Chapters 4 and 6, leaching is unlikely to occur for the duration of the proposed experiment. Considering the need to find an alternative to ^{137}Cs particle tracer, applying the above recommendations are encouraged. Potassium is harmless to the environment, and therefore would be a desirable particle tracer.

Based on the findings of this research, the concentrations of the element show high correlations with absorption feature parameters within the shortwave infrared only at very high concentrations and under laboratory conditions [Luleva et al., 2011]. At concentrations typically applied by farmers, the influence of moisture and clay content limit the application of the technique in field conditions.

The detailed spatial patterns vary wildly between phases of the experiment, although in some cases they are logical with movement of K and clay. Varying moisture contents obscure clear results. Also the amount

of water applied did not cause any visible erosion in the form of rills, the relatively high clay content creates a relatively stable structure.

However, common features can be observed from the correlation plots. These coincide with the processes that are taking place (runoff, infiltration, absorption and solution of K, movement of clay particles). In future experiments where higher rate of erosion is created (e.g. with a rainfall simulator) or under field circumstances with heavy rainfall, the results might be clearer.

In most plots, a movement of clay particles was observed. Detailed roughness analysis and identifying indicators for where puddles and micro-sedimentation occur, could widen the scope for further explanation of the crusting process. In addition, studies of pesticides absorbing to the clay on the soil surface, could benefit from these results, but further investigation is necessary.

Infrared cameras should replace the use of ASD spectrometer in order to reduce cross contamination and noise introduced during the measurements. Studies use information derived from the thermal infrared part of the spectrum [Yitagesu et al., 2009] where it is seen that clays rich in K show distinct absorption based on the concentration of the element. Exploring this part of the spectrum could provide a mean to deal with the noise introduced by clay content in the shortwave infrared. Due to these limitations, the study was terminated at an experimental stage. Considering that K is applied by farmers in relatively low concentrations, rapid particle tracing detection might not prove successful in uncontrolled fields. Nevertheless, if the method is applied on fields that are fertilized with higher amounts of K_2O , the method has potential. A condition that has to be met is that the initial concentration of K before fertilizer application is known.

Upscaling the experiment to hyperspectral remotely sensed imagery was initially intended, however this would only be successful once the above limitations are handled. A possible continuation of the study will have to look into testing new methodologies outside the controlled experimental setting prior to image interpretation.

Bibliography

L. C. Alatorre and S. Begueria. Identification of eroded areas using remote sensing in a badlands landscape on marls in the central Spanish Pyrenees. *CATENA*, 76(3):182–190, 2009.

J. Ali, K. Pramod, and S. Ansari. Near-infrared spectroscopy for nondestructive evaluation of tablets. *Systematic Reviews in Pharmacy*, 1:17–23, 2010.

Alterra. Desire project, http://www.desire-project.eu/. *DESIRE*, 2007.

T. J. Andersen, O. A. Mikkelsen, A. L. Moller, and P. Morten. Deposition and mixing depths on some European intertidal mudflats based on 210Pb and 137Cs activities. *Continental Shelf Research*, 20(12–13):1569–1591, 2000.

K. Anderson and N. J. Kuhn. Variations in soil structure and reflectance during a controlled crusting experiment. *International Journal of Remote Sensing*, 29(12):3457–3475, 2008.

A. C. Andrello and C. R. Appoloni. Spatial variability and Cesium-137 inventories in native forest. *Brazilian Journal of Physics*, 34:800–803, 2004.

M. Askegaard and J. Eriksen. Potassium retention and leaching in an organic crop rotation on loamy sand as affected by contrasting potassium budgets. *Soil Use and Management*, 16(3):200–205, 2000.

G. P. Asner and K. B. Heidebrecht. Imaging spectroscopy for desertification studies: comparing AVIRIS and EO-1 Hyperion in Argentina drylands. *Geoscience and Remote Sensing, IEEE Transactions on*, 41(6):1283–1296, 2003.

J. Baartman, A. Veldkamp, J. Schoorl, J. Wallinga, and L. Cammeraat. Unravelling late Pleistocene and Holocene landscape dynamics: The upper Guadalentin basin, SE Spain. *Geomorphology*, 125(1):172 – 185, 2011.

E. M. Barnes, K. A. Sudduth, J. W. Hummel, S. M. Lesch, D. L. Corwin, C. H. Yang, C. S. T. Daughtry, and W. C. Bausch. Remote- and ground-based sensor techniques to map soil properties. *Photogrammetric Engineering and Remote Sensing*, 69(6):619–630, 2003.

P. Barre, C. Montagnier, C. Chenu, L. Abbadie, and B. Velde. Clay minerals as a soil potassium reservoir: observation and quantification through X-ray diffraction. *Plant and Soil*, 302(1):213–220, 2008.

M. Baumgardner, L. Silva, L. Biehl, and E. Stoner. Reflectance properties of soil. *Advances in Agronomy*, 38:1–44, 1985.

M. Belivermis. Vertical distributions of 137Cs, 40K, 232Th, and 226Ra in soil samples from Istanbul and its environs, Turkey. *Radiation Protection Dosimetry*, 2012.

E. Ben-Dor. *Quantitative remote sensing of soil properties*, volume 75, pages 173–243. Academic Press, 2002.

E. Ben-Dor and A. Banin. Near infrared analysis (NIRA) as a method to simultaneously evaluate spectral featureless constituents in soils. *Soil Science*, 159(4):259–270, 1995.

E. Ben-Dor, N. Goldlshleger, Y. Benyamini, M. Agassi, and D. G. Blumberg. The spectral reflectance properties of soil structural crusts in the 1.2 to 2.5 micrometers spectral region. *Soil Sci Soc Am J*, 67(1):289–299, 2003.

E. Ben-Dor, D. Heller, and A. Chudnovsky. A novel method of classifying soil profiles in the field using optical means. *Soil Sci. Soc. Am. J.*, 72(4): 1113–1123, 2008.

H. D. Betts and R. C. DeRose. Digital elevation models as a tool for monitoring and measuring gully erosion. *International Journal of Applied Earth Observation and Geoinformation*, 1(3–4):235–235, 1999.

J. Boardman. Soil erosion science: Reflections on the limitations of current approaches. *CATENA*, 68(2–3):73–86, 2006.

J. Boardman and B. Evans. *Britain*, pages 439–453. John Wiley & Sons, Ltd, 2006.

J. Boardman, L. Ligneau, A. de Roo, and K. Vandaele. Flooding of property by runoff from agricultural land in Northwestern Europe. *Geomorphology*, 10(1–4):183–196, 1994.

J. Boardman, M. L. Shepheard, E. Walker, and I. D. L. Foster. Soil erosion and risk-assessment for on- and off-farm impacts: A test case using the Midhurst area, West Sussex, UK. *Journal of Environmental Management*, 90(8):2578–2588, 2009.

P. Bogaert and D. D'Or. Estimating soil properties from thematic soil maps: The Bayesian maximum entropy approach. *Soil Sci Soc Am J*, 66 (5):1492–1500, 2002.

I. Bogrekci and W. S. Lee. Effects of soil moisture content on absorbance spectra of sandy soils in sensing phosphorus concentrations using UV-VIS-NIR spectroscopy. *Trans. ASABE*, 49(4):1175–1180, 2006.

CAMO Software AS. The unscrambler, 2010.

B. L. Campbell, R. J. Loughran, and G. L. Elliott. Caesium-137 as an indicator of geomorphic processes in a drainage basin system. *Australian Geographical Studies*, 20(1):49–64, 1982.

R. Casa, F. Castaldi, S. Pascucci, A. Palombo, and S. Pignatti. A comparison of sensor resolution and calibration strategies for soil texture estimation from hyperspectral remote sensing. *Geoderma*, 197âĂŞ198(0):17–26, 2013.

O. Cerdan, G. Govers, Y. Le Bissonnais, K. Van Oost, J. Poesen, N. Saby, A. Gobin, A. Vacca, J. Quinton, K. Auerswald, A. Klik, F. J. P. M. Kwaad, D. Raclot, I. Ionita, J. Rejman, S. Rousseva, T. Muxart, M. J. Roxo, and T. Dostal. Rates and spatial variations of soil erosion in Europe: A study based on erosion plot data. *Geomorphology*, 122(1–2):167–177, 2010.

S. Chabrillat, A. F. H. Goetz, L. Krosley, and H. W. Olsen. Use of hyperspectral images in the identification and mapping of expansive clay soils and the role of spatial resolution. *Remote Sensing of Environment*, 82(2–3): 431–445, 2002.

A. Chappell. Modelling the spatial variation of processes in the redistribution of soil: digital terrain models and 137Cs in southwest Niger. *Geomorphology*, 17(1–3):249–261, 1996.

A. Chappell. Using remote sensing and geostatistics to map 137Cs-derived net soil flux in South-west Niger. *Journal of Arid Environments*, 39(3): 441–455, 1998.

A. Chappell. The limitations of using 137Cs for estimating soil redistribution in semi-arid environments. *Geomorphology*, 29(1–2):135–152, 1999.

A. Chappell, T. M. Zobeck, and G. Brunner. Using on-nadir spectral reflectance to detect soil surface changes induced by simulated rainfall and wind tunnel abrasion. *Earth Surface Processes and Landforms*, 30(4): 489–511, 2005.

R. N. Clark, T. V. V. King, M. Klejwa, G. A. Swayze, and N. Vergo. High spectral resolution reflectance spectroscopy of minerals. *J. Geophys. Res.*, 95(B8):12653–12680, 1990.

A. L. Collins, D. E. Walling, H. M. Sichingabula, and G. J. L. Leeks. Using 137Cs measurements to quantify soil erosion and redistribution rates for areas under different land use in the Upper Kaleya river basin, Southern Zambia. *Geoderma*, 104(3–4):299–323, 2001.

H. Croft, K. Anderson, and N. J. Kuhn. Characterizing soil surface roughness using a combined structural and spectral approach. *European Journal of Soil Science*, 60(3):431–442, 2009.

R. C. Dalal and R. J. Henry. Simultaneous determination of moisture, organic carbon, and total nitrogen by near infrared reflectance spectrophotometry. *Soil Sci Soc Am J*, 50(1):120–123, 1986.

S. Dasgupta, J. J. Qu, X. Hao, and S. Bhoi. Evaluating remotely sensed live fuel moisture estimations for fire behavior predictions in georgia, usa. *Remote Sensing of Environment*, 108(2):138–150, 2007.

B. S. Dayal and J. F. MacGregor. Recursive exponentially weighted PLS and its applications to adaptive control and prediction. *Journal of Process Control*, 7(3):169–179, 1997.

H. de Bakker. *Major soils and soil regions in the Netherlands*. W. Junk, PUDOC, The Hague etc. ; Wageningen, 1979.

S. M. de Jong and V. G. Jetten. Estimating spatial patterns of rainfall interception from remotely sensed vegetation indices and spectral mixture

analysis. *International Journal of Geographical Information Science*, 21 (5):529–545, 2007.

S. M. de Jong, M. L. Paracchini, F. Bertolo, S. Folving, J. Megier, and A. P. J. de Roo. Regional assessment of soil erosion using the distributed model SEMMED and remotely sensed data. *CATENA*, 37(3–4):291–308, 1999.

J. B. deGraffenried Jr and K. D. Shepherd. Rapid erosion modeling in a Western Kenya watershed using visible near infrared reflectance, classification tree analysis and 137Cesium. *Geoderma*, 154(1–2):93–100, 2009.

S. H. Doerr, R. A. Shakesby, and R. P. D. Walsh. Soil water repellency: its causes, characteristics and hydro-geomorphological significance. *Earth-Science Reviews*, 51(1–4):33–65, 2000.

M. Eghbal, M. Hajabbasi, and H. Golsefidi. Mechanism of crust formation on a soil in central Iran. *Plant and Soil*, 180(1):67–73, 1996.

W. Ellison. Studies of raindrop erosion. *Journal of Agricultural Engineering*, 25:131–136, 1944.

J. Estrany, C. Garcia, and D. E. Walling. An investigation of soil erosion and redistribution in a Mediterranean lowland agricultural catchment using Caesium-137. *International Journal of Sediment Research*, 25(1):1–16, 2010.

R. Evans. An alternative way to assess water erosion of cultivated land — field-based measurements: and analysis of some results. *Applied Geography*, 22(2):187–207, 2002.

J. S. Famiglietti, J. A. Devereaux, C. A. Laymon, T. Tsegaye, P. R. Houser, T. J. Jackson, S. T. Graham, M. Rodell, and P. J. van Oevelen. Ground-based investigation of soil moisture variability within remote sensing footprints during the Southern Great Plains 1997 (sgp97) hydrology experiment. *Water Resour. Res.*, 35(6):1839–1851, 1999.

FAO. World reference base for soil resources. Technical Report Reports 103, ISRIC, ISSS, 1998.

FAO. World reference base for soil resources. Technical Report Reports 103, Food and Agriculture Organization of the United Nations, 2006.

J. Farifteh, F. van der Meer, C. Atzberger, and E. J. M. Carranza. Quantitative analysis of salt-affected soil reflectance spectra: A comparison of two

adaptive methods (PLSR and ANN). *Remote Sensing of Environment*, 110 (1):59–78, 2007.

D. Flanagan and J. Laflen. USDA water erosion prediction project, WEPP. *Eurasian soil science*, 30(5):524–530, 1997.

L. S. Galvao and I. Vitorello. Variability of laboratory measured soil lines of soils from Southeastern Brazil. *Remote Sensing of Environment*, 63(2): 166–181, 1998.

D. E. Garrett. *Potash: Deposits, Processing, Properties and Uses*. Chapman & Hall, London, first edition edition, 1996.

N. Goldshleger, E. Ben-Dor, R. Lugassi, and G. Eshel. Soil degradation monitoring by remote sensing: Examples with three degradation processes. *Soil Sci. Soc. Am. J.*, 74(5):1433–1445, 2010.

N. Goldshleger, I. Livne, A. Chudnovsky, and E. Ben-Dor. New results in integrating passive and active remote sensing methods to assess soil salinity: A case study from jezre'el valley, israel. *Soil Science*, 177(6): 392–401, 2012.

C. Gomez, P. Lagacherie, and G. Coulouma. Continuum removal versus plsr method for clay and calcium carbonate content estimation from laboratory and airborne hyperspectral measurements. *Geoderma*, 148 (2):141–148, 2008.

M. F. Guimaraes, V. F. N. Filho, and J. Ritchie. Application of cesium-137 in a study of soil erosion and deposition in Southeastern Brazil. *Soil Science*, 168(1):45–53, 2003.

D. M. Haaland and E. V. Thomas. Partial least-squares methods for spectral analyses. 1. relation to other quantitative calibration methods and the extraction of qualitative information. *Analytical Chemistry*, 60(11):1193–1202, 1988.

D. Haase, J. Fink, G. Haase, R. Ruske, M. Pécsi, H. Richter, M. Altermann, and K. D. Jäger. Loess in Europe — its spatial distribution based on a European loess map, scale 1:2,500,000. *Quaternary Science Reviews*, 26 (9–10):1301–1312, 2007.

H. Hasegawa. Spectroscopic studies on the color reaction of acid clay. iii. the coloration with polyenes and polyacenes. *The Journal of Physical Chemistry*, 67(6):1268–1270, 1963.

S. N. Haubrock, S. Chabrillat, C. Lemmnitz, and H. Kaufmann. Surface soil moisture quantification models from reflectance data under field conditions. *International Journal of Remote Sensing*, 29(1):3–29, 2008.

T. Hengl, D. G. Rossiter, and A. Stein. Soil sampling strategies for spatial prediction by correlation with auxiliary maps. *Soil Research*, 41(8):1403–1422, 2003.

J. Hernandez Bastida, N. Vela De Oro, and R. Ortiz Silla. Electrolytic conductivity of semiarid soils (Southeastern Spain) in relation to ion composition. *Arid Land Research and Management*, 18(3):265–281, 2004.

W. Herrmann, M. Blake, M. Doyle, D. Huston, J. Kamprad, N. Merry, and S. Pontual. Short wavelength infrared (SWIR) spectral analysis of hydrothermal alteration zones associated with base metal sulfide deposits at Rosebery and Western Tharsis, Tasmania, and Highway-Reward, Queensland. *Economic Geology*, 96(5):939–955, 2001.

R. Hessel and V. Jetten. Suitability of transport equations in modelling soil erosion for a small Loess plateau catchment. *Engineering Geology*, 91(1): 56–71, 2007.

A. Holden. Engineering soil mapping from airphotos. *Photogrammetria*, 23(6):185–199, 1968.

G. Hunt and J. Salisbury. Visible and near-infrared spectra of minerals and rocks: I silicate minerals. *Modern Geology*, 1:283–300, 1970.

ITT Visual Information Solutions. IDL core version 7.1.1, 2009.

P. M. Jacobs and J. A. Mason. Late Quaternary climate change, loess sedimentation, and soil profile development in the central Great Plains: A pedosedimentary model. *Geological Society of America Bulletin*, 119 (3–4):462–475, 2007.

M. Jalali. Site-specific potassium application based on the fertilizer potassium availability index of soil. *Precision Agriculture*, 8(4):199–211, 2007.

M. Jalali and D. Rowell. Potassium leaching in undisturbed soil cores following surface applications of gypsum. *Environmental Geology*, 57(1): 41–48, 2009.

M. Jalali and D. L. Rowell. The role of calcite and gypsum in the leaching of potassium in sandy soils. *Experimental Agriculture*, 39(04):379–394, 2003.

L. J. Janik, R. H. Merry, and J. O. Skjemstad. Can mid infrared diffuse reflectance analysis replace soil extractions? *Australian Journal of Experimental Agriculture*, 38(7):681–696, 1998.

V. Jetten, G. Govers, and R. Hessel. Erosion models: quality of spatial predictions. *Hydrological Processes*, 17(5):887–900, 2003.

C. T. Johnston. Probing the nanoscale architecture of clay minerals. *Clay Minerals*, 45(3):245–279, 2010.

R. J. A. Jones, G. Spoor, and A. J. Thomasson. Vulnerability of subsoils in europe to compaction: a preliminary analysis. *Soil and Tillage Research*, 73(1–2):131–143, 2003.

Y. Julien and J. A. Sobrino. The yearly land cover dynamics (ylcd) method: An analysis of global vegetation from NDVI and LST parameters. *Remote Sensing of Environment*, 113(2):329–334, 2009.

M. Khawlie, M. Awad, A. Shaban, R. Bou Kheir, and C. Abdallah. Remote sensing for environmental protection of the eastern Mediterranean rugged mountainous areas, Lebanon. *ISPRS Journal of Photogrammetry and Remote Sensing*, 57(1–2):13–23, 2002.

R. Kimura. Estimation of moisture availability over the Liudaogou river basin of the loess plateau using new indices with surface temperature. *Journal of Arid Environments*, 70(2):237–252, 2007.

C. King, N. Baghdadi, V. Lecomte, and O. Cerdan. The application of remote-sensing data to monitoring and modelling of soil erosion. *CATENA*, 62 (2–3):79–93, 2005.

R. F. Kokaly and R. N. Clark. Spectroscopic determination of leaf biochemistry using band-depth analysis of absorption features and stepwise multiple linear regression. *Remote Sensing of Environment*, 67(3):267–287, 1999.

Z. Kolahchi and M. Jalali. Effect of water quality on the leaching of potassium from sandy soil. *Journal of Arid Environments*, 68(4):624–639, 2007.

F. Kwaad, A. de Roo, and V. Jetten. *The Netherlands*, pages 477–487. John Wiley & Sons, Ltd, 2006.

F. J. P. M. Kwaad and H. J. Mücher. Degradation of soil structure by welding — a micromorphological study. *CATENA*, 23(3–4):253–268, 1994.

X. Lai, Y. Zheng, I. Sondergaard, H. Josephsen, H. Lowenstein, J. N. Larsen, H. Ipsen, and S. Jacobsen. Determination of aluminium content in aluminium hydroxide formulation by FT-NIR transmittance spectroscopy. *Vaccine*, 25(52):8732–8740, 2007.

Y. Le Bissonnais, O. Cerdan, V. Lecomte, H. Benkhadra, V. Souchère, and P. Martin. Variability of soil surface characteristics influencing runoff and interrill erosion. *CATENA*, 62(2–3):111–124, 2005.

J.-C. Lee and M. H. Ramsey. Modelling measurement uncertainty as a function of concentration: An example from a contaminated land investigation. *The Analyst*, 126(10):1784–1791, 2001.

M. Lemenih, E. Karltun, and M. Olsson. Assessing soil chemical and physical property responses to deforestation and subsequent cultivation in smallholders farming system in Ethiopia. *Agriculture, Ecosystems & Environment*, 105(1–2):373–386, 2005.

Y. Li, M. J. Lindstrom, J. Zhang, and J. Yang. Spatial variability of soil erosion and soil quality on hillslopes in the Chinese Loess Plateau. *Acta Geologica Hispanica*, 35(3–4):261–270, 2000.

X. Liu. Airborne lidar for dem generation: some critical issues. *Progress in Physical Geography*, 32(1):31–49, 2008.

D. B. Lobell and G. P. Asner. Moisture effects on soil reflectance. *Soil Sci. Soc. Am. J.*, 66(3):722–727, 2002.

F. Lopez-Granados, M. Jurado-Exposito, J. M. Pena-Barragán, and L. Garcia-Torres. Using geostatistical and remote sensing approaches for mapping soil properties. *European Journal of Agronomy*, 23(3):279–289, 2005.

M. Luleva, H. Van Der Werff, F. Van Der Meer, and V. Jetten. Observing change in potassium abundance in a soil erosion experiment with field infrared spectroscopy. *Chemistry*, 22(1):91–109, 2013.

M. I. Luleva, H. van der Werff, V. Jetten, and F. van der Meer. Can infrared spectroscopy be used to measure change in potassium nitrate concentra-

tion as a proxy for soil particle movement? *Sensors*, 11(4):4188–4206, 2011.

M. I. Luleva, H. Van Der Werff, F. Van Der Meer, and V. Jetten. Gaps and opportunities in the use of remote sensing for soil erosion assessment. *Chemistry*, 21(5):748–764, 2012.

L. Lyles. Basic wind erosion processes. *Agriculture, Ecosystems & Environment*, 22 – 23(0):91 – 101, 1988.

L. Mabit, M. Benmansour, and D. E. Walling. Comparative advantages and limitations of the fallout radionuclides 137Cs, 210Pbex and 7Be for assessing soil erosion and sedimentation. *Journal of Environmental Radioactivity*, 99(12):1799–1807, 2008.

G. W. McCarty, J. B. Reeves III, V. B. Reeves, R. F. Follett, and J. M. Kimble. Mid–infrared and near–infrared diffuse reflectance spectroscopy for soil carbon measurement. *Soil Science Society of America Journal*, 66(2): 640–646, 2002.

G. I. Metternicht and A. Fermont. Estimating erosion surface features by linear mixture modeling. *Remote Sensing of Environment*, 64(3):254–265, 1998.

G. I. Metternicht and J. A. Zinck. Evaluating the information content of jers-1 sar and landsat tm data for discrimination of soil erosion features. *ISPRS Journal of Photogrammetry and Remote Sensing*, 53(3):143 – 153, 1998.

K. Meusburger, N. Konz, M. Schaub, and C. Alewell. Soil erosion modelled with USLE and PESERA using QuickBird derived vegetation parameters in an Alpine catchment. *International Journal of Applied Earth Observation and Geoinformation*, 12(3):208–215, 2010.

M. S. Moran, D. C. Hymer, J. Qi, and Y. Kerr. Comparison of ERS-2 SAR and Landsat TM imagery for monitoring agricultural crop and soil conditions. *Remote Sensing of Environment*, 79(2–3):243–252, 2002.

R. Morgan. *Soil erosion and conservation.* Blackwell, Malden, third edition edition, 2005.

V. Mulder, S. de Bruin, M. Schaepman, and T. Mayr. The use of remote sensing in soil and terrain mapping - a review. *Geoderma*, 162(1-2):1 – 19, 2011.

M. Nael, H. Khademi, and M. A. Hajabbasi. Response of soil quality indicators and their spatial variability to land degradation in central Iran. *Applied Soil Ecology*, 27(3):221–232, 2004.

S. E. Nicholson and T. J. Farrar. The influence of soil type on the relationships between NDVI, rainfall, and soil moisture in semiarid Botswana. i. NDVI response to rainfall. *Remote Sensing of Environment*, 50(2): 107–120, 1994.

R. Nigel and S. Rughooputh. Mapping of monthly soil erosion risk of mainland Mauritius and its aggregation with delineated basins. *Geomorphology*, 114(3):101–114, 2010.

M. F. Noomen, A. K. Skidmore, F. D. van der Meer, and H. H. T. Prins. Continuum removed band depth analysis for detecting the effects of natural gas, methane and ethane on maize reflectance. *Remote Sensing of Environment*, 105(3):262–270, 2006.

L. Oldeman. The extent of human-induced soil degradation, in oldeman, l.r. et al., world map of the status of human-induced soil degradation. In *United Nations Environment Programme and International Soil Reference and Information Centre*. Wageningen, The Netherlands, 1991.

C. T. Omuto and D. P. Shrestha. Remote sensing techniques for rapid detection of soil physical degradation. *Int. J. Remote Sens.*, 28(21):4785–4805, 2007.

Y. Onda, H. Kato, Y. Tanaka, M. Tsujimura, G. Davaa, and D. Oyunbaatar. Analysis of runoff generation and soil erosion processes by using environmental radionuclides in semiarid areas of Mongolia. *Journal of Hydrology*, 333(1):124–132, 2007.

M. Owe, R. de Jeu, and J. Walker. A methodology for surface soil moisture and vegetation optical depth retrieval using the microwave polarization difference index. *IEEE Transactions on Geoscience and Remote Sensing*, 39(8):1643–1654, 2001.

A. Palacios-Orueta and S. L. Ustin. Remote sensing of soil properties in the Santa Monica mountains i. spectral analysis. *Remote Sensing of Environment*, 65(2):170–183, 1998.

S. Park, J. J. Feddema, and S. L. Egbert. Impacts of hydrologic soil properties on drought detection with MODIS thermal data. *Remote Sensing of Environment*, 89(1):53–62, 2004.

A. J. Parsons and I. D. L. Foster. What can we learn about soil erosion from the use of 137Cs? *Earth-Science Reviews*, 108(1–2):101–113, 2011.

A. V. Peterburgsky and F. V. Yanishevsky. Transformation of forms of potassium in soil during long-term potassium fertilization. *Plant and Soil*, 15(3):199–210, 1961.

J. Poesen, J. Nachtergaele, G. Verstraeten, and C. Valentin. Gully erosion and environmental change: importance and research needs. *CATENA*, 50(2–4):91–133, 2003.

V. O. Polyakov and M. A. Nearing. Rare earth element oxides for tracing sediment movement. *CATENA*, 55(3):255–276, 2004.

P. Porto, D. E. Walling, and V. Ferro. Validating the use of Caesium-137 measurements to estimate soil erosion rates in a small drainage basin in Calabria, Southern Italy. *Journal of Hydrology*, 248(1–4):93–108, 2001.

D. F. Post, A. Fimbres, A. D. Matthias, E. E. Sano, L. Accioly, A. K. Batchily, and L. G. Ferreira. Predicting soil albedo from soil color and spectral reflectance data. *Soil Science Society of America Journal*, 64(3):1027–1034, 2000.

V. Prasannakumar, H. Vijith, S. Abinod, and N. Geetha. Estimation of soil erosion risk within a small mountainous sub-watershed in Kerala, India, using revised universal soil loss equation (RUSLE) and geo-information technology. *Geoscience Frontiers*, 3(2):209–215, 2012.

J. B. Reeves III, G. W. McCarty, and J. J. Meisinger. Near infrared reflectance spectroscopy for the analysis of agricultural soils. *Journal of Near Infrared Spectroscopy*, 7(3):179–193, 1999.

A. S. Relman. The physiological behavior of Rubidium and Cesium in relation to that of Potassium. *Yale Journal of Biology and Medicine*, 29 (3):248–262, 1956.

K. G. Renard, G. R. Foster, G. A. Weesies, and J. P. Porter. RUSLE: Revised universal soil loss equation. *Journal of Soil and Water Conservation*, 46 (1):30–33, 1991.

N. Richter, T. Jarmer, S. Chabrillat, C. Oyonarte, P. Hostert, and H. Kaufmann. Free iron oxide determination in Mediterranean soils using diffuse reflectance spectroscopy. *Soil Sci. Soc. Am. J.*, 73(1):72–81, 2009.

S. J. Rodway-Dyer and D. E. Walling. The use of 137Cs to establish longer-term soil erosion rates on footpaths in the UK. *Journal of Environmental Management*, 91(10):1952–1962, 2010.

M. Sac, E. Yumurtaci, G. Yener, B. Camgoz, A. Ugur, and B. Ozden. Soil erosion determinations by using 137Cs technique in the agricultural regions of Gediz Basin, Western Turkey. *Environmental Geology*, 55(3): 477–483, 2008.

J.-A. Sanchez-Cabeza, M. Garcia-Talavera, E. Costa, V. Pea, J. Garcia-Orellana, P. Masque, and C. Nalda. Regional calibration of erosion radiotracers (210Pb and 137Cs): Atmospheric fluxes to soils (Northern Spain). *Environmental Science & Technology*, 41(4):1324–1330, 2007.

A. Savitzky and M. J. E. Golay. Smoothing and differentiation of data by simplified least squares procedures. *Analytical Chemistry*, 36(8): 1627–1639, 1964.

T. Schmid, A. Palacios-Orueta, S. Chabrillat, E. Bendor, A. Plaza, M. Rodriguez, M. Huesca, M. Pelayo, C. Pascual, P. Escribano, and V. Cicuendez. Spectral characterisation of land surface composition to determine soil erosion within semiarid rainfed cultivated areas. *Proceedings of IGARSS, 2012, Munchen, Germany, 22-27 July 2012*, pages 7082 –7085, july 2012.

E. E. Schulte and K. A. Kelling. Understanding plant nutrients: soil and applied potassium. *University of Wisconsin Extension*, Publ. A2521, 1998.

P. Seiden, R. Bro, L. Poll, and L. Munck. Exploring fluorescence spectra of apple juice and their connection to quality parameters by chemometrics. *Journal of Agricultural and Food Chemistry*, 44(10):3202–3205, 1996.

A. Sharma. Integrating terrain and vegetation indices for identifying potential soil erosion risk area. *Geo-Spatial Information Science*, 13(3):201–209, 2010.

A. N. Sharpley. Relationship between soil potassium forms and mineralogy. *Soil Science Society of America Journal*, 53(4):1023–1028, 1989.

K. D. Shepherd and M. G. Walsh. Development of reflectance spectral libraries for characterization of soil properties. *Soil Sci Soc Am J*, 66(3): 988–998, 2002.

K. D. Shepherd and M. G. Walsh. Diffuse reflectance spectroscopy for rapid soil analysis. *Encyclopedia of Soil Science: Second Edition*, pages 480 – 484, 2006.

M. Shoshany. Satellite remote sensing of natural mediterranean vegetation: A review within an ecological context. *Progress in Physical Geography*, 24(2):153–178, 2000.

D. P. Shrestha, J. A. Zinck, and E. Van Ranst. Modelling land degradation in the Nepalese Himalaya. *CATENA*, 57(2):135–156, 2004.

D. P. Shrestha, D. E. Margate, F. v. d. Meer, and H. V. Anh. Analysis and classification of hyperspectral data for mapping land degradation: An application in Southern Spain. *International Journal of Applied Earth Observation and Geoinformation*, 7(2):85–96, 2005.

R. B. Shruthi, N. Kerle, and V. Jetten. Object-based gully feature extraction using high spatial resolution imagery. *Geomorphology*, 134:260–268, 2011.

M. J. Smith and C. D. Clark. Methods for the visualization of digital elevation models for landform mapping. *Earth Surface Processes and Landforms*, 30(7):885–900, 2005.

J. A. Sobrino and N. Raissouni. Toward remote sensing methods for land cover dynamic monitoring: Application to Morocco. *International Journal of Remote Sensing*, 21(2):353–366, 2000.

W. Spaan, H. Winteraeken, and P. Geelen. Adoption of SWC measures in South Limburg (The Netherlands): Experiences of a water manager. *Land Use Policy*, 27(1):78–85, 2010.

B. Stenberg, R. A. Viscarra Rossel, A. M. Mouazen, J. Wetterlind, and L. S. Donald. *Visible and Near Infrared Spectroscopy in Soil Science*, volume 107, pages 163–215. Academic Press, 2010.

A. Stevens, T. Udelhoven, A. Denis, B. Tychon, R. Lioy, L. Hoffmann, and B. van Wesemael. Measuring soil organic carbon in croplands at regional scale using airborne imaging spectroscopy. *Geoderma*, 158(1–2):32–45, 2010.

N. Syversen, L. Oygarden, and B. Salbu. Cesium-134 as a tracer to study particle transport processes within a small catchment with a buffer zone. *J. Environ. Qual.*, 30(5):1771–1783, 2001.

I. Takken, L. Beuselinck, J. Nachtergaele, G. Govers, J. Poesen, and G. Degraer. Spatial evaluation of a physically-based distributed erosion model (LISEM). *CATENA*, 37(3–4):431–447, 1999.

A. K. Thurmond, M. G. Abdelsalam, and J. B. Thurmond. Optical-radar-DEM remote sensing data integration for geological mapping in the Afar depression, Ethiopia. *Journal of African Earth Sciences*, 44(2):119–134, 2006.

A. Q. Timothy, G. Gerard, E. W. Desmond, Z. Xinbao, J. J. D. Philippe, Z. Yusheng, and V. Karel. Erosion processes and landform evolution on agricultural land – new perspectives from Caesium-137 measurements and topographic–based erosion modelling. *Earth Surface Processes and Landforms*, 22(9):799–816, 1997.

D. Troufleau and H. Sogaard. Deriving surface water status in the sahel from the pathfinder AVHRR land data set. *Physics and Chemistry of The Earth*, 23(4):421–426, 1998.

A. N. Tyler. *In situ and airborne gamma-ray spectrometry*, volume 11, pages 407–448. Elsevier, 2008.

T. Udelhoven, C. Emmerling, and T. Jarmer. Quantitative analysis of soil chemical properties with diffuse reflectance spectrometry and partial least-square regression: A feasibility study. *Plant and Soil*, 251(2):319–329, 2003.

L. S. Unganai and F. N. Kogan. Drought monitoring and corn yield estimation in southern africa from AVHRR data. *Remote Sensing of Environment*, 63(3):219–232, 1998.

F. van der Meer. Analysis of spectral absorption features in hyperspectral imagery. *International Journal of Applied Earth Observation and Geoinformation*, 5(1):55–68, 2004.

F. van der Meer. The effectiveness of spectral similarity measures for the analysis of hyperspectral imagery. *International Journal of Applied Earth Observation and Geoinformation*, 8(1):3–17, 2006.

G. Van Lynden. European soil resources. current status of soil degradation, causes, impacts and need for action. *Nature and Environment*, (71):1–99, 1995.

L. Van Reeuwijk. Procedures for soil analysis. Technical report, 2002.

R. A. Viscarra Rossel. Parles: Software for chemometric analysis of spectroscopic data. *Chemometrics and Intelligent Laboratory Systems*, 90(1): 72–83, 2008.

R. A. Viscarra Rossel, D. J. J. Walvoort, A. B. McBratney, L. J. Janik, and J. O. Skjemstad. Visible, near infrared, mid infrared or combined diffuse reflectance spectroscopy for simultaneous assessment of various soil properties. *Geoderma*, 131(1–2):59–75, 2006.

R. A. Viscarra Rossel, P. A. B. McBratney, D. B. Minasny, B. Stenberg, and R. A. V. Rossel. *Diffuse Reflectance Spectroscopy for High-Resolution Soil Sensing Proximal Soil Sensing*, volume 1 of *Progress in Soil Science*, pages 29–47. Springer Netherlands, 2010.

A. Vrieling. Satellite remote sensing for water erosion assessment: A review. *CATENA*, 65(1):2–18, 2006.

P. J. Wallbrink and A. S. Murray. Use of fallout radionuclides as indicators of erosion processes. *Hydrological Processes*, 7(3):297–304, 1993.

D. E. Walling and T. A. Quine. Calibration of Caesium-137 measurements to provide quantitative erosion rate data. *Land Degradation & Development*, 2(3):161–175, 1990.

F. L. Wang and P. M. Huang. Effects of organic matter on the rate of potassium adsorption by soils. *Canadian Journal of Soil Science*, 81(3): 325–330, 2001.

S. D. Warren, H. Mitasova, M. G. Hohmann, S. Landsberger, F. Y. Iskander, T. S. Ruzycki, and G. M. Senseman. Validation of a 3-D enhancement of the universal soil loss equation for prediction of soil erosion and sediment deposition. *CATENA*, 64(2–3):281–296, 2005.

L. Weidong, F. Baret, G. Xingfa, T. Qingxi, Z. Lanfen, and Z. Bing. Relating soil surface moisture to reflectance. *Remote Sensing of Environment*, 81 (2–3):238–246, 2002.

S. L. West, G. N. White, Y. Deng, K. J. McInnes, A. S. R. Juo, and J. B. Dixon. Kaolinite, halloysite, and iron oxide influence on physical behavior of formulated soils. *Soil Sci. Soc. Am. J.*, 68(4):1452–1460, 2004.

F. Westad, M. Hersleth, P. Lea, and H. Martens. Variable selection in pca in sensory descriptive and consumer data. *Food Quality and Preference*, 14 (5–6):463–472, 2003.

H. J. Winteraeken and W. P. Spaan. A new approach to soil erosion and runoff in South Limburg – The Netherlands. *Land Degradation & Development*, 21(4):346–352, 2010.

W. Wischmeier and D. Smith. *Predicting rainfall erosion losses : a guide to conservation planning*. Supersedes agriculture handbook no. 282, "Predicting rainfall-erosion losses from Cropland East of the Rocky Mountains". Science and Education Administration United States Department of Agriculture (USDA), Purdue Agricultural Experiment Station, 1978.

S. Wold, M. Sjöström, and L. Eriksson. Pls-regression: a basic tool of chemometrics. *Chemometrics and Intelligent Laboratory Systems*, 58(2): 109–130, 2001.

N. Xiaojun, W. Xiaodan, L. Suzhen, G. Shixian, and L. Haijun. 137Cs tracing dynamics of soil erosion, organic carbon and nitrogen in sloping farmland converted from original grassland in Tibetan plateau. *Applied Radiation and Isotopes*, 68(9):1650–1655, 2010.

F. A. Yitagesu, F. van der Meer, H. van der Werff, and W. Zigterman. Quantifying engineering parameters of expansive soils from their reflectance spectra. *Engineering Geology*, 105(3–4):151–160, 2009.

F. A. Yitagesu, F. van der Meer, H. van der Werff, and C. Hecker. Spectral characteristics of clay minerals in the 2.5–14 μm wavelength region. *Applied Clay Science*, 53(4):581–591, 2011.

P. Zhang, L. Li, G. Pan, and J. Ren. Soil quality changes in land degradation as indicated by soil chemical, biochemical and microbiological properties in a karst area of southwest guizhou, china. *Environmental Geology*, 51 (4):609–619, 2006.

P. Zhou, O. Luukkanen, T. Tokola, and J. Nieminen. Effect of vegetation cover on soil erosion in a mountainous watershed. *CATENA*, 75(3): 319–325, 2008.

M. Zribi, S. Le Hégarat-Mascle, C. Ottlé, B. Kammoun, and C. Guerin. Surface soil moisture estimation from the synergistic use of the (multi-incidence and multi-resolution) active microwave ERS wind scatterometer and SAR data. *Remote Sensing of Environment*, 86(1):30–41, 2003.

M. Zribi, N. Baghdadi, N. Holah, and O. Fafin. New methodology for soil surface moisture estimation and its application to ENVISAT-ASAR multi-

incidence data inversion. *Remote Sensing of Environment*, 96(3–4):485–496, 2005.

Summary

Assessing soil erosion over large areas has been a challenge for decades. The large spatial extent of the process creates difficulties in data acquisition, for both measuring and validation. Remotely sensed data provide spatial coverage and are used to derive information for various soil erosion parameters, such as vegetation cover, topography, and soil moisture.

As part of this work, various applications of remotely sensed data in soil erosion studies were reviewed to identify gaps in current soil erosion research. To date, infrared spectroscopy has been applied in only a limited number of studies. A way to better integrate these data in studies of soil erosion was to detect the chemical composition of the soil and apply the method for soil chemical particle tracing.

To identify a potential soil particle tracer that has similar physical and chemical properties as the commonly used radioactive isotope Ceasium-137 (^{137}Cs), but at the same time does possess a distinctive spectral signature, a number of abundant in the environment chemical elements were tested. Wavelength ranges that statistically predict and quantify soluble fractions of chemical elements, from infrared spectroscopy were identified. Partial least squares regression (PLSR) was used to develop prediction models for naturally occurring Calcium (Ca), Magnesium (Mg), Potassium (K), Sodium (Na), Iron (Fe), and acidity (pH) in silt loam soil samples. Significant wavelength ranges were determined by establishing direct and indirect relationships between soil spectra and soluble fractions of these elements.

The feasibility of using Partial Least Squares Regression for identifying soluble fractions of soil chemical elements in silt loam soils using infrared

spectroscopy was tested. By outlining wavelength ranges where the change in reflectance was associated with change in the concentration of the element, Potassium was identified as having the closest to ^{137}Cs properties that can be predicted from infrared spectra.

A laboratory based study on the use of Potassium (K) as a potential replacement of ^{137}Cs in soil particle tracing was then conducted. The element was found to have similar electrical, chemical and physical properties. In order to test the suitability of the element as a particle tracer, heavy clay, clay loam, loam, silty loam and sandy loam and fine sand soils were sampled for the study. Sensitivity analyses were performed on soil chemical properties and spectra to identify the wavelength range related to K concentration. Different concentrations of K fertilizer were added to soils with varying texture in order to establish spectral characteristics of the absorption feature associated with K.

Quantifying concentrations of K by using commercial fertilizer and infrared spectroscopy was possible for soils with sandy and sandy silt texture. The current study suggested the method as a new approach that could potentially grow to a technique for rapid monitoring of soil particle movement. A flow experiment was conducted in the area of the Guadalentin basin in Murcia, South East Spain in order to identify soil particle movement using Potassium fertilizer and infrared spectroscopy in the field. The severe soil erosion that takes place in the region, as well as the silty loam texture of the soil, determined the selection of the field area.

This experiment allowed identification of key factors that determine the detection of K, when tested as a potential particle tracer. A follow up experiment was designed to take into consideration soil clay content, runoff data and concentrations of applied fertilizer. Consequently, a field-based water flow experiment was conducted on 6 plots in silty loam soils in the Netherlands. The field area was selected due to the fact that the soils were developed on Loess, and were characterized with limited clay content. The plots were treated with various concentrations of K_2O and one plot was used as reference. Infrared reflectance spectra were collected to observe spatial variation in available K, before and after application of fertilizer, and after runoff simulation by water flow. The runoff sediment was also collected in order to establish potential removal of fertilizer under the influence of the water flow.

Exploring K as a soil particle tracer introduced a number of advantages to current erosion studies. It is applied annually as a fertilizer and therefore does not have a half-life as radioactive elements do. The scope of the study, however, was limited to K concentrations that are not harmful to the environment, and are regularly applied during agricultural practices. Although high concentrations of Potassium in the laboratory show promising results, high amounts of fertilizer were not used in the field experiments. Thus, the methodology would be suitable for effective monitoring of early signs of soil erosion.

The focus of this study was put on the removal of K under the influence of water flow. Therefore, in order to establish whether sedimentation and deposition can be measured, additional tests should be conducted at the locations where the flow stops. Moreover, it was recommended that further tests on K leaching should be performed, despite that leaching is unlikely to occur for the duration of the proposed experiment. There is a strong need to find an alternative to ^{137}Cs for soil erosion modeling, considering the radioactive properties and half life of the element. If used as a particle tracer, potassium is environmentally friendly, readily available in the form of a fertilizer, and its abundance can be detected with infrared spectroscopy in dry, silty loam or sandy soils, with low clay content.

Samenvatting

Het waarnemen van bodemerosie over grote landoppervlaktes is al voor langere tijd een uitdaging in de wetenschap. De ruimtelijke schaal waarop dit proces zich afspeelt maakt het moeilijk gegevens te vergaren voor zowel het meten van het proces als het valideren van deze meetgegevens. Aardobservatie geeft de benodigde ruimtelijke dekking en wordt gebruikt om informatie te verkrijgen over verscheidene bodem erosie parameters, zoals vegetatie bedekking, topografie en bodemvocht gehalte.

Als deel van dit onderzoek werd een overzicht gemaakt van verscheidene toepassingen van aardobservatie voor bodemerosie, en mogelijkheden die in huidig onderzoek naar bodem erosie onbenut bleken, konden daarmee geïdentificeerd worden. Infrarood spectroscopie werd tot nu toe gebruikt in slechts een beperkt aantal studies, en een mogelijkheid voor het gebruik van deze techniek bleek te liggen in het meten van de chemische samenstelling van bodems en het volgen van verplaatsende bodemdeeltjes.

Gewoonlijk wordt in bodem erosie studies het radio-actieve Caesium-137 (^{137}Cs) isotoop gebruikt voor volgen van verplaatsende bodemdeeltjes. Dit element heeft echter geen absorptie kenmerken heeft in het infrarode spectrum. Er werd daarom gezocht naar een alternatief element dat vergelijkbare fysische en chemische eigenschappen heeft, maar wel spectraal actief is.

Partial Least Squares regressie (PLSR) werd gebruikt om de absorptie golflengtes te bepalen die statistisch de wateroplosbare fractie van chemische elementen voorspellen, waarbij zowel directe alsook indirecte relaties tussen spectra en de elementen gebruikt werden. Van de natuurlijk voorkomende elementen Calcium (Ca), Magnesium (Mg), Kalium (K),

Natrium (Na), IJzer (Fe), en van de zuurtegraad (pH), konden in silt leem bodem monsters de golflengtes vastgesteld worden die een significante voorspelling geven.

Uit het systematisch testen van veranderingen in het absorptie spectrum als gevolg van veranderende concentraties van opgeloste elementen, bleek dat PLSR gebruikt kon worden voor het identificeren van de wateroplosbare fracties van bodem elementen in silt leem bodems. Van de bovengenoemde elementen, die alle spectroscopisch detecteerbaar zijn, komt Kalium chemisch met meest overeen met ^{137}Cs .

Een laboratorium onderzoek werd uitgevoerd om de geschiktheid van Kalium (K) als mogelijke vervanger van ^{137}Cs te bepalen. Een gevoeligheidsanalyse werd uitgevoerd tussen infrarood spectra en bodemchemische eigenschappen van klei, klei leem, leem, silt leem en zand leem bodem monsters, waaraan verschillende concentraties van een Kalium houdende kunstmest toegevoegd werden. Hiermee werden de absorptie golflengtes gerelateerd aan veranderingen in Kalium concentratie vastgesteld. Het bleek dat het vaststellen van deze Kalium concentratie met behulp van infrarood spectroscopie aleen mogelijk was in zand of zand leem bodems.

In dit proefschrift is dit gegeven gezien als een mogelijkheid om beweging van bodemdeeltjes te observeren. Om beweging van bodemdeeltjes in het veld te observeren, werd een vloei experiment met Kaliumhoudende kunstmest en infrarood spectroscopie uitgevoerd in het Guadalentin bekken, nabij Murcia in Zuidoost Spanje. Dit gebied heeft bodems met een overwegend silt leem textuur en gaat tevens gebukt onder hevige erosie. Dit experiment belichtte een aantal sleutel factoren die het detecteren van Kalium beinvloeden. In een vloei experiment gedaan in een Loess gebied in Zuid Nederland, dat gekenmerkt worden door bodems met een relatief laag klei gehalte, werd ook de invloed van klei gehalte, stroomsterkte van water en de concentratie van de toegevoegde kunstmest bepaald. Hiertoe werden vijf plekken in een silt leem grond voorzien van verschillende concentraties K_2O, terwijl één plek als referentie gebruikt werd. Infrarood spectra werden gebruikt om de ruimtelijke variatie van Kalium te bepalen voor en na het vloeien van water. Het verplaatste sediment werd opgevangen om het transport van kunstmest door het water vast te stellen.

Het gebruik van Kalium als indicator voor transport van bodemdeeltjes geeft nieuwe mogelijkheden aan bodemerosie studies. Kalium wordt jaar-

lijks opgebracht als meststof, en het heeft geen beperkende halfwaarde tijd zoals radioactieve elementen. Dit onderzoek bleef beperkt tot het gebruik van Kalium concentraties die gebruikelijk jaarlijks opgebracht worden en die niet schadelijk zijn voor het milieu. Hoewel het gebruik van hogere concentraties Kalium in laboratorium experimenten duidelijker resultaten laat zien, en daarmee geschikt zou zijn om de eerste signalen van bodemerosie op te vangen, zijn deze hoge hoeveelheden in het veld niet gebruikt.

Deze studie was gericht op het verwijderen van Kalium door het laten vloeien van water. Om vast te stellen of erosie en sedimentatie daadwerkelijk gemeten kan worden, zou in toekomstige experimenten ook metingen gedaan moeten worden op plaatsen waar de waterstroom stopt. Ook zou het weglekken van Kalium in de bodem beter gecontroleerd moeten worden, hoewel zulks niet waarschijnlijk is in de korte tijdsduur die vloei experimenten nemen.

Voor bodemerosie modelering is het belangrijk een alternatief voor ^{137}Cs te vinden, gezien de radio-activiteit en half-waarde tijd van dit element. Voor deze toepassing, Kalium is milieu vriendelijk, beschikbaar in de vorm van kunstmest, en kan gedetecteerd worden in droge, silt leem of zandige bodems met infrarood spectroscopie.

Resume

Mila Luleva was born on January, 18th, 1984 in Sofia, Bulgaria. In 2005, she obtained her Bachelor degree in Geography and Environmental Science with Honors, from University of Sussex, UK, with specialization in soil contamination. She then completed a Masters of Science course in Geo-information science and Earth Observation for Environmental Modeling and Management from University of Southampton, University of Lund, University of Warsaw and ITC. The topic of her MSc thesis was 'Identification of Soil Property Variation Using Spectral and Statistical Analyses on Field and ASTER Data - A Case Study of Tunisia'. In 2007 she began her PhD funded by the EU DESIRE Project. Mila is currently an environmental GIS and remote sensing consultant.

Publications

Peer Reviewed First Author Publications

- Luleva M., van der Werff, H., van der Meer, F., Jetten, V., 2013, Observing change in Potassium abundance in a soil erosion experiment with field infrared spectroscopy, Chemistry, 22(1): 91 - 109
- M. I. Luleva, H. Van Der Werff, F. Van Der Meer, and V. Jetten., 2012, Gaps and opportunities in the use of remote sensing for soil erosion assessment. Chemistry, 21(5): 748 - 764
- Luleva, M.I., van der Werff, H., Jetten, V., van der Meer, F., 2011. Can Infrared Spectroscopy Be Used to Measure Change in Potassium Nitrate Concentration as a Proxy for Soil Particle Movement? Sensors 11, 4188 – 4206
- Luleva M., van der Werff, H., van der Meer, F., Jetten, V., Predicting Soluble Fractions of Chemical Elements in Silt Loam Soils Using Infrared Spectroscopy, Pedosphere (submitted)
- Luleva, M., 2007, Economic Impact of Global Worming: The Ever-Lasting Debate, Economy Life, In Press, [In Bulgarian]
- Luleva M., Ignatova, M, 2007, NATURA 2000 in Bulgaria: The Current Situation of the Country in Respect to the EU Directives, Economy Life, submitted and approved [In Bulgarian]
- Luleva M., 2007, Environmental Tax on Airplanes: Is it a Feasible Idea?, Economy Life, submitted and approved [In Bulgarian]

Conference Proceedings

- Luleva, M, van der Meer, F, van der Werff, H., Jetten, V., Tracing soil particle movement using Potassium Nitrate and Infrared spectral response, DESIRE Conference, May, 2010, Enschede, The Netherlands
- Luleva, M, van der Meer, F, van der Werff, H., Jetten, V., Applying Partial Least Squares Regression technique for rapid detection of soil chemical composition related to land degradation, High Resolution Geological Remote Sensing, GRSG Annual General Meeting, 10-11 December, 2008-10-01, The Geological Society of London

MSc Thesis

- Luleva, M, 2007, Identification of Soil Property Variation Using Spectral and Statistical Analyses on Field and ASTER Data. A Case Study of Tunisia. Available: http://www.itc.nl/library

ITC dissertations

A complete list of ITC dissertations is online on the ITC website: www.itc.nl/research/phd/phd_graduates.aspx.

This dissertation has number 228.